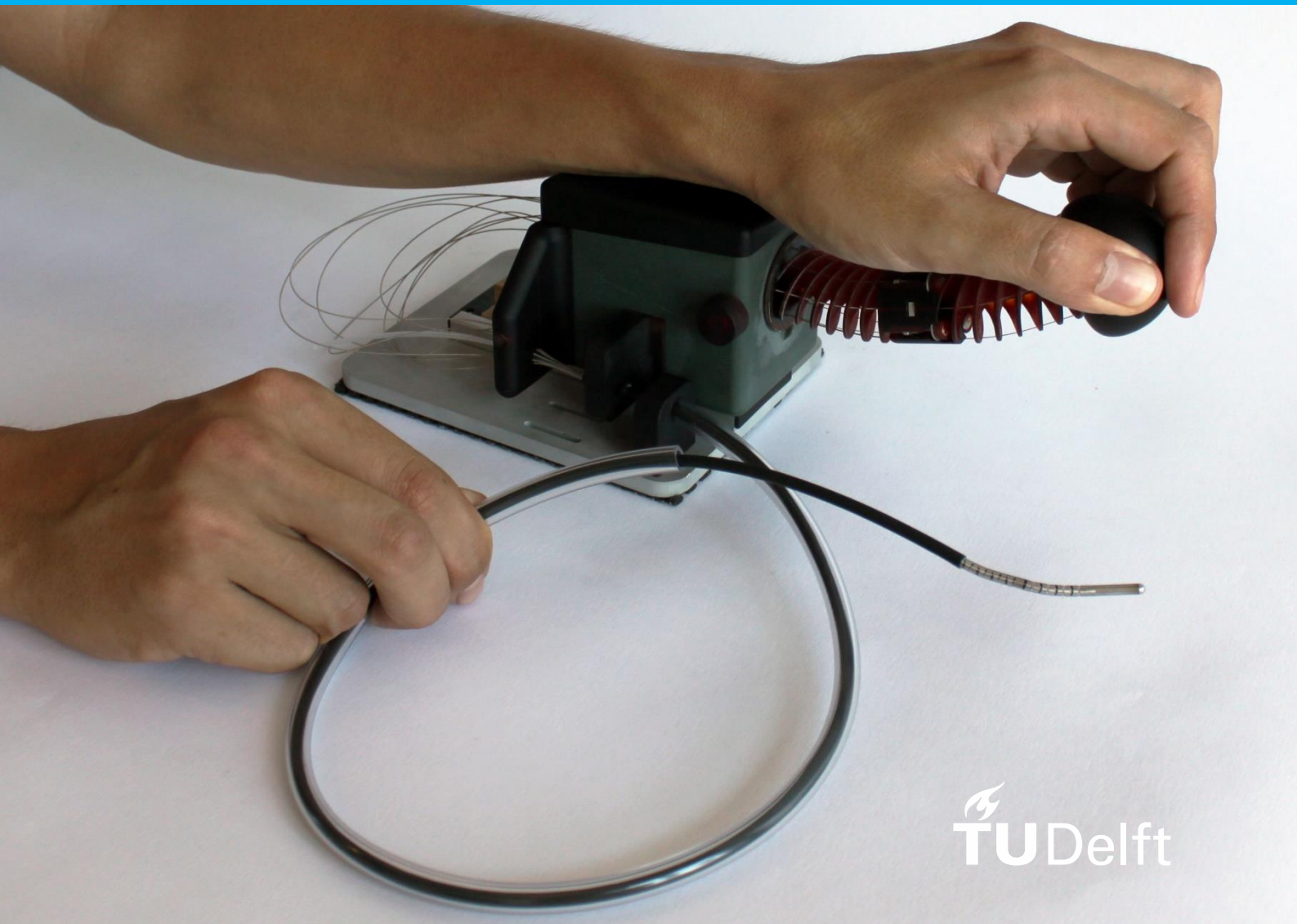


Design and Evaluation of the Epsilon Catheter

*Single-Handed Control of a Five Degrees of Freedom
Multi-Steerable Heart Catheter*

Master Thesis
BioMechanical Design
Mechanical Engineering
Delft University of Technology
J.W.L. Mulckhuyse
May 29, 2019



Design and Evaluation of the Epsilon Catheter

Single-Handed Control of a Five Degrees of Freedom Multi-Steerable Heart Catheter

By

Joppe Willem Leendert Mulckhuyse

in partial fulfilment of the requirements for the degree of

Master of Science
in Mechanical Engineering

at the Delft University of Technology,
to be defended publicly on Wednesday May 29, 2019 at 14:00.

Thesis committee:	Paul Breedveld	TU Delft, Chairman
	Costanza Culmone	TU Delft, Daily supervisor
	Awaz Ali	TU Delft, Daily supervisor
	Michaël Wiertlewski	TU Delft, External member

This thesis is confidential and cannot be made public until December 31, 2021.

An electronic version of this thesis is available at <http://repository.tudelft.nl/>.

Contents

Abstract.....	1
1. Introduction.....	1
1.1. Interventional cardiology	1
1.2. Steerable catheters	2
1.3. Multi-steerable Sigma catheter.....	2
1.4. Aim of this study.....	3
1.5. Paper lay-out	4
2. Theoretical framework	4
2.1. Interventional environment.....	4
2.2. Interventionist.....	6
2.3. Instrumentation control.....	6
3. Design	7
3.1. Design requirements	7
3.2. Functional design.....	8
3.3. Handle design.....	9
3.4. Prototype design	12
4. Prototype	15
4.1. Basic components.....	15
4.2. Assembly	16
4.3. Steering cable fixation	16
4.4. Functionality test	18
5. Evaluation	18
5.1. Experimental design.....	18
5.2. Experimental results.....	21
6. Discussion	23
6.1. Catheter design.....	23
6.2. Experimental findings.....	24
6.3. Cardiac application	25
6.4. Future recommendations	25
7. Conclusion.....	26
Acknowledgements	26
References.....	26
Appendix A: List of symbols.....	30
Appendix B: Technical drawings Epsilon prototype	31
Appendix C: Informed consent form	55
Appendix D: Instructions.....	57
Appendix E: Intake questionnaire	59
Appendix F: Technical drawings experimental design	60
Appendix G: TLX questionnaire	68
Appendix H: Final questionnaire	69
Appendix I: Raw data of experiment.....	70
Appendix J: MATLAB code for data processing of the experiment.....	71

Design and Evaluation of the Epsilon Catheter

Single-Handed Control of a Five Degrees of Freedom Multi-Steerable Heart Catheter

Joppe Mulckhuysen – 4234006

Delft University of Technology, Department of Mechanical Engineering

May 29, 2019

Abstract

Objectives – Over the past decades, more and more cardiac diseases have been treated in interventional cardiology. Catheters are generally used to access the heart through the blood vessels. The previously developed steerable *Sigma* catheter at Delft University of Technology, tackles cable related challenges of conventional mechanically controlled catheters by an improved tip and shaft design. With its two finger-controlled joysticks, the handle allows full actuation of the four degrees of freedom catheter tip. However, this input control method is not specifically designed for optimal user experience. Therefore, the aim of this research is to design an input control method for the *Sigma* catheter tip and shaft design to improve task performance while reducing workload for the interventionist. **Methods** – A theoretical framework was composed and analysed to form design requirements. After detailing the functional and geometrical design, a functional prototype, the *Epsilon* catheter, was fabricated. To evaluate the proposed control method, an experimental setup was prepared and the control method of both catheters were compared. Six participants were asked to conduct the task, which consisted of contacting targets with the catheter end-point. Target-to-target times were measured and a self-report questionnaire was conducted.

Results – The theoretical analysis was divided in the interventional environment, the interventionist who controls the catheter, and the instrumentation. A functional design was made, including catheter control through combining multiple fingers and the wrist using positive input-output coupling. The geometrical design achieved these functionalities through bending flexures and a 180° bended shaft. Data analysis of the experiment showed differences in target-to-target times and self-reported measures. **Conclusion** – The *Epsilon* prototype showed to fulfil on the requirements in a functionality test. The prototype allows steering the catheter tip in five degrees of freedom, single-handed in a handheld design. In the experimental setup, participants using the control method of the *Epsilon* catheter, performed the targeting task faster than using the *Sigma* catheter with reduced workload. **Significance** – Allowing the interventionist to control all manoeuvrability of the catheter tip single handed, may change the operational procedure during interventional cardiology. A single interventionist could perform extended treatment using two individually controlled multi-steerable catheters. Further developments will be towards design optimisations to further improve user experience and evaluation of the fifth degree of freedom.

Keywords – Steerable heart catheter, interventional cardiology, catheterization, multi-steerable instruments, manoeuvrability, medical device design

1. Introduction

1.1. Interventional cardiology

According to the Global Burden of Disease (GBD) consortium, cardiovascular disease has a major contribution to the confinement of the expectation and quality of life of the world population [1-4]. In 2015, it was approximated that worldwide, 422 million people were suffering from cardiovascular disease. Complaints can be prevented or reduced by influencing risk factors as physical activity, nutrition and smoking [1,5]. Still, more than 250.000 patients were hospitalised in the Netherlands in 2015, mostly for heart failure and atrial fibrillation [1]. In these patients, prudent

treatments like diets, physical activity programs or medication are not sufficient and more extensive treatment is required.

Extensive treatment often implies heart surgery in which, for example, septal defects are closed or leakage of heart valves is reduced. During heart surgery, the heart lung machine can be used to take over the blood and air flow of the patient and allow temporary heart arrest [1,6]. The heart is accessed through an incision in the chest. Therefore, the surgeon has direct vision of the heart and can accurately manipulate heart tissue by their hands or instrumentation. Despite a successful performance of the procedure, patients endure chest trauma and risks of postoperative

complications like infections, pain, blood clots and heart arrhythmia [7,8]

To reduce the trauma of the treatment, new treatment strategies were explored and found in the use of catheters. The use of catheters expanded from vascular procedures to extensive heart treatments. The development coincides with the demand of accurate treatment for cardiovascular disease. This resulted in newer and less invasive procedures to arise, and the broadened fields of like interventional cardiology and electrophysiology. The newer and less invasive techniques do not replace open-heart procedures, but rather extended the capabilities of the clinicians.

To access the heart with a catheter, initially, an incision for catheter entrance is made. The natural openings in the cardiovascular system (blood vessels and heart chambers) are used to guide the catheter to the heart. This procedure allows treatment in and on the heart while the heart is in naturally beating condition. Catheters are used for placement of artificial heart valves, septal occluders and stents without opening the chest [9]. Catheters are also used for treatment of heart arrhythmia caused by electrical rhythm disturbance. This technique is called ablation. Heat or cold is produced at the catheter tip to cause scar tissue on the heart wall, to isolate the electrical leakage.

While these interventional procedures are generally less invasive than open heart surgery, they present new challenges. The noisy 2-dimensional (2D) images from ultrasound or computed tomography scanners show a limited visualisation of the 3-dimensional (3D) operational site [10,11]. Object details and depth perception as during direct visual sight are absent. Moreover, for treatment of the heart, the catheter should not only be able to reach the heart through the blood vessels but also be able to manipulate tissue within the heart. This requires steerability of the tip segment of the catheter in the complex 3D environment of the heart.

1.2. Steerable catheters

Steerable catheters are available in a broad range of constructions. Initially, catheters consisted solely of hollow, flexible tubes which are passively steered by a push-pull motion along the shaft and by rotation around the shaft axis [12]. Pre-curved catheter tips can force the catheter to follow the desired pathway when a rotation around the shaft axis is applied [12]. If the interventionist desires a different curvature of the tip, a guidewire is placed through the catheter [12]. This allows removal of

the catheter while leaving the guidewire in place. A second catheter is inserted along the guidewire. The interventionist can continue the desired trajectory with the second catheter at the crossing where the first catheter was removed.

Additional developments resulted in actively steerable catheters which use a steering mechanism in the tip to adapt the curvature of the tip [13]. This allows interventionist to reach multiple locations on the heart in real-time without interchanging catheters. This changes the functionality of the catheter from treatment at a single location, for example, during stenting, to treatment at a series of locations, for example, during ablation. Most of the clinically used steerable catheters can steer in up to two planes [14]. An overview of steerable catheters and their steering mechanisms is presented by Ali et al. [14].

Some systems can steer over three planes using external actuation methods as for example in the Niobe magnetic navigation system (Stereotaxis, St-Louis, USA) [15-17]. This catheter is steered by a magnetic field induced by large magnets near the patient. The interventionist can enter the desired orientation and location of the catheter into a computer. The system adapts the magnetic field in order to move the catheter to the desired location.

Currently, steerable catheters are clinically used but not broadly applied. This is partly caused by guidelines which only recommend the interventional approach for inoperable or high operative risk patients. This is for example the case in patients who need replacement of the aortic valve [18]. Nevertheless, studies show similar or improved outcomes of the interventional approach compared to the surgical approach of aortic valve replacement [19,21]. During ablation procedures, magnetic navigation systems show similar efficiency to mechanically steerable catheterization systems [22]. On the other hand, the use of mechanical catheterization systems results in lower complication rates and total radiation exposure [22].

1.3. Multi-steerable Sigma catheter

Despite positive clinical outcomes of available steerable catheters, difficulties are reported [23]. Especially the magnetic and robotic systems require large investments, adapted operating rooms, new operational skills of the interventionist and limited force application [24,25].

Ali et al. [26] performed an analysis of mechanically actuated steerable catheters to indicate challenges and propose solutions. First of

all, mechanically actuated steerable catheters do not require such major investments because low-cost internal steering cables are used [26]. However, typical cable related problems occur like buckling, wedging, lack of push-ability and limited maximum pull force [26]. The torque applied by the clinicians, to steer the catheter, in combination with low torsional stiffness of the catheter shaft, results in shock-wise and unpredictable behaviour of the catheter [26-28]. The catheter behaviour is also disturbed by limited axial stiffness of the catheter shaft [26]. This results in shortening of the shaft and unexpected displacement of the tip [29]. Due to the tortuous vascular pathway, friction appears between steering cables and their sleeves resulting in steering difficulties [26]. Moreover, mechanically actuated steerable catheters do not allow complex or multi-planar curves to be made inside the heart [30,31].

In addition to these technical challenges, clinical challenges arise as a result of the dynamic cardiovascular environment. Rotation and exchange of catheters contribute to complications as vessel damage and cardiac arrhythmias [32,34].

Ali et al. [26] proposed solutions according to the analysed challenges and combined them into the multi-steerable *Sigma* catheter, as shown in Figure 1. The catheter tip is controlled at the handle by the thumb and index finger using two joysticks. The catheter tip is constructed of two

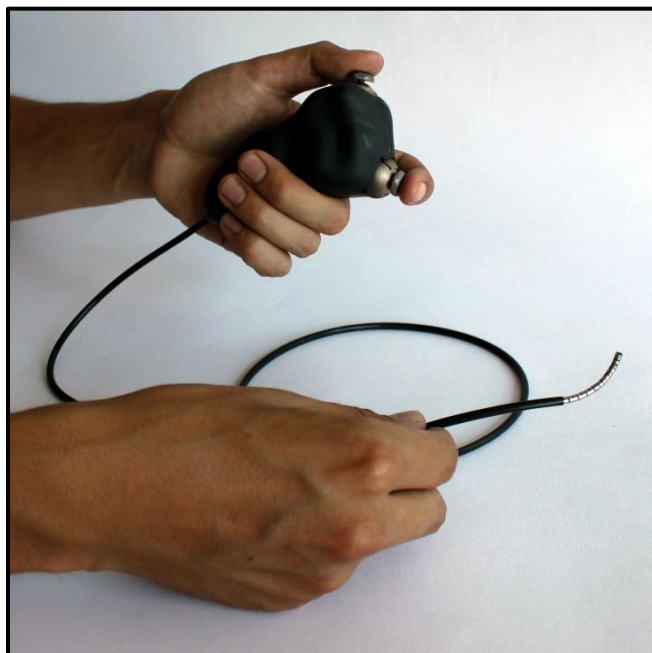


Figure 1: The *Sigma* catheter represented in a functional prototype. Tip of the catheter (right) is controlled at the handle (top) by thumb and index finger. Tip and handle are connected by a flexible shaft.

steering segments, where each segment is controlled by an individual finger. A detailed photo of the catheter tip is shown in Figure 2. Both segments can steer in two planes perpendicular to each other. Combining both segments results in steering in four Degrees of Freedom (DOF), further referred to as omni-steerability. This omni-steerability results in two lateral movements and two angular rotations of the catheter tip end-point. Due to the omni-steerability, torque application to the shaft is no more required. Steerability is also independent from the path followed by the shaft or from the steering direction. The longitudinal movement is controlled by the second hand of the interventionist, like clinically used catheters. The catheter, with an outer $\varnothing 3$ mm, is designed as a steerable sheath having a lumen of $\varnothing 1.5$ mm.

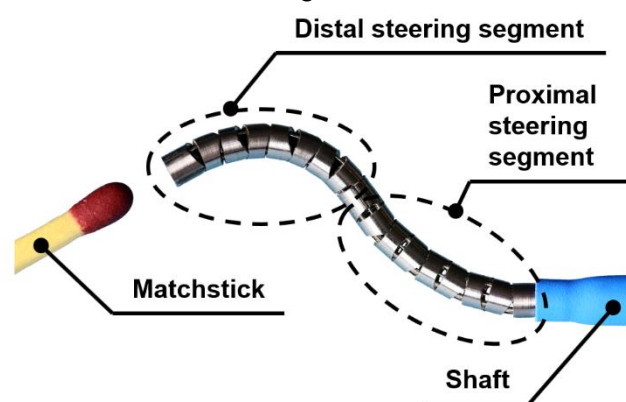


Figure 2: Detailed photo of the omni-steerable dual-segmented *Sigma* catheter tip. Both steering segments are steered in opposite direction. A matchstick is added to the photo to visualise the scale of the steering segment elements.

1.4. Aim of this study

The *Sigma* catheter tackles cable related challenges of mechanically controlled catheters resulting in reliable omni-steerability [26]. The *Sigma* catheter allows manoeuvring tasks to be achieved by steering the catheter tip from location and orientation A to location and orientation B [26]. Performance of such tasks is a trade-off between speed and accuracy [35]. However, since the interventionist controls the catheter, task performance depends on both the mechanical system and the input control method [26]. On top of that, two finger-controlled joysticks allow full actuation of the *Sigma* catheter but are not specifically designed for optimal user experience [26].

Therefore, the aim of this study is designing an input control method for the *Sigma* catheter tip and shaft design which improves task performance, while reducing workload of the interventionist.

1.5. Paper lay-out

At first, additional information from the literature focussing on the interventional environment, the interventionist and instrumentation control is gathered, analysed and presented in Section 2 *Theoretical framework*. Subsequently, the main elements from the literature are formed to design requirements in Section 3 *Design*. According to the requirements, a functional design is presented which shows the demand for a handle design. Once the handle design is described, further details are reported to adapt the design for building a functional prototype. Section 4 *Prototype*, describes the manufacturing and assembly of the *Epsilon* catheter prototype with in the end, a functionality test. Section 5 *Evaluation* describes the experimental design and results of the evaluation of the *Epsilon* catheter. Then, Section 6 *Discussion* describes a reflection on the design, evaluation and future applications, followed by Section 7 *Conclusion*.

2. Theoretical framework

2.1. Interventional environment

Before forming design requirements, more relevant information about using heart catheters is gathered as a foundation for the input control method design. To cover all relevant information, the theoretical framework is divided in three topics. At first, the catheter functions in an operation room. This is described by the interventional environment. Next, the catheter is controlled by the interventionist who leads the procedure. Finally, information about controlling complex systems is described in the instrumentation section.

The operation room is an intricate environment with many people working closely together under many protocols and strict legislation while patient's life is at stake. Not only the clinical components of the procedure are challenging but also the additional support systems and instrumentation require close attention from the whole surgical team. For the catheterization system the following topics are discussed: visualisation of the heart, handheld versus robotic systems and interventional tasks.

Visualisation of the heart – During the preparation of interventional procedures, pre-operative magnetic resonance imaging (MRI) scans of the heart and blood vessels are used for path planning. On these 3D images it is clear to distinct several kinds of soft tissue like muscles, tendons, fat and plaque [36]. During most interventional procedures MRI cannot be used

since magnetic materials of the instruments disturb the image [36]. Additionally, the MRI scanner limits the working environment of the interventionist since the patient is inside the cavity of the MRI scanner [36].

The main visualisation technique used in interventional cardiology is computed tomography (CT) combined with fluoroscopy [36]. CT shows accurately bone tissue and (magnetic) instrumentation in real-time, but distinction between different soft tissues is very limited as shown in Figure 3.

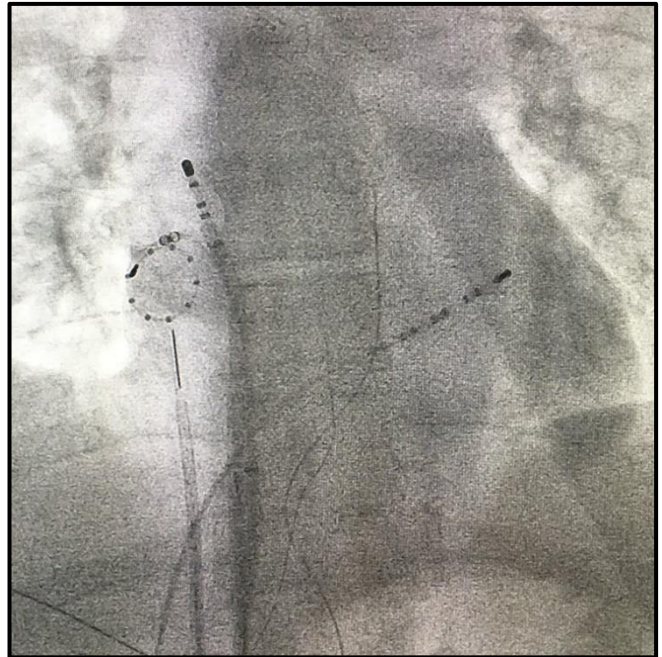


Figure 3: CT image taken during an ablation procedure at the Erasmus Medical Centre in Rotterdam. The patient's spinal cord (from top to bottom) and instrumentation (catheters with dotted tips) can be identified. Distinction between soft tissue, to visualise the heart, is limited.

Using fluoroscopy, the image can be improved by the insertion of contrast fluid in the patient's blood [36]. The contrast fluid highlights the blood vessels of the patient for a few seconds on the image. This is used to detect a blockage in a blood vessel or leakage of a heart valve. However, due to both the radiation of the CT and the contrast fluid this imaging technique has to be used within limits for patient's health.

Another main visualisation technique is echography, sometimes referred to as ultrasound, which shows real-time images with clear soft tissue distinction and can highlight blood flow [36]. MRI and CT allow imaging of the entire patient's cross-section, while the signal penetration depth of echography is limited [36]. On top of that, bone tissue blocks the signal which results in visualized

areas behind bone. Due to the patient's ribs, echography cannot be used to visualise the heart from the patient's chest. Transoesophageal echocardiography can supply images of the heart since the oesophagus is located just behind the heart [36,37]. Due to gagging and pain, general anaesthesia has to be applied to the patient with this visualisation method. This increases the impact of the procedure on the patient [36].

The last technique discussed here focuses on cardiac mapping. A catheter is used to map the heart on beforehand to build-up a 3D representation of the heart [38]. At first, this 3D representation assists the interventionist, to orient the catheter within the heart. Secondly, during ablation procedures, the system keeps track of ablated locations. An example of this method is shown in Figure 4.

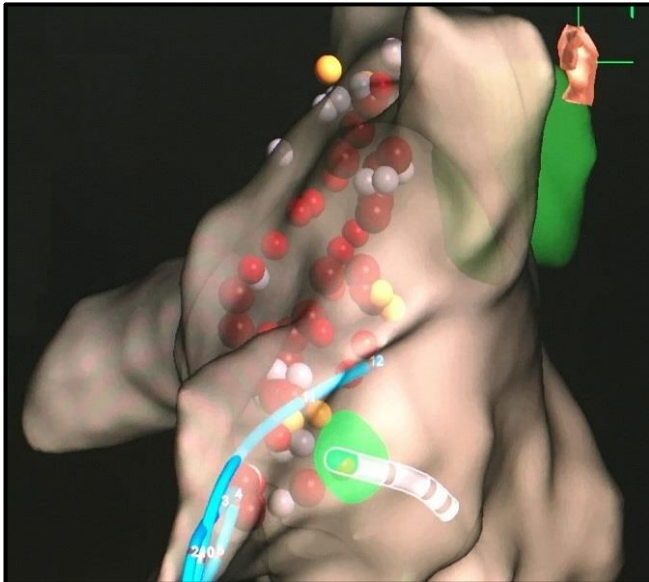


Figure 4: 3D representation of the heart mapped by the Advisor FL Circular Mapping Catheter of St. Jude Medical, Minnesota, USA during an ablation procedure at the Erasmus Medical Centre in Rotterdam. During this procedure scar tissue is made by heat at the tip to treat heart arrhythmia. The coloured dots show the already ablated locations.

All visualisation techniques show their images on a large 2D display. This results in limited 2D visual information of the work domain of the interventionist [39]. Misorientation often occurs between the intended actions of the interventionist and the shown movements of the catheter on the display [40].

Altogether, the visualisation of the cardiac environment is limited and it can cause orienting difficulties for the interventionist. Therefore, it should instantly be clear, for the interventionist, how to steer the catheter tip to a new location.

When a misorientation occurs, the interventionist should be able to restore the misorientation.

Handheld versus robotic systems – Robotic-controlled catheterization systems like the Niobe magnetic navigation system or surgical robotic systems like the Da Vinci robotic system (Intuitive Surgery, Mountain View, CA, USA) allow extended movability with comfortable user experience [41]. However, this is at cost of valuable space in the operation room by the accompanying peripheral equipment [41]. In addition, these robotic-controlled systems require huge investment costs and often adaption of the operation rooms [42]. The contrast is tremendous with handheld systems which require no additional space or adaption of the operating room and only a fraction of the costs [43]. The inclusion of electro-mechanical actuators in handheld devices should be taken into consideration since this will decrease the user experience by added weight and size of the instrument [44].

To extend application of the catheterization systems over surgical approaches, handheld devices are preferred over robotic systems. The costs are limited and adaptations to existing locations or systems are not required. On top of that, user experience of handheld systems can be improved by exclusion of electro-mechanical actuators in the handheld device.

Interventional tasks – Inserting the catheter from the groin to the heart is performed by the interventionist within a minute. The control challenges arise when the catheter tip is within the heart cavity. When analysing commonly applied ablation procedures, fundamental tasks are steering the catheter tip from location A, to location B. Orientation of the tip has no impact on the outcome. For the positioning of artificial heart valves, the catheterization system is feed-forwarded through the blood vessels up to the natural valve location. Influencing the orientation of the artificial valve is not possible with the currently applied catheters.

A rotational DOF around the shaft, does not have to be implemented in the design. Since the *Sigma* catheter is designed as a steerable sheath, during treatment a functional tool is passed through the lumen. This tool can be rotated around its central axis.

To extend the possibilities of interventional procedures, the orientation of the catheter tip needs to be integrated in the steerability of the device.

Deduction of the interventional environment – The operation room is a hectic and crowded environment by all individual specialists and

surrounding support systems. On top of that, visualising the working environment in the heart is limited. Together with the limited steerability this results in a complex interventional environment.

2.2. Interventionist

Prior to the procedure, the interventionist determines how the procedure will be executed. Pathways, methods and instrumentation are selected. During the procedure, the interventionist controls the instrumentation to perform a certain task. The interventionist's role and capabilities will be further explained in the following topics: double-handed, DOF in the hand, precise surgical tasks and human neuromuscular control.

Double-handed – Although technology of alternative input systems like eye and head movement tracking is emerging, these systems are not fully developed for clinical implementation [45]. In clinically available mechanical catheters, the primary hand of the interventionist is used to control the DOF in the catheter tip [12]. The second hand is used to push or pull the shaft in the longitudinal direction and is close to the insertion point to prevent buckling of the catheter shaft [12]. Therefore, using the catheter requires both hands of the interventionist.

When both hands of the interventionist are occupied to control the catheter, the control capabilities of the interventionist are limited. Single-handed control could allow the interventionist to perform additional functions with his second hand as, for example, applying contrast fluid into the patient's blood vessel.

DOF in the hand – The human hand consists of 22 DOF [46]. A single human finger is able to control three DOF [46]. The human arm can control seven DOF: three DOF in the shoulder, one DOF in the elbow and three DOF in the wrist [46].

To control 5 DOF of the catheter, only a selection of the 22 DOF of the fingers, wrist, arm and shoulder is needed. Simultaneous actuation of all DOF is difficult for the user, especially when DOF are interrelated to each other. Using an individual finger for each DOF could be a solution but may not be the ideal configuration.

Precise surgical tasks – Initially, surgical instruments are used during surgery to access the operation site. Then, high precision tasks, which are part of the procedure, come next. According to described surgical techniques for precise instrument handling, scalpels or tweezers are applied and held in a pencil grip [47,48]. Movements of multiple fingers and the wrist are

combined for accurate handling. The wrist is resting to reduce fatigue of the arm.

Since the pencil grip is commonly accepted as a reliable method to control instrumentation during high precision tasks, it should be considered to be included in the design.

Human neuromuscular control – The human hand is controlled by the human neuromuscular system. This contains two types of motor control, which are feedforward and feedback control [49]. Feedforward control is used when no perturbations are present. In order to execute the movements accurately, a well-developed internal model of interaction is acquired by extensive training [50]. When significant or unpredictable perturbations are present, feedback control uses sensory information to execute the movements [49]. The interaction of multiple muscles can result in fatigue which induces motor noise and perturbations [49].

For optimal functioning of the feedforward control, fatigue of the arm of the interventionist should be minimized. This can be achieved by limiting the amount of involved muscular systems or resting of the arm.

Deduction of the interventionist – During the intervention procedures both hands of the interventionist are occupied. Their hands and arm consist of an extensive manoeuvrable system controlled by a combination of feedforward and feedback control.

2.3. Instrumentation control

Without adequately designed instrumentation control, the interventionist cannot successfully perform interventional procedures. Two techniques to improve user experience using adequate instrumentation control are described as follows.

Multi-segment control – For multi-segmented instruments the input control method can be separated in parallel single-segment control (SSC) in which each segment has an independent controller, serial SSC in which each segment has a dependent controller or integrated SSC where only the distal segment has an independent controller [51]. A visual representation of the described input control methods is shown in Figure 5. Integrated SSC allows direct control of the end-point of the catheter [51]. This simplifies the control task of the interventionist since mentally combining several inputs is not required [51].

Integrated SSC should be incorporated in the design since it shifts the translation from input to output from the interventionist to the mechanical

system. This decreases the mental and physical demands of the interventionist which simplifies the task.

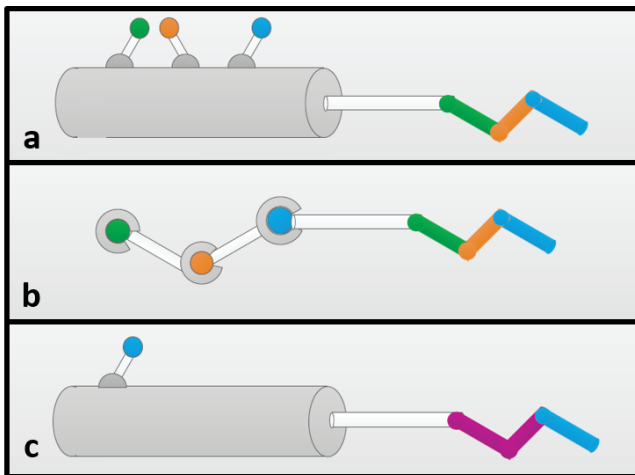


Figure 5: Input control strategies for multi-segment instruments. Controllers are shown at the left and steering segments are shown at the right. a) parallel SSC (Single Segment Control): one uncoupled controller for each steering segment b) serial SSC: one coupled controller for each steering segment c) integrated SSC: a single controller controls only the most distal (blue) segment. The purple segments position depends on the position of the distal segment. Adapted from Fan et al. [51]

Input-output coupling – Besides the number and interactional relationships of input controllers, coupling of input and output has a major effect on the control effort. According to a study of Fan et al. [52] positive input-output coupling can improve novice participant's task performance, reduce training time and their cognitive workload. Positive input-output coupling implies that the steering direction of the input controller is in the same direction as the catheter tip [52]. This applies also on the distinction between lateral and angular motions.

Additional simplification of the control method for the interventionist by coupling the input and output movements should be implemented in the design to further reduce the workload.

Deduction of the instrumentation control – Both integrated single segment control and positive input-output coupling attribute to the user experience of the input control method.

3. Design

3.1. Design requirements

The theoretical framework includes a wide range of information. This requirements subsection captures the essential functions into functional

requirements and elements related to sizes into dimensional requirements.

Functional requirements – Elements from the theoretical framework which are related to the functions of the design are described by the following functional requirements:

- **Five DOF steerability** – The end-point of the omni-steerable *Sigma* catheter tip consists of four DOF [26]. The fifth DOF is present in the longitudinal direction of the catheter, by pushing forward the entire shaft. The input control method needs to control these five described DOF.

- **Positive input-output coupling** – To improve user experience of the control method, a positive coupling between input of the handle and output of the catheter tip is required.

- **Single-handed** – To extend the capabilities of the interventionist during performing treatment, all five DOF should be single-handed controlled.

- **Handheld** – Due to the impact of robotic systems on operational space and costs, the design should be guided towards a compact handheld solution. Additionally, the design cannot be dependent of other equipment of the operation room like surgical tables or equipment waggon.

- **Pencil grip** – To control the catheter tip accurately a combination of thumb, index finger, middle finger and the wrist should be used, further referred to as the pencil grip. This pencil grip also includes resting of the forearm to reduce fatigue of the arm.

- **Mechanical actuation** – A mechanical solution for the input control method is required to limit complexity, weight and size of the instrument to improve user experience.

Dimensional requirements – Elements from the theoretical framework which are related to the sizing and range of motion are described by the following dimensional requirements:

- **Sigma catheter** – The input control method should not be designed solely for a single catheter but for cable actuated omni-steerable five DOF catheters. To evaluate the control method, the design will be adjusted to the *Sigma* catheter [26]. Each segment of the *Sigma* catheter must steer up to 90° resulting in approximately 25 mm lateral displacement [26]. The outer diameter of the *Sigma* catheter shaft is Ø3 mm with a lumen of Ø 1.5 mm and a total shaft length of 1 m [26]. Eight stainless steel steering cables (1x19 construction, stainless steel 1.4401, Engelmann, Hannover, Germany) of Ø0.25 mm must be used to steer the tip. The steering cables are covered by stainless steel guiding springs of inner Ø0.3 mm and outer Ø0.5 mm.

- **Heart cavity** – Since the input control method aims for manipulation within the heart cavity, the range of longitudinal motion is set to 50 mm.

- **Input range of motion** – The fingers and wrist of the human hand have a limited range of motion. The design should be adapted to the range of motions described by DINED anthropometry database [53].

An overview of the numerical design requirements is shown in Table 1.

Table 1: Overview of dimensional requirements

Description	Value
Total amount of DOF	5
Steerable segments	2
DOF per segment	2
Tip deflection per segment	90°
Longitudinal shaft movement	50 mm

3.2. Functional design

The required functions of the design are described using the design requirements and further elaborated by the theoretical framework. For easy resemblance with the theoretical framework the same categorisation is applied. A schematic

overview of the functional design is shown in Figure 6.

Interventional environment – Due to limited torsional stiffness of the shaft and the limited 2D visual information, the input-output coupling is often disturbed. In Section 2, it was already suggested to include realignment in the design. Since the system does not require a rotational DOF around the shaft, the control method is free to be rotated over the central axis to allow realignment of the input-output coupling. For proper functionality of the design, the user should be able to block this additional DOF.

Interventionist – During the interventional tasks no large perturbations are expected. Perturbations caused by fatigue are minimized by resting the forearm. Without the perturbations, feed-forward control of the task is feasible and allows the interventionist to feed the system with precise and direct input. Although the clinician should train to develop an internal model of interaction for the control task, similar previously obtained skills can accelerate the acquisition of the internal model of interaction [50]. Since the pencil grip has high resemblance with pen writing, the human internal model of interaction is already highly developed for these tasks. This reduces required training to familiarize the control tasks.

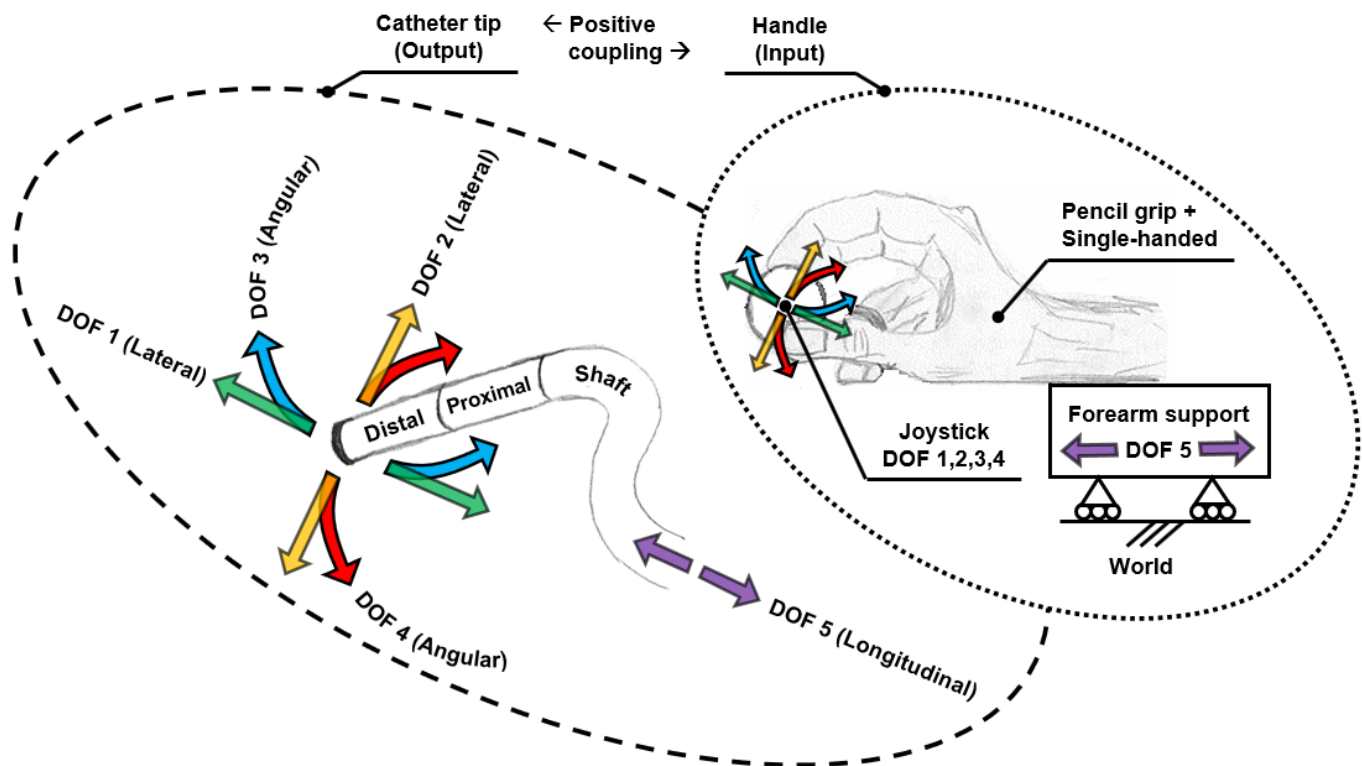


Figure 6: Schematic overview of the functional design. The basic elements of the output (catheter tip) are the steering segments (distal and proximal) and the shaft. The input (handle) consists of a joystick (which is used in the pencil grip) and a forearm support. The most trivial element to reach the project goal (improved task performance, with reduced workload) is the positive coupling between the DOF of the input and output.

On top of that, visual feedback of the location of the catheter tip is available to the surgeon to finetune the control action.

Instrumentation control – Integrated SSC strategy is preferred over serial or parallel SSC since it simplifies the control task for the interventionist while maintaining all available steerability [51]. Therefore, the use of multiple input controllers is not suitable. However, the pencil grip allows angular motions by mutual movement of the thumb, index finger and middle finger and lateral movements by the wrist on a single controller. Besides, the pencil grip allows precise movements when the forearm is rested to prevent muscle fatigue. However, longitudinal movement by the fingers is limited to approximately 15 mm where 50 mm is required [53]. Scaling is undesired since this reduces the control accuracy. Therefore, the wrist support should be movable solely in the longitudinal direction, just as in pen writing in which the wrist is relocated after a few letters. The design should be handheld and should be independent of equipment in the operational room. For now, as a demonstrative prototype, a base plate will be used as fixation of the wrist support to the world.

A positive input-output coupling should be designed due to the positive effect on task performance and workload [52]. When this input-output relation is disturbed by incorrect imaging or twisting of the shaft, re-alignment should allow restoration of the positive input-output coupling. The just described pencil grip allows this positive input-output coupling by independent angular and lateral input movements. A mechanical system to translate the input movements into cable displacement and subsequently the correct catheter tip end-point movements is required. This requires further analysis of the catheter tip construction.

3.3. Handle design

Once the functional design is set, a mechanical solution is sought to acquire a positive input-output coupling between the hand of the interventionist and the catheter tip.

Tip analysis – To correctly couple the input to the output, the tip design of the *Sigma* catheter described by Ali et al [26] is analysed. Each segment of the catheter tip can be steered by four pulling cables, one set of two cables for each DOF. When one cable is pulled, the tip bends to that direction and the counter cable should give way in equal proportion. Pretension is applied to the cable sets to minimize play. Perpendicular to these cables, two other cables can be pulled to

bend the tip in a perpendicular plane as the first set of cables. The distal segment is placed on top of the proximal segment but rotated 45° in order to pass the cables of the distal segment through the proximal segment. Combining movement of both segments results in lateral or angular movement of the catheter tip end-point.

Steering segments in series – The steering segments in series, with the 45° rotated orientation, results in a complex input-output relation between cable displacement and behaviour of the catheter tip end-point. To acquire a system in the handle, dealing with this relation, the segment in series design of the tip is mimicked in the handle. The handle is composed out of two bendable segments in series (including 45° rotated orientation between both segments).

At first, this method was evaluated in a 2D plane using two segments with two cables per segment. To acquire a positive input-output coupling, the output should steer in the same direction as the input. Steering lateral and angular of the input should correspond to an output as shown in Figure 7.

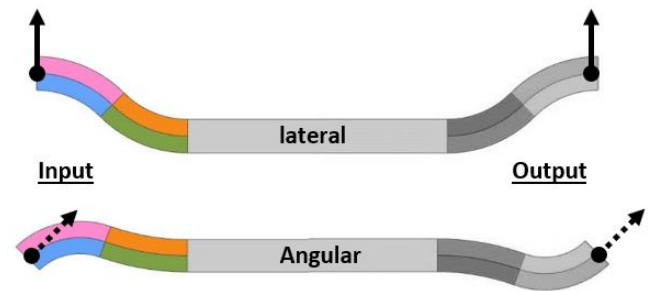


Figure 7: 2D evaluation of applying steerable segments in series at both handle (input) and tip (output). Each segment is controlled by two cables and each individual cable set is shown in a separate colour. Positive input-output coupling is visualised while steering lateral (top) and angular (bottom).

The cables of a set cannot be interchanged since this will block movability of the system. However, the set itself can be placed at the proximal or distal end of the shaft. When both sets are placed at the same side, the configuration is normal. If the set at the input is proximal and at the output is distal (or the other way around), the set is mirrored. The same normal or mirrored configurations are present between top and bottom position. These two possibilities result in four configurations. These configurations are evaluated in a lateral and angular input. For some configurations one of the tasks is correct, but none of the configurations result in correct input-output coupling for both lateral and angular steering. An overview of the configurations is shown in Figure 9.

The cables in the shaft are assembled in a Bowden construction which allows the shaft to bend in any shape. When the shaft is bent over 180°, cable displacement in the handle and tip match for both lateral and angular steering. Therefore, this cable configuration will be applied in the design. The 180° cable configuration is shown in Figure 8. An additional advantage of this handle design is that the handle forms a visual representation of the tip's shape. This can assist the interventionist with his mental visualisation of shape of the catheter tip in the cardiac environment.

Cable adjustment system – Since the cables are glued in the tip, continuous adjustment of the cables is required in the handle to equalize the pretension in the cables when needed. Since the cables are only Ø0.25 mm, clamping will damage or fracture the cables. On top of that, accurate cable guiding is also required to prevent overbending of the tip which can result in cable fracture. The handle should also be axially and rotationally stiff to limit undesired forces on the cables. Cable slack should also be minimized

since this will lead to play and dysfunction of the catheter.

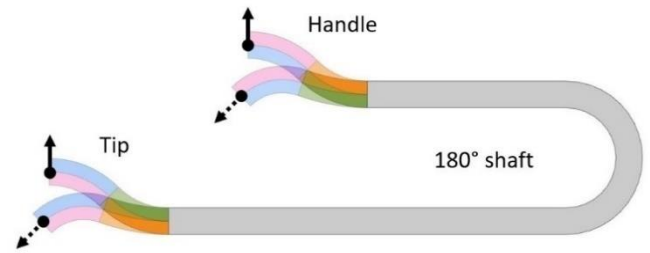


Figure 8: Cable configuration in 2D using the 180° bended shaft. Using this configuration, both lateral and angular steering directions of the handle and tip match.

Bending flexure – A suitable joint is needed to convert the movement of the handle to the desired cable displacements. Jelínek et al. [54] presented a classification of joints used in steerable instruments for minimally invasive surgery. Qualitative evaluation showed high potential for the bending flexure (Figure 11a and Figure 11b) for several merits related to the joint geometry and

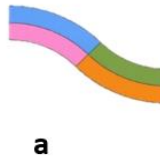

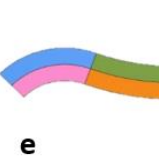
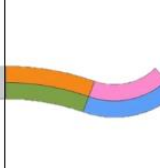
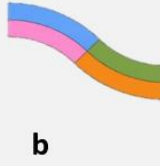

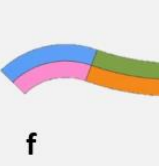
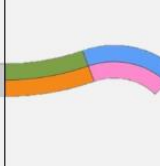



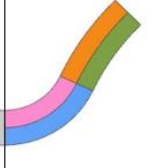


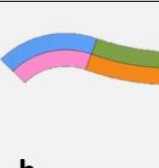
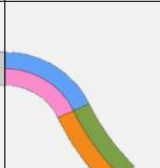
Configuration type	Lateral steering			Angular steering		
	Handle	Shaft	Tip	Handle	Shaft	Tip
Top / down = normal Proximal / distal = normal	 a	Incorrect		 e	Correct	
Top / down = mirrored Proximal / distal = normal	 b	Correct		 f	Incorrect	
Top / down = normal Proximal / distal = mirrored	 c	Correct		 g	Incorrect	
Top / down = mirrored Proximal / distal = mirrored	 d	Incorrect		 h	Incorrect	

Figure 9: Overview of cable configurations in 2D. The catheter design of four sets of cables results in four configuration types. Still, no configuration type results in positive input-output coupling for both lateral and angular steering.

motion. Since axial and transverse split is prevented, the joint is very accurately and axially stiff. These characteristics are crucial for cautious guiding of steering cables. Sadly, the basic shape is not torsionally stiff. Torsional stiffness is incorporated in the bending flexure design by adding more material off-centre without influencing the bending stiffness by a helix as shown in Figure 11c and Figure 11d. Combining two bending flexures in series (Figure 11e) results in the desired four DOF: two angular DOF and two lateral DOF.

Detailing of the handle – The basic shape of Figure 11 is further detailed in this paragraph to adjust to the overall design. For equal bending stiffness in both directions four helices are designed as shown in separate colours in Figure 10. Begin and end-points of the helix are shifted 45° degrees to further distribute the bending stiffness. Steering 45° with the bending flexures should result in movement within the range of motion of the human hand. Using the full 115 mm for the bending segments results in motions over the range of motion of the hand. A segment length of 40 mm is ideal. The spacing between the helices is determined to remain open, while bending the segment 45°.

The diameter of the central rod of the bending flexure defines for the greater part the bending stiffness. To determine the most appropriate diameter three test segments were printed (printing is described in more detail in the next section). The thickness of the helix is determined at 1.5 mm in the centre and increases outwards. The thickness cannot be smaller because then the cables break loose and increasing the thickness results in closing of the cable openings during printing. The variation in thickness is included to add more material off-centre to increase the

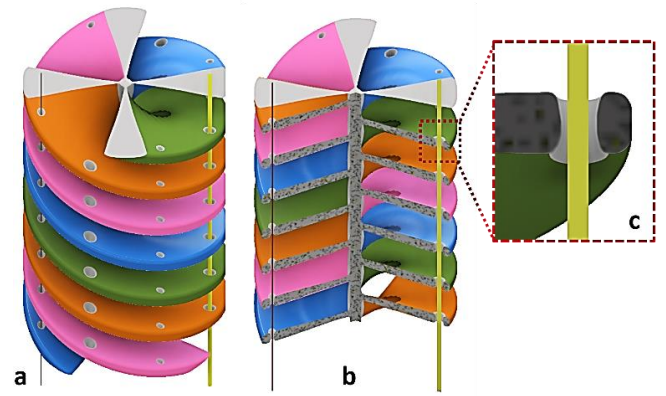


Figure 10: 3D representation of the handle design. a) Overview of a single bending flexure of the handle. Each helix is shown in a different colour (blue, green, orange and pink). A steering cable is shown at the left in red and a guiding spring in yellow on the right. b) Section view located at the cabling. c) Close-up of the perpendicular section view of the cable guiding opening.

influence on torsion stiffness with less influence on the bending stiffness. The outer diameter of the helix originates from the magnification factor between input and output as described in the next paragraph. This determines the diameter on which the cable openings are placed. The outer edge of the helix is designed to be flat to print the openings in a homogeneous layer. Exact dimensions of the helix are shown in Appendix B.

For the steering cables and guiding springs, openings are present through the entire structure. These openings are not straight but slightly curved to both nicely guide the cable when the structure is curved and to minimize closing of the openings during printing, as shown in Figure 10c. Between both segments an opening is required to stop the guiding spring while allowing passage of the steering cable. This resolution is not achievable

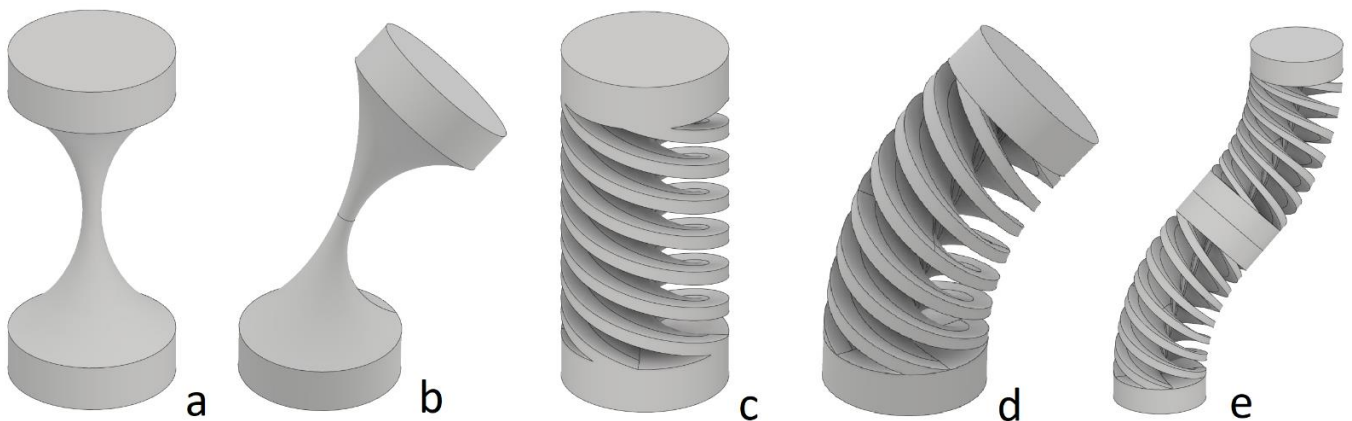


Figure 11: Joint design. a) Bending flexure design presented by Jelínek et al. [54]. b) Bending flexure bended to 45°, c) Bending flexure including helix, d) Bending flexure including helix bended to 45°, e) Two bending flexures in series bended to 45° in opposite directions.

with available additive manufacturing machines at the DEMO workshop (Delft University of Technology, Delft, The Netherlands). Therefore, these stops of the guiding spring are made of aluminium inserts (Bowden stop as shown in Figure 14).

Magnification factor – A magnification factor between input and output is required to overcome hysteresis between steering cables and guiding springs and the limited motion of the human hand. The distance in the tip between the centre of two steering cables of the same set is 2.35 mm. In the handle of the *Sigma* catheter, this distance is 20 mm. This results in a theoretical magnification factor of 8.5. Steering 45° with the joystick of the *Sigma* prototype results in 90° steering angle of the tip. So, due to hysteresis, a magnification factor of two is remained. To ensure that the bending flexures will not have to exceed 45° bending in order to steer the tip to 90°, the theoretical magnification factor is increased to 10.

3.4. Prototype design

The positive coupling between the input and output is achieved by a handle consisting of two bending flexures in series. To show the functioning of this design a functional prototype was fabricated at the DEMO workshop. However, this required detailing of the functional and handle design to a prototype design.

Handle fabrication method – Combining a screw shaped bending flexure with openings for cable guiding results in a complicated handle design in which additive manufacturing appears to be more suitable than conventional machining. Polymer materials can be used which are suitable for bending. Additive manufacturing also enables the handle to be fabricated in one piece, reducing alignment and assembly challenges. The additive manufacturing process is also referred to as printing.

Test segments – As previously described in the handle design subsection, test segments were printed to evaluate dimensions of the bending flexure. At the DEMO workshop a Perfactory 4 Mini XL printer (EnvisionTEC, Gladbeck, Germany) is available. This printer uses R5 photopolymer material (EnvisionTEC, Gladbeck, Germany) which is designed for functional parts due to its mechanical and fabricating properties [56]. The test segments are shown in Figure 12. The dimensional differences are hardly visible but exact dimensions are shown in Table 2.

The three test segments were printed with various diameters of the central rod to determine the bending stiffness. Different opening diameters

allows evaluation of the minimum printing size. The openings were evaluated by passing through both the steering cables and the guiding springs. At the bottom of the steering segment, a gap is present where the rotation stop knob fixates the rotational freedom of the steering segment. Using the elementary house and the test segments, the most suitable dimensions for the gap were determined.

Table 2: Overview of dimensions of the test segments. The shaded boxes represent the most suitable dimension.

Test segment	a	b	c
Central rod [mm]	Ø1.0	Ø1.5	Ø2.0
Steering cable opening [mm] (Ø0.25 mm)	Ø0.4	Ø0.55	Ø0.7
Guiding spring opening [mm] (inner Ø0.3 mm, outer Ø0.5 mm)	Ø0.7	Ø0.85	Ø1.0
Gap with [mm]	5.0	4.0	3.0
Gap depth [mm]	2.0	1.5	1.25

Print processes and support – The Perfactory printer uses light to harden the material from liquid to solid. After hardening a layer, the printed structure was lifted to allow new liquid photopolymer to flow underneath the structure. The handle was printed from the housing to the ball-end to acquire circular openings. Since the bending flexure allowed bending of the handle during the printing process, the handle end-point was not exactly restored back to the correct position. This resulted in printing inaccuracies as can be noticed in Figure 13. Support was added

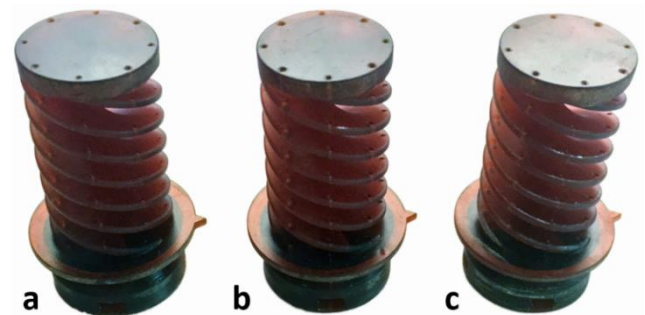


Figure 12: Test segments a, b and c fabricated with different dimensions. Dimensions vary in diameter of the central rod, steering cable opening, guiding cable opening and with and depth of the gap for the rotation stop knob. This image shows the test segment and indicates the minuscule variance in dimensions of the test segments.

to the design to increase the bending stiffness of the handle which resulted in a correctly printed handle. The support was removed after the printing process using a scalpel and sandpaper. Before assembly, the cable openings in the handle were checked by passing through the (twined) steering cable. By pushing and pulling this cable, printing inaccuracies were rubbed off the openings which improved smooth cable guiding. To remove all small debris from additive manufactured components, the parts were placed for a few minutes in an ultrasonic cleaner. This bath filled with isopropanol vibrates at a high frequency which removes debris from the component.

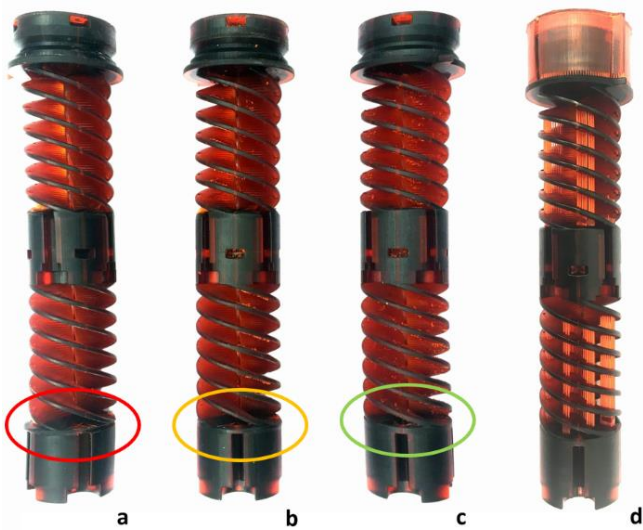


Figure 13: The handle printed from the top to bottom. a) First printing trial (no support) resulted in a bulge at the bottom. b) The second printing trial (minimal support) reduced the bulge. c) Final printing trial without a bulge using full support as shown in d).

Threads – Tapping thread directly in photopolymer results in fragile inner threads. Thread inserts (HELICOIL, Böllhoff, Bielefeld, Germany) were placed within photopolymer parts to provide stronger threads by improved force distribution over more thread windings.

Cable adjustment system – Due to the additive manufacturing, the cable adjustment system can be incorporated in the handle without extra production effort. Since the handle can be adapted in many ways, a continuous adjustment using standardised bolts, washers and nuts is used as shown in Figure 14. The hexagonal shape of the nut is also applied in the handle to restrain rotation about the central axis of the nut. A washer is applied to reduce wear and friction between the handle and the bolt. To allow more grip on the bolt

for manual usability a printed bolt knob was designed.

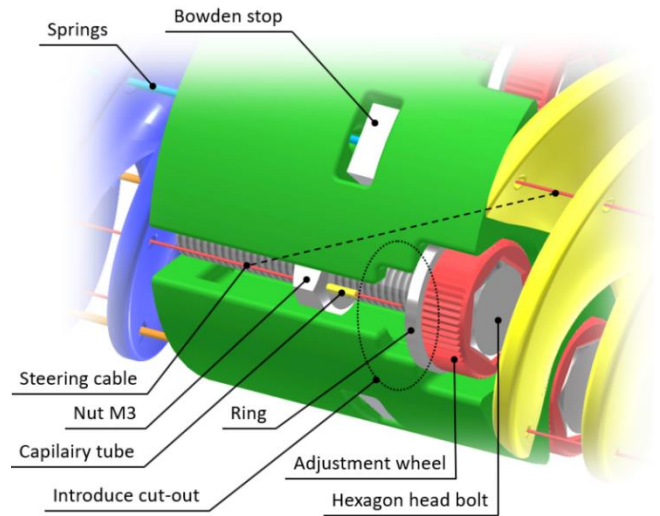


Figure 14: Close-up view of the artist impression of the cable adjustment system

Control point – The handle is held in a pencil grip and rotated by the thumb, index finger and middle finger. A ball of Ø45 mm is designed as control point, since the clamping of the fingers can freely be adjusted at the circular shape. The distance between this control point and the wrist support is set to 115 mm, determined by average human hand sizes [52]. The horizontal cross-section of the wrist support is set to 60 mm (width of the arm) x 80 mm (length of the arm).

Housing – Initially, the wrist support was designed from aluminium plates assembled by alignment pins and bolts. The design was adapted for additive manufacturing to reduce production and assembly time. Besides, the top of the wrist support can easily be adapted to any desired curved surface for convenient support when printing is used.

Printing of the handle and housing allows an indicator on top of the handle as shown in Figure 15. At the housing, indicational grooves are set each 22.5° and an end-stop is placed at 180° to prevent twisting of the cabling inside the housing. The re-aligning can continuously be constrained by two adapted M4 socket head screws with 90° ends which fall into a v-groove in the handle. The printed knobs enable manual usability.

Longitudinal motion – The housing with wrist support has to be guided during the longitudinal motion. Various types of linear guides are commercially available for such applications. The exact guide applied is further clarified in the next section.

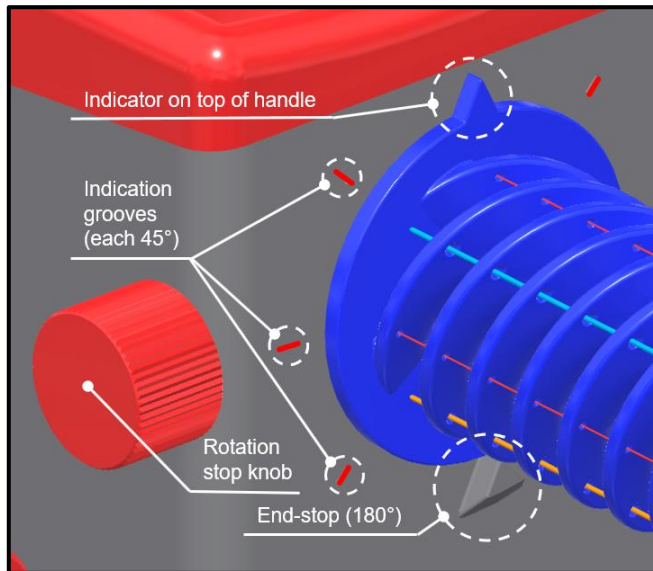


Figure 15: Close-up view of the artist impression of the housing and handle. An indicator on top of the handle indicates the angular rotation of the handle using grooves in housing. The rotation stop knob can be tensioned to block the angular rotation of the handle.

To enable longitudinal motion, the shaft should be connected to the housing. Because clamping the entire shaft will damage the cabling, the design was adapted to guide the cabling outwards. This allows clamping of the lumen by rubber disks.

The longitudinal motion of the wrist support was initially designed by two hardened steel shafts fixed in the housing as shown in Figure 16. The shafts slide over brass inserts in the aluminium base frame. During the first fabrication attempt, the position of the shaft in the house was slightly off due to printing inaccuracies, which required increasing the fit between the shafts and the brass inserts. This wide fit resulted in pitching of the housing and accordingly jamming of the guiding. To position the shaft in the housing more accurately, a new house was printed and openings were milled but still, the guiding jammed.

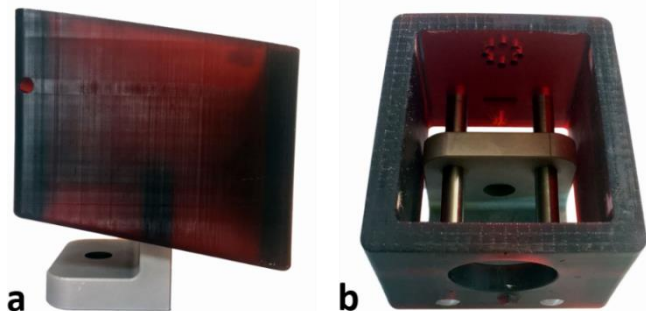


Figure 16: Initial design of the housing using steel shafts and brass inserts. a) Side view. b) Front/top view.

Since this design option resulted in unsuccessful prototypes a proven commercially available solution was sought and found in standardised slide bearings. The linear guide systems of IGUS consist of a polymer wagon which slides in an aluminium guide rail [55]. This combination results in low friction, wear-resistance and self-lubricating linear guide [55]. Costly ball bearing linear guides with even lower friction coefficients are available but due to costs and sufficient friction properties of slide bearings the latest option was chosen. A combination of guide rail (IGUS Drylin NS-01-40, Cologne, Germany) and wagon (IGUS Drylin NW-01-40, Cologne, Germany) was selected which allows solely longitudinal movement. End caps (IGUS Drylin NSK-40) clamped to the rail prevent the wagon to exit the rail. The wagon was bolted to the house.

Guiding tube – Longitudinal motion of the wrist support should correspond to longitudinal motion of the catheter shaft. Since this motion is not directly applied at the catheter entry point, pushing forward the catheter will result in deflection of the catheter shaft outside the patient. To prevent this buckling, a guiding tube is used to guide the catheter shaft from the wrist support to the catheter entry point. Available tubing in silicon and PVC for the guiding tube was examined for different dimensions. PVC tubing with inner Ø5 mm and outer Ø8 mm appeared to guide the shaft the most adequately. The shaft smoothly glided through the guide tube and the guide tube did not buckle. The length of the tubing should be adapted to the procedure since the shaft's length is fixed but the pathway in the patients can be variable. For the examination a tubing length of 200 mm was used. The guiding tube is clamped in a printed part (guide clamp) which is fixed to the base plate by screws.

Shaft clamp – The lumen was clamped to the lumen clamp through rubber disks. The disks were die-cut from a rubber plate using a custom-made tube with sharp edges. To allow assembly of the shaft, some clearance was left between the lumen and outer shaft. This causes play when pushing the shaft forward using the lumen. Therefore, an additive manufactured component was added to the design (shaft clamp). This component fixates the outer shaft to the housing which eliminates the play of the lumen.

An exploded view of all components is shown in Figure 17.

4. Prototype

4.1. Basic components

In order to examine the proposed design, a demonstrative prototype, subsequently referred to as *Epsilon* catheter, was fabricated and assembled. This prototype shows the practical functioning of the design and allows evaluation of user experience. Technical drawings of the prototype are shown in appendix B.

Some proposed design choices functioned different than was expected. This required reconsideration of the design and further prototyping. At first, the fabrication of the main components of the prototype is described.

Tip and shaft – The tip elements are fabricated similar to the *Sigma* catheter. Also, the same steering cables and guiding springs are used [26]. The outer shaft material is replaced by the outer sheet of FT038-BK (Thorlabs, Newton, USA) furcation tubing, outer Ø3.8 mm. This material is smoother than the shaft material of the *Sigma* catheter which improves gliding through the guiding tube. The inner tube of FT030-BLUE (Thorlabs, Newton, USA) furcation cable, inner Ø1.0 mm, is used as lumen because of enhanced buckling resistance in respect to the lumen of the *Sigma* catheter.

Base plate – The prototype is assembled on a 5.0 mm aluminium (7075-T6) base plate which can be connected to a tripod or table depending

on the evaluation setup. The base plate contains tapped openings (M4) to attach the linear guide as further explained in the following paragraphs. Two slots are milled for adjustable fixation of the guide clamp to the base plate using M3 socket head screws.

Additive manufactured components – The house, lid, lumen clamp, shaft clamp, handle, ball, rotation stop knobs and bolt knobs are fabricated by additive manufacturing using the Perfactory 4 Mini XL printer. However, during the fabrication process, R5 was temporarily out of stock at the DEMO workshop. Therefore, the house was made from HTM 140 V2 (EnvisionTEC, Gladbeck, Germany) which is designed as casting material. Due to the intended rigidity of the housing, HTM 140 V2 was also suitable. The designed house did not fit within the printing area of the Perfactory 4 Mini XL printer (115 x 72 x 220 mm) which required to manufacture the lumen clamp separately. The lumen clamp is bolted (M3) to the house and is aligned by an edge at the housing.

Additional components – The Bowden stops were made from aluminium (7075-T6) using drilling and wire Electrical Discharge Machining (EDM). Openings in the M3 hexagon nuts for the cable adjustment system were made by small hole drilling EDM. The head of a M3 hexagon head bolt was glued (Second Glue, Bison, Goes, NL) to the ball and was subsequently bolted to the handle.

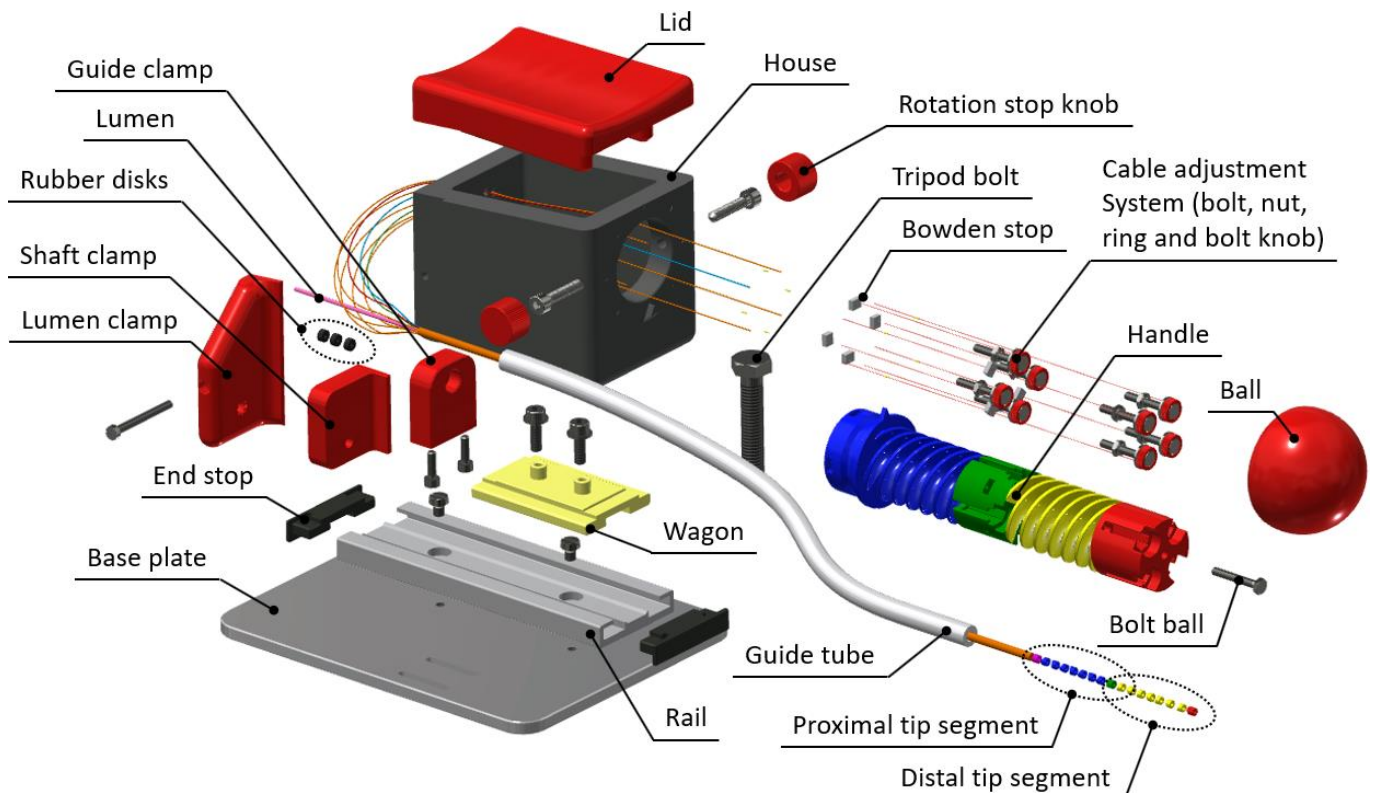


Figure 17: Exploded view of the artist impression of the prototype design.

4.2. Assembly

When all components were fabricated the prototype was assembled. Since there was minimal play between the steering cables and guiding springs, dust from the environment could already badly influence the prototype by adding friction. Therefore, the cabling was assembled on special fabric and the prototype was stored in a closed off box.

Cabling – At first the steering cables and guiding springs were cut to length. The steering cables were passed through the tip segments under a microscope using tweezers and subsequently glued to the tip. After 24 hours, the glue is completely hardened and the guiding springs were placed over the steering cables. Steering of the tip was tested by manually pulling the steering wire while careful pinching the guide spring to the table. Then the lumen was placed over a small bulged of the proximal tip component. The cables were taped at the lumen and passed through the outer shaft. Then, the assembled shaft was passed through the guide clamp and shaft clamp. The lumen clamp has a central opening for the lumen and individual openings for each steering cable. Next, the top of the tip was marked and again manually steered. It is important to place the correct cable through the correct openings in the lumen clamp, housing and handle. Once this was verified, the tip was placed over the table edge and pulled downwards by the gravitational force. The cable to steer the tip upwards, against gravity, was pulled until the tip was straight. Then the cable was connected to the nut using soldering the capillary tube. Then, the handle was rotated 180° and the counter cable was pulled and connected and so on. Using this pulling against gravity all play is forced out of the system.

Introduce cut-out – The cable adjustment system (bolt, nut, ring and bolt knob) of the distal segment was introduced from the distal end. At the proximal segment, the distal segment obstructed placement of the cable adjustment system. Therefore, at the knob side a cut-out was made in the handle in order to introduce the cable adjustment system from the lateral side when the nut is screwed to the knob side (shown in Figure 14).

Gluing – The shaft clamp was glued (Second Glue, Bison, Goes, NL) to the outer shaft and the housing. During this gluing, the base plate was clamped in a bench vise with the handle pointing downwards. The glue was placed drip by drip through an injection needle. When accidentally too

much glue was added, it flowed downwards on the outside of the shaft and not inside the shaft.

Reconnect steering cabling – The steering cables were, for a certain moment, fixated in the handle using pinching of a capillary tube at the cable (described in the next subsection). This caused sudden loosening of the cables. To reconnect the cable, the cable was pulled back from the handle and housing. Then, carefully peeling off the guide spring from the steering wire by pushing a nail between two windings was possible. Then the guiding spring was cut off. This resulted in a shortened U-turn of the cable at the back of the house but allowed to introduce the cable again through the handle. Then, the cable was pulled to force play out of the system and reconnected by pinching a capillary tube.

4.3. Steering cable fixation

The Ø0.25 mm stainless steel steering cables (1x19 construction) were glued (Griffon Combi Metal Blister, Bison, Goes, NL) in a slit at the tip of the *Sigma* catheter. Back in the handle, cables were clamped between two plates. A screw was used to loosen and clamp the cable. This clamping fixation method showed to be reliable but adjustments damaged the cables. The cable adjustment system in the *Epsilon* catheter was designed to continuously adjust the tension in the cables without damaging the cables. A bolt nut construction was designed with the cable glued to a slit in the nut. The same glue as for the tip connection was used. Unfortunately, this fixation immediately broke when steering the handle. To determine a more reliable fixation, several possibilities were verified in an experimental setup.

Experimental setup – According to the fabricant of the steering cables, the minimum breaking load is 59 N [57]. This was verified using stainless-steel clamps. From an obsolete *Sigma* prototype, cables glued in the tip were tested to verify the glue method. Another common applied fixation method for cabling is pinching a capillary tube. A Ø0.3 mm hole was drilled in the nut through which the cable can be introduced. The capillary tube (outer Ø0.50, wall thickness of 0.10 mm and a length of 2.0 mm) will fixate the cable behind the nut. To prevent lateral displacement of the capillary tube in respect to the hole, a Ø0.55 mm hole (depth of 0.5 mm) was drilled in the nut. Soldering was also tested by soldering the cable just behind the capillary tube. Flux (S-39-RVS, Bison, Goes, NL) was added to provide a strong bond between the solder tin and the stainless steel.

At one end, the cable clamps were placed in a bench vise. At the other side a mechanical force gauge (SS-LG-20N, Chatillon, Largo, USA) [58] was used to pull the cable vertically and measure the applied force at the breaking load, as shown in Figure 18a. For the capillary tubes, a stainless-steel spare part with $\varnothing 0.3$ mm openings was used as top fixation. For accuracy, the measurements were intended to be repeated five times.

Table 3: Results from cable fixation experiment. The steering cables were loaded by manual pulling. The maximum breaking load [N] was measured by a force gauge. Using the first fixation method, clamping using the stainless-steel clamps at both sides, was performed as benchmark. Using the second method, the steering cable was clamped at the bottom using a stainless-steel clamp and glued in a slit (just as the tip) at the top. Using capillary pinching a capillary tube was pinched over the cable at the top. Using capillary soldering the steering cable was soldered to the capillary tube at the top. M1-M5 stands for measurement 1 to 5. Symbols are listed in Appendix A.

Breaking load [N]	M1	M2	M3	M4	M5	μ	σ
Method							
Stainless-steel clamps	58	57	53	56	53	55	2,3
Glue	42	41	43	-	-	42	1,0
Capillary pinching	32	30	36	30	27	31	3,3
Capillary soldering	53	57	53	56	53	54	1,9

Results – The initial test of the breaking load resulted in 55 N on average over five measurements. It was observed that the cable broke close to the clamp. In the tip with glued cables, only three cables were left. On average this resulted to a breaking load of 42 N. The cable broke twice out of the glue, as shown in Figure 19a. The location where the outer cables of the 1x19 construction were glued, is still present in the remained glue. One cable was broken half way. Using the capillary pinching method, the average breaking load was 31 N. All cables broke at the pinch location as shown in Figure 19b. The end of the cables is visible on the left but no cable sticks out at the right. Using the capillary soldering method, the breaking load was 54 N. All the cables broke out of the soldering. Just like the glue method, the print of the individual cables was still noticeable. A close-up view of the soldering method can be observed in Figure 19c. The solder was placed over the cable and capillary tube and probably also crept into the tube. An overview of the individual measurements, mean breaking load

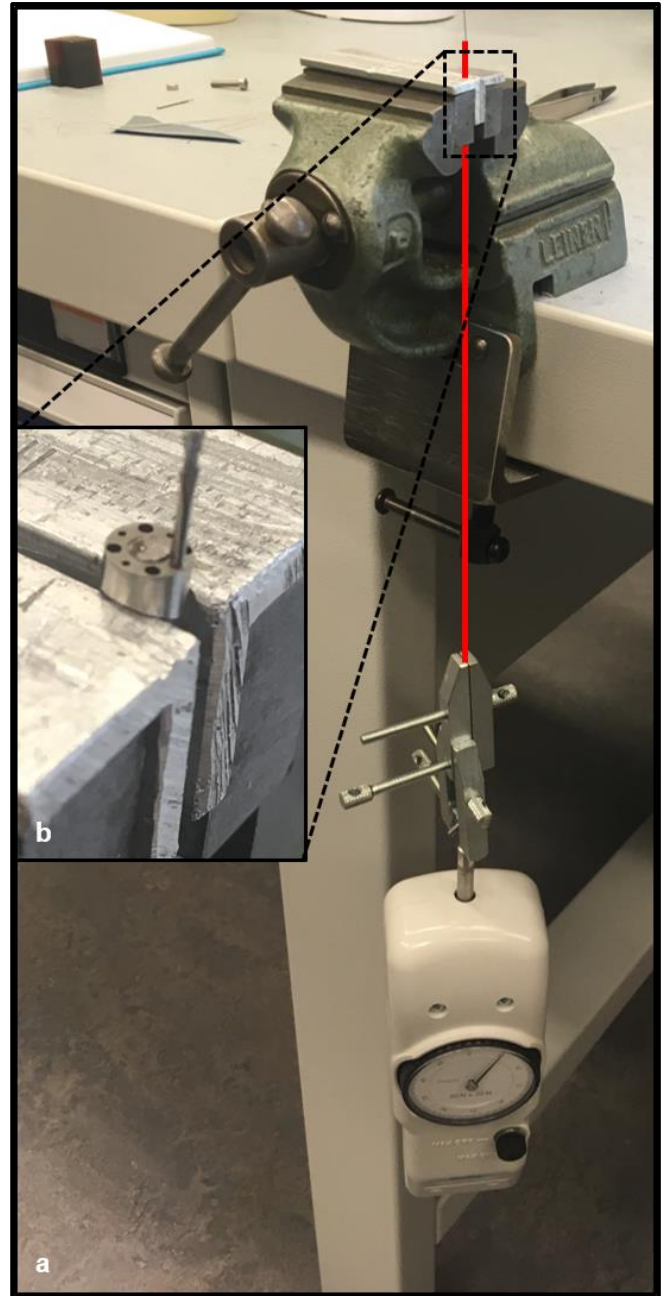


Figure 18: Overview of cable fixation experiment setup. a) Elements from top to bottom: bench vise, steering cable (shown in red for visibility), stainless-steel clamps and a mechanical force gauge. The setup is vertical since this allows initial tensioning of the cable by the gravitational force. Additional force is applied by manual pulling the force gauge downwards. b) The close-up at the bench vise shows a stainless-steel spare part with $\varnothing 0.55$ mm openings for fixation of the capillary tubes.

and standard deviation of the breaking load can be found in Table 3.

Discussion – Using the stainless-steel clamps, the theoretical minimum breaking load was almost achieved. This suggested that the clamping method was close to the optimal clamping

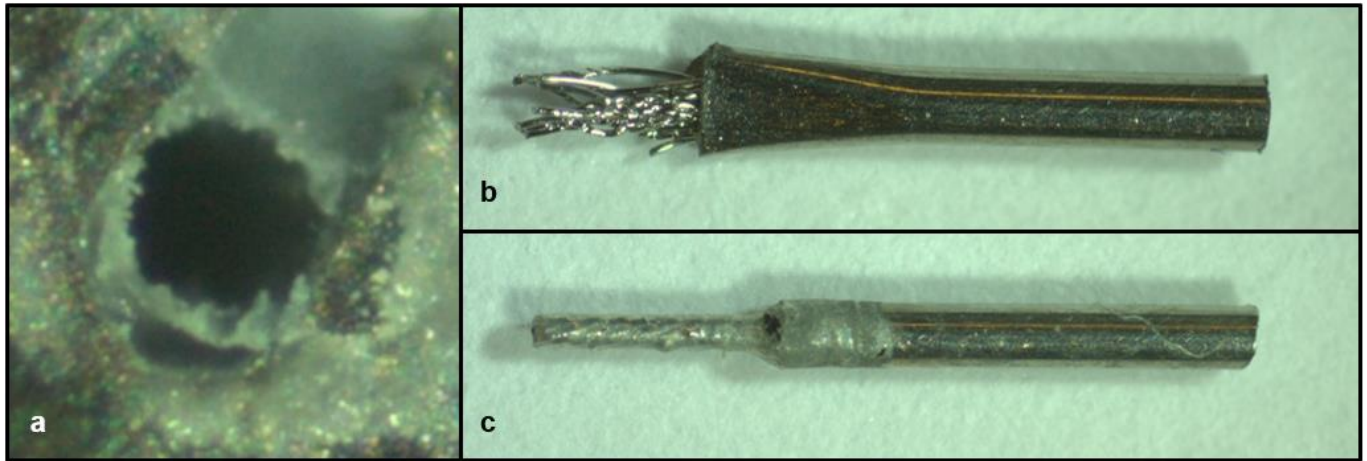


Figure 19: Close-up view of test components after the experiment. a) Top view of the hole in which the steering cable was glued for the glue method. The outline of the individual cables of the steering cable assembly are still visible. b) Using the capillary pinching method, the capillary tube was pinched to clamp the steering cable. The load applied to the steering cable was towards the right. This is because of the circular shape of the capillary tube which fits into a hole in the adapted nut. From the picture can be noticed that the cable is broken inside the capillary tube. c) Using the capillary soldering method, the steering cable was soldered to the capillary tube. The load was applied in the same direction as the pinching method and the steering cable is also broken inside the capillary tube.

method. The glue method loosened earlier. Due to the larger span in the adjustment system, the cable can laterally move and probably peel off from the slit. Therefore, in the actual tip design, a larger clamping force can be expected. The pinching method appeared to be insufficient. Perhaps, the pinching method fixates a few cables instead of the whole set. When pulling the cable, only these cables are exposed to the force and will break. This reduces the overall strength of the cable construction. Using the capillary soldering method approximately the same breaking load as the steel clamps was observed. The soldering captured the whole cable construction in position instead of only a few individual cables. The standard deviation over both methods is approximately 4% of the breaking load and can therefore be concluded as reliable. Additionally, the lowest breaking load for both methods is 53 N.

Conclusion – Using stainless-steel clamps or capillary soldering results in approximately the same average breaking load, close to the theoretical minimum breaking load. However, soldering allows a more compact solution which allows continuous adaption of the cable tension. Therefore, the most appropriate clamping method of the steering cables in the *Epsilon* catheter prototype is capillary soldering.

4.4. Functionality test

A proof-of-concept test of the *Epsilon* catheter was performed to confirm the behaviour of the proposed design. The user was able to steer the catheter tip in all four DOF up to 45° per segment as shown in Figure 20. The intended magnification

factor of two was reduced to one. Longitudinal movement of the catheter over the full 50 mm was feasible. The housing was smoothly guided by the rail and was pushed through the 200 mm transparent guiding tube. Re-aligning of the steering orientation functioned adequately and did not noticeable affect the steerability of the catheter tip.

Initially it was planned to connect the base plate to a tripod or clamp the base plate to a table. During the functionality test it seemed that an anti-slip mat between base plate and table was sufficient to maintain the base plate at the desired location.

5. Evaluation

5.1. Experimental design

Improved task performance with reduced workload of the input control method of the *Epsilon* catheter, is compared to the input control method of the *Sigma* catheter in an experimental setup. In this section the experimental design and setup is described, results are presented and processed using statistical techniques.

Catheter prototypes – Both the *Sigma* and the *Epsilon* catheter were constructed using an identical shaft and tip. In addition, the longitudinal motion of the *Epsilon* is restricted and the non-dominant hand was used for the longitudinal push/pulling of the shaft. This allowed fair comparison of both input control methods. The *Sigma* catheter tip was steered using user's thumb and index finger. The *Epsilon* catheter tip was steered using user's fingers and wrist.

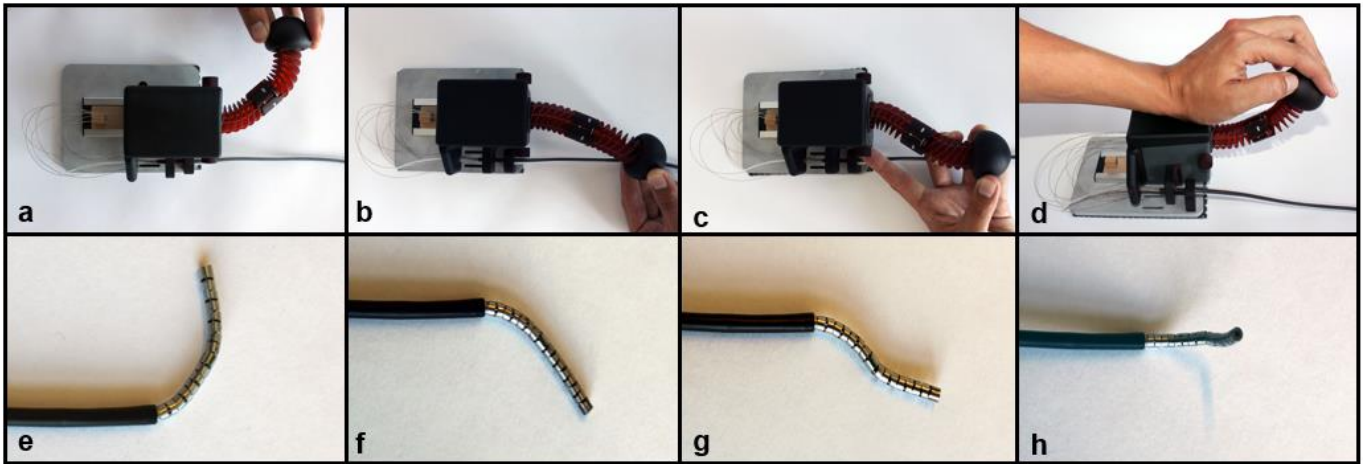


Figure 20: The Epsilon catheter handle (a-d) and corresponding tip's shapes (e-h). From left to right: steering both segments (a/e), steering only proximal segment (b/f), lateral steering (c/g) and vertical steering (d/h). The forearm is not placed on the wrist rest as intended due to visibility of the handle.

For the experimental setup, blunt 15 mm long stainless-steel pointers were added to the tip of both catheters. The function of these pointers will be described in the next paragraph.

Experimental setup – The experiment was prepared in a within-subject design to compare both conditions (condition 1: Sigma | condition 2: Epsilon) with a defined number of participants. The participants encountered both conditions, which induced learning curves and other carry-over effects. These effects were reduced by counterbalancing the conditions order and providing obligated practice sessions before conducting the task. An overview of the experimental setup is shown in Figure 23.

Before conducting the experiment, the participants received an informed consent form (Appendix C) in which the purpose of the research, procedure, risks and benefits were explained. Then, the participants received an instruction form (Appendix D) with a task description and usability instructions of the prototypes. Prior to the task, the participants were given two minutes to get acquainted with the prototype, focussed on manoeuvring the prototype and reaching targets.

An intake questionnaire (Appendix E) was carried out before the task with general information about the participant like: gender, age, educational phase, study direction, dominant hand and video game experience.

Experimental task – The task consisted of contacting targets using the pointer attached to the catheter tip. The task time started when target 1 was contacted. A correct hit was indicated by a buzzer. Then, the participant proceeded to target 2, 3, 4 and again target 1. The targets, insertion block and grip of the secondary hand is shown in

Figure 21. Technical drawings of the experimental setup are shown in Appendix F.

It was mentioned to the participants that they should try to hit the targets as fast as possible while handling the prototypes carefully. This trade-off between speed and accuracy is comparable with application of catheters during treatment. It was also mentioned that not only the task completion time but also the numbers of errors were recorded.



Figure 21: Close-up of the experimental setup. The four targets are indicated by a number. The secondary hand is placed in front of the insertion block to push and pull the shaft.

The targets consisted of Ø5 mm openings in a 1 mm thick polymer plate placed at 65 mm (50 mm from the tip and pointer and 15 mm additional space) from the insertion block. Behind the openings in the polymer plate, stainless steel plates were placed with a 1.5 mm slit as shown in Figure 24.

When the pointer connected the stainless-steel plates, a signal is measured by the Multifunction I/O Device (USB-6008, National Instruments, Austin, USA) [59] and stored on a laptop (Elitebook 8570w, Hewlett-Packard, Palo Alto, USA). A block scheme of the electrical circuit is shown in Figure 22. The blunt end of the pointer enables contacting two plates at various orientations. The insertion point was taken as central reference point and the targets were placed 12.5 mm above, below and sideways. This is half of the maximum achievable lateral displacement of the tip. Since it was unclear where the pointer was located when the

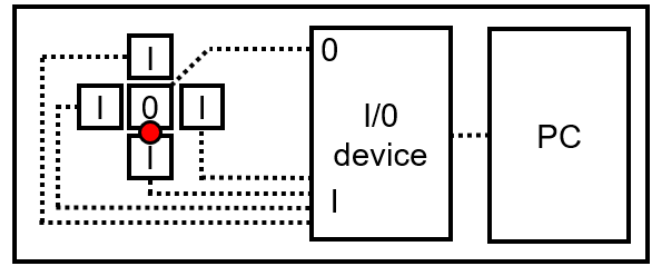


Figure 22: Simplified block scheme of the electrical circuit of the experimental setup. Once the catheter tip (shown in red) connects two steel plates (squares noted with 1 or 0) the I/O device sends a signal with a time stamp to the PC. Afterwards target-to-target times can be calculated.

measurement started, the task completion time started when the first target was hit. The targets were marked with a number and the participants contacted the targets in the fixed order from one to four and at last the first target again. This results in four target-to-target time intervals (one trail).

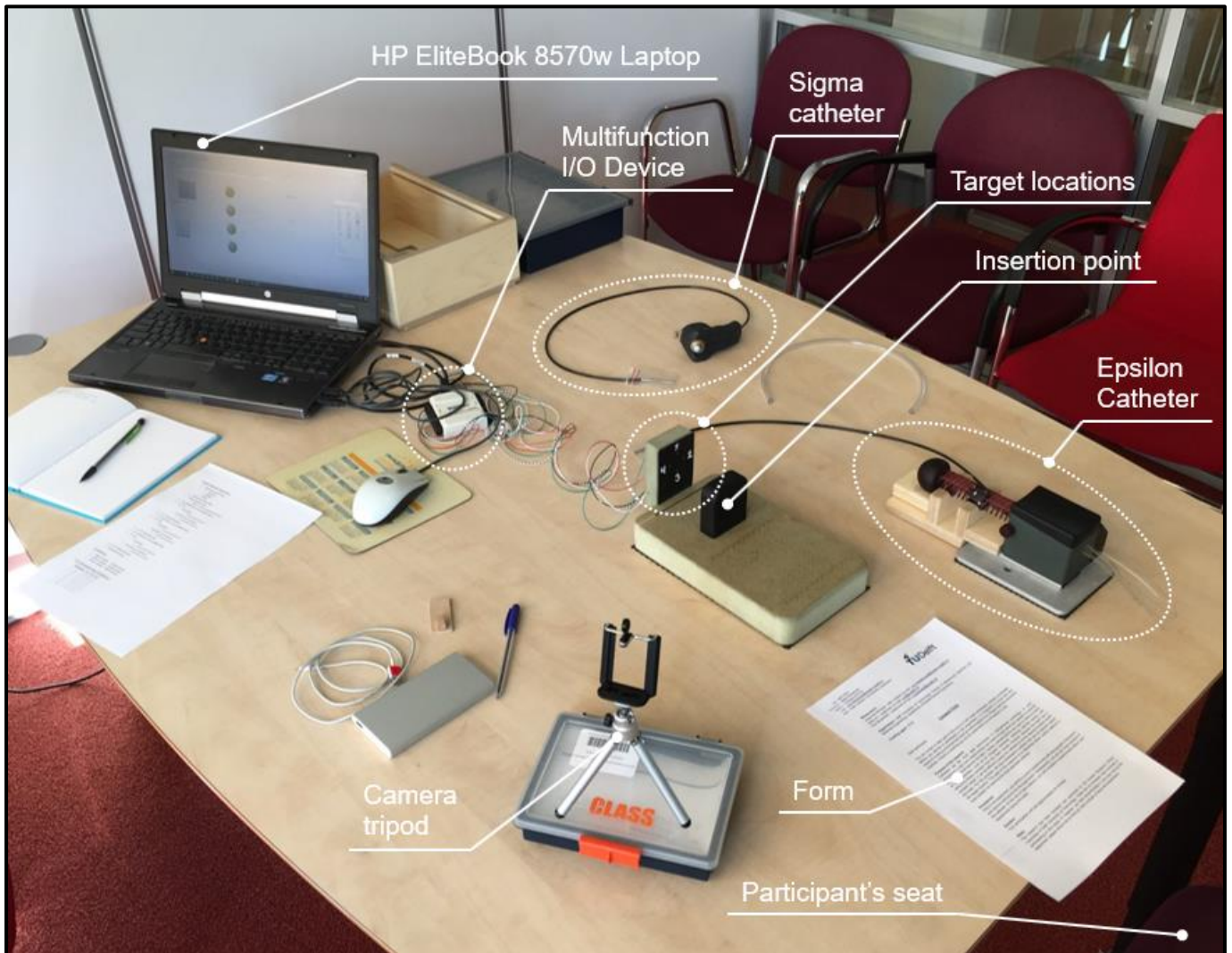


Figure 23: An overview of the experimental setup. The participant is seated on the right, a camera is used to record the experiment. Data is measured by the multifunction I/O device and stored on a laptop.

After this sequence, the measurement was reset and the trial was repeated twice to obtain twelve target-to-target intervals. These repetitions are required to increase the test-retest correlation [60]. The task is video recorded (iPhone SE, Apple, Cupertino, USA) to allow afterwards clarification of outliers or measurement errors.

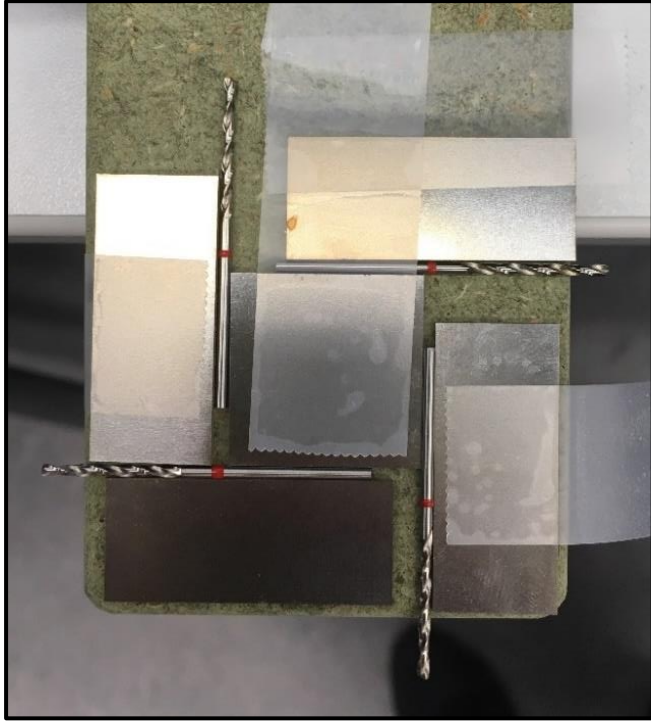


Figure 24: The experimental setup under construction. Stainless steel plates were glued to a fibreboard back plate. In order to acquire an exact slit of 1.5 mm, drills of $\varnothing 1.5$ mm were used during the assembly.

Self-reported measure – Using the target-to-target time intervals, the mean task completion time are calculated. The video records allow counting of attempts to reach the targets. These measures give insight in the task performance. To also get insight in the effort and mental or physical load of the task, a self-reported questionnaire was carried out after each condition.

A commonly used self-report questionnaire in human suspect research is the NASA – Raw Task Load Index (TLX) questionnaire [61]. Each of the six subscales (mental demand, physical demand, temporal demand, performance, effort and frustration) are rated from -10 to 10. High scores indicate a high task load. The total TLX score will be calculated unweighted [62]. The exact form used in the experiment is shown in appendix G.

When both conditions were conducted, a final questionnaire was carried out. The participants were asked which prototype they preferred and which prototype was the easiest, fastest and most precise to steer. At the end of the form,

participants were asked to leave comments regarding the prototypes or experiment. The exact form is shown in Appendix H. An overview of the experimental procedure is shown in Figure 25.

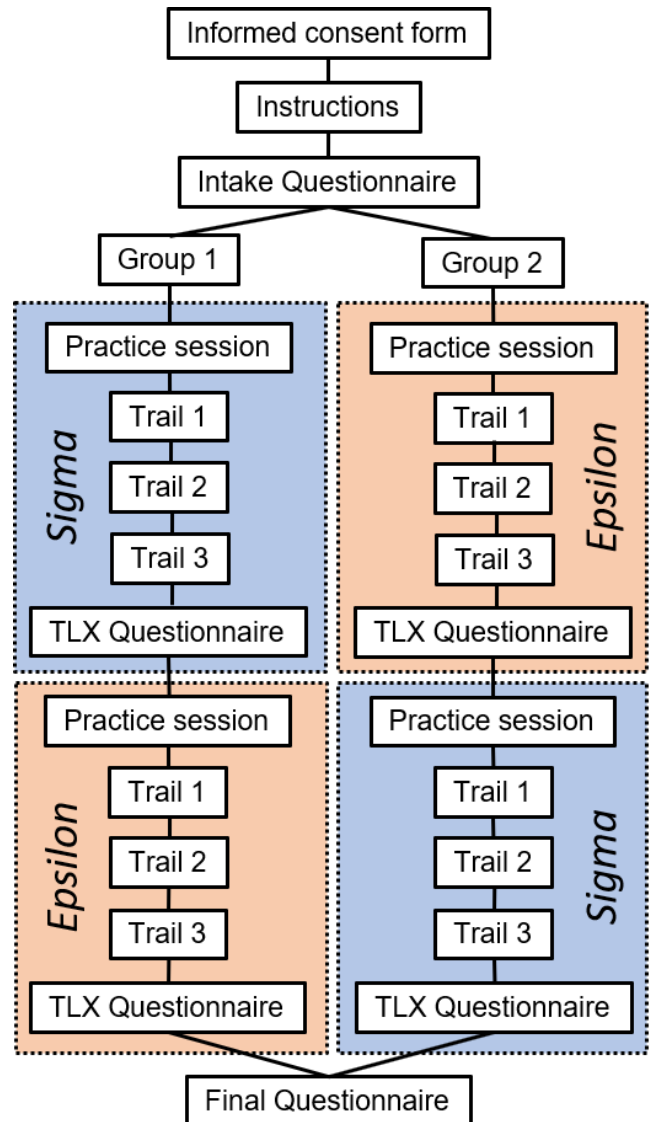


Figure 25: Scheme of the experimental procedure (from top to bottom).

5.2. Experimental results

The obtained data, shown in Appendix I, from the experiment is analysed and presented in this section. The statistical data is processed using G*Power [63] and MATLAB 2017a (The MathWorks, Inc., Natick, MA) using the m-file which can be found in Appendix J.

Demography and background – Six volunteers (four male and two female) from the Delft University of Technology participated in the experiment. All participants were master students and between 23 and 26 years ($\mu = 25$ years, $\sigma = 0.98$ years) old. One participant was left handed and no one had prior experience with controlling steerable catheters.

Experiment observations – During the experiment it was noticed that the participants could easier control the *Epsilon* catheter. Using the *Sigma* catheter, many participants repeatedly overshoot the target. Frustration of the participants was noticed while performing the task using the *Sigma* catheter by deep sighs. When completing the task, some verbally indicated that they were relieved that the task was completed.

Task performance – Combining 3 trials resulted in 12 target-to-target times. The results are visually shown in Figure 26 in a boxplot representation to show both median, spread and outliers of the target-to-target time. Initial visual interpretation of the boxplot, shows differences between the catheters but also between participants. Subsequently, the average target-to-target time, 20.2 s ($\sigma = 17.4$ s) for the *Sigma* catheter and 6.6 s ($\sigma = 4.6$ s) for the *Epsilon* catheter indicates differences in task performance between both catheters.

However, to statistically confirm the effect, a paired samples t-test (both tailed, $\alpha = 0.05$) was carried out over the data for each participant [64]. ‘Paired samples’ is applied since each participant performed the task with both catheters. ‘Both

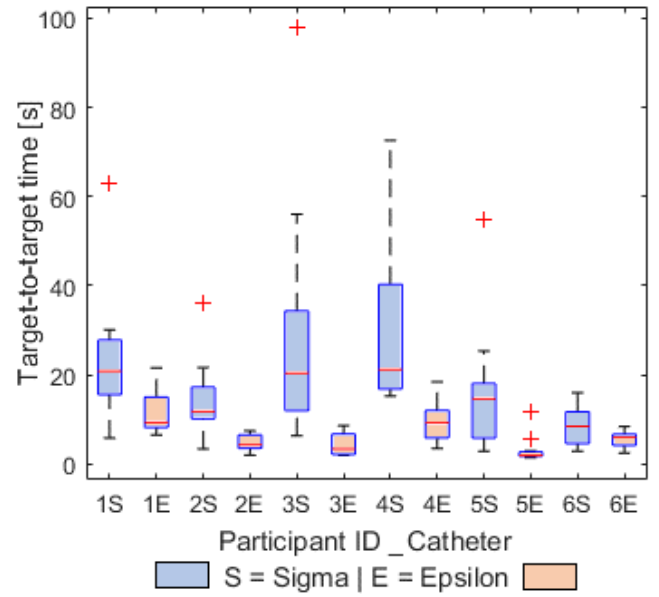


Figure 26: Target-to-target time for each participant using both catheters shown in a Boxplot representation. Outliers are shown in a ‘+’ symbol

Table 4: Statistics of the t-test for the target-to-target times. Participant 6 is shaded since the p-value is above the significance level of 0.05.

Statistics		Sigma		Epsilon		Sigma versus Epsilon			
ID		μ [s]	σ [s]	μ [s]	σ [s]	effect size	t-statistic	p-value	statistical power
1		23.8	14.2	12.1	5.1	1.10	2.71	0.020	100%
2		14.2	8.7	4.8	1.8	1.49	3.66	0.004	100%
3		28.9	25.1	4.4	2.5	1.33	3.32	0.007	100%
4		30.1	19.6	9.7	4.7	1.43	3.65	0.004	100%
5		15.9	14.1	3.1	3.0	1.25	2.90	0.015	100%
6		8.5	4.3	5.6	1.9	0.90	2.01	0.070	99%
Total		20.2	17.4	6.6	4.6	1.07	6.71	3.995E-09	100%

Table 5: Statistics of the t-test for the Raw TLX scores. Temporal demand is shaded since the p-value is above the significance level of 0.05 and the statistical power below 80%.

Statistics Topic	Sigma		Epsilon		Sigma versus Epsilon			
	μ [%]	σ [%]	μ [%]	σ [%]	effect size	t-statistic	p-value	statistical power
Mental Demand	74	13	38	22	2.06	7.42	0.001	100%
Physical Demand	58	24	27	11	1.70	3.85	0.012	100%
Temporal Demand	51	17	42	18	0.52	1.61	0.168	38%
Performance	67	15	23	9	3.58	4.97	0.004	100%
Effort	70	19	46	30	0.96	3.24	0.023	86%
Frustration	63	22	19	9	2.61	4.54	0.006	100%
Total	64	19	32	20	1.63	8.91	1.606E-11	100%

tailed' indicates that the hypothesis was tested in both directions to determine if one catheter performs better or worse than the other. The significance level is set at $\alpha = 0.05$, a commonly used value in human suspect research.

Next to testing the data of individual participants, the data of all participants was combined and tested. An overview of all statistics of the target-to-target time is shown in Table 4. The t-statistic, effect size (Cohen's d [65]) and statistical power are also shown there. An effect size between 0.2 and 0.3 is considered as a small effect, an effect size around 0.5 as a medium effect and an effect size larger than 0.8 is a large effect [66]. Generally, statistical power above 80% is considered to be sufficient.

Workload – The raw data of the Raw TLX questionnaire is shown in Table 7 and Table 8 at Appendix I. The responses range from -10 to 10 and are in the data processing transferred to a percentage scale. High percentages indicate a high task load and low percentages indicate a low task load. The total Raw TLX score is 64% ($\sigma = 19\%$) for the *Sigma* catheter and 32% ($\sigma = 20\%$) for the *Epsilon* catheter. Means and variance of the individual topics are shown in Table 5, which shows that the *Epsilon* catheter results in lower TLX percentages than the *Sigma* catheter on all topics.

To statistically confirm the difference between TLX scores of both catheters, a paired samples t-test (both tailed, $\alpha = 0.05$) is calculated and shown for each individual topic in Table 5. A significant difference ($p\text{-value} < \alpha$) with sufficient statistical power ($> 80\%$) is found on all topics except temporal demand.

Final questionnaire – All participants preferred the *Epsilon* prototype on personal preference, easy steering and precision steering. One of the six participants chose the *Sigma* catheter for the fastest steering.

At the remarks question, some participants indicated that the *Sigma* catheter could be more precise but it was hard to control. One mentioned that the *Sigma* catheter 'randomly' moved. Another participant noted that the index finger was sufficient to perform the task using the *Sigma* catheter.

6. Discussion

6.1. Catheter design

Additive manufacturing – Especially during initial prototyping, additive manufacturing appeared to be very useful. The housing was made of a single part, which not only reduced

assembly, but also allowed to integrate the rotational indicators.

A main disadvantage of additive manufacturing is the minimum printing size of the openings. Especially the handle design does not allow to drill open the closed openings afterwards, due to the length. Since some play is left between the cables and the guiding, at first, bending the handle does not result in cable displacement. The initial steering results in attachment of the cable to one side of the guiding, whereupon bending the handle further induces cable displacement.

Since the R5 additive material hardens by light, flexibility of the handle reduces over time. When adaption of the cable clamping required to dismantle the cables from the tip, a new handle was made which was not affected by additional light. This also allowed to improve the fit of the hexagonal nut of the cable displacement system.

Handle – Position of preference of the handle was not incorporated in the design. Now, the handle bends downwards by gravitational force. When leaving the handle for some time in this position, the neutral position could shift to this bended position. Therefore, a handle holder was made when the prototype was stored (Figure 27).

Although the handle segments bend like designed, some lateral displacement in one segment is possible. Since this does not result in cable displacement, the tip will not react. This could result in disturbance of the input-output coupling.

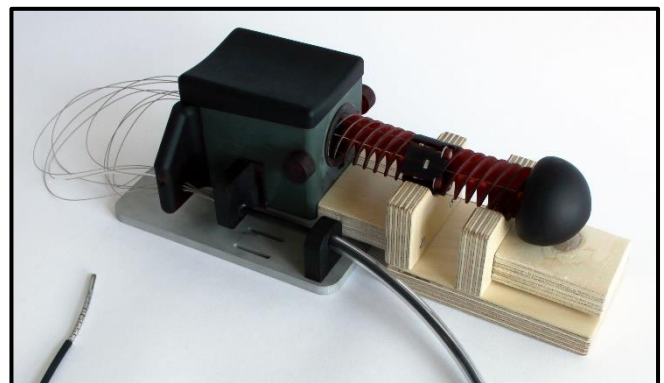


Figure 27: *Epsilon* catheter including handle holder to prevent permanent deformation of the handle while in rest position.

Oiling – Lubrication of mechanical systems is widely applied to reduce friction or wear. Since the steering cables are surrounded by the guiding springs for approximately 1 m and make a 180° bend, it was decided to apply lubrication. The effect on the additive manufacturing material is unknown and since the play between cable and guiding is sufficient the oil was not applied on the

inside of the handle. Since the scale of this mechanical system is comparable to mechanical watches, fines wristwatch oil (Koch 1, Klüber Lubrication, München, Germany) was applied. Using an injection needle, small drops were placed over the 180° bend. The prototype was placed in a bench vise with the shaft downwards. This made it possible to add oil drip by drip into the shaft until the oil reached the tip.

Despite all this effort, over the long range of the steering cable the oil seemed to stick the steering cable to the guiding spring. This was noticed when the handle was dismantled in order to adapt to the cable clamping. Before oiling it was possible to steer the tip manually. This means that the guiding spring was clamped to the table by a finger and the steering cable was pulled by the other hand. After oiling, this manually steering was not possible anymore. The sticky behaviour of the oil causes the inside of the tip to stick together, which limits the bending. Also, the oil attracts dust to the tip, which induces additional friction. Using an ultrasonic cleaner (bath filled with propanol), the oil was removed and after reassembling the prototype, the shaft was not oiled.

6.2. Experimental findings

Measured effects – The target-to-target time over all measurements showed a significant difference between both catheters. On this specific task novice participants were able to reach the targets faster using the control method of the *Epsilon* catheter than using the control method of the *Sigma* catheter. Since the effect size is above 0.8, the effect can be considered as large. The statistical power is also above 80%.

A significant difference was also determined for participant 1 to 5 with an effect size above 0.8. However, the time samples of participant 6 resulted in $t(11) = 2.01$, $p = 0.07$. This indicates that the impact of the steering method on the task performance also depends on the skills of the participant.

The combined TLX score showed a significant difference between both catheters. It can be concluded that performing this specific task by the novice participants using the control method of the *Epsilon* catheter results in less workload than using the control method of the *Sigma* catheter. This effect can be considered as large.

When focusing on individual topics, the difference in temporal demand is insignificant. The effect of the other topics can be considered as large. The temporal demand topic focusses on the pace of the task. Although the participants could feel some time pressure since their pace was

lower with the *Sigma* catheter, it is likely that this effect was too small to measure with the questionnaire.

The data analysis showed significant differences ($p\text{-value} < \alpha$) between both conditions using a paired samples t-test. This shows that there is a certain difference between both conditions, but it does not show the size of the effect or reliability of this conclusion. The size of the effect is stated by the effect size or t-statistic (related to the effect size). The reliability of the test is expressed by the statistical power. Although the sample size was small (6 participants), in general, the statistical power is above 80% and often close to 100%. The statistical power is a function of the effect size, sample size, α , tails and measurement error [66]. Since the measured effect size between both conditions is large, the statistical power is still sufficient regardless of the low sample size. Although the conclusions of the data analysis may be reliable, the small group of participants could be a poor representation of the entire population or the population of interventionists. The participants consist of students with a technical background which may perform outstanding on one condition in respect to the other condition. Therefore, a larger group with participants with different backgrounds (or even interventionists) is required to confirm the difference between both conditions in general.

Experimental setup – During the task, orientation of the pointer is undervalued in respect to the position. Approximately $\pm 30^\circ$ variance perpendicular to the target plane was allowed. Initially, it was planned to place a transparent window, with Ø5 mm openings, 10 mm in front of the target plane as shown in Figure 28. This should have restricted the participants to touch the target perpendicular. However, when the pointer was within the transparent window it was not able to freely move. When a participant was steering in the wrong direction this was not noticed. This could damage the prototype and obstruct the experiment. Therefore, this restriction was left out of the task.

A third condition was initially planned in which all five DOF of the *Epsilon* catheter were evaluated. During the proof-of-concept test, a guide tube of 200 mm allowed longitudinal movement of the prototype. This distance was estimated to guide the shaft from the prototype's base to the entry point at the patient's groin in real practice. In the experimental setup, only the tip was inserted which requires a guide tube of 530 mm. Over this distance the shaft did not smoothly move through the guide tube. Both the length and

curves resulted in additional static friction. When the user exerted additional force, suddenly the shaft slid through, which could have damaged the prototype. Besides, this does not represent the actual functioning of the design. Therefore, the longitudinal movement was excluded from the experiment.

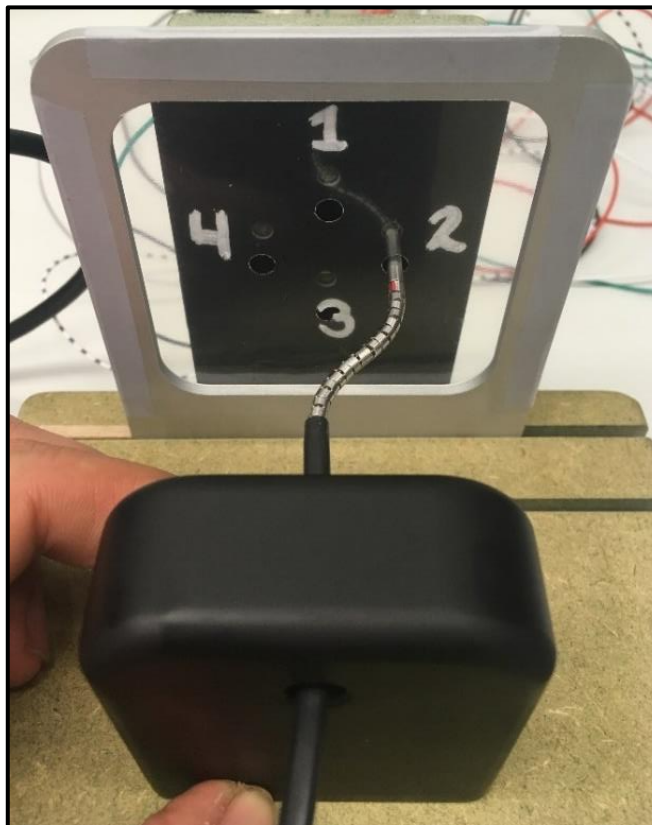


Figure 28: Experimental setup including transparent window. The transparent window was initially planned to force the participant to reach the target perpendicular. Due to unintended harm to the prototype this transparent window was not applied during the experiment.

6.3. Cardiac application

Current practice during interventional techniques is an interventionist, whose hands are both occupied, controlling a single catheter. After extended training the interventionist is able to adequately control the catheter.

Workload – Using the designed input control method, the interventionist can control all 5 DOF of the catheter single-handed. In the experiment, novices without any experience or extended training were able to reach targets with the catheter in a reasonable period of time. This indicates that the input control method results in ‘natural’ behaviour of the catheter tip end-point. This could indicate that the control method does not only allows extended steerability with respect to existing clinical devices but also decrease the

workload of controlling the catheter. This allows more attention of the interventionist to the treatment itself and perhaps reduce operational time.

Extended procedures – If the interventionist can control the catheter single-handed, standardised treatments can be reconsidered. For example, treatment using two catheters approaching the heart from different pathways could extend the possibilities of the interventionist, since the interventionist can control both catheters simultaneously.

6.4. Future recommendations

To proceed the development of less demanding multi-steerable catheters further progress has to be made.

Design – Further improvement of user experience of the *Epsilon* catheter can be acquired by reducing play in the handle. Extended printing accuracy or metal inserts could reduce the play in which steering from a neutral position will be more direct. Eliminating the position of preference would also improve user experience since this allows to let go of the handle without undesired tip movement.

The handle is based on a bending flexure joint to reduce play and allow accurate cable guiding. However, the bending stiffness requires force application of the user. During long procedures, this could be fatiguing. Redesigning the joint in combination with extended design possibilities of additive manufacturing could further improve the control method.

The *Epsilon* prototype is yet far from clinical use. The reliability of the photopolymer material over time is unknown. User experience challenges, such as mentioned in the previous paragraphs, should be overcome to convince interventionist of the capabilities of this design. In the end, design improvement should be towards cleanability of the device for reusability and large-scale production.

Experiment – The executed evaluation showed potential for the input control method of the *Epsilon* catheter but the longitudinal movement is not evaluated yet. The guide tube should be adapted to smoothly guide the catheter shaft. Potentially, oil could reduce friction between shaft and guiding tube.

Further evaluation of the *Epsilon* catheter could be performed by an extended task. Including orientation, depth variation, target disturbances (beating of the heart) and limited 2D visualisation would improve the resemblance of the task with the clinical setting. Instead of contacting targets,

the task could be adapted to grasping of objects and subsequently placement of these objects for even improved resemblance.

To show the magnitude of improvement of the proposed steering method, the task could be performed using currently applied catheters as baseline reference.

Clinical use – To identify further improvements, the prototype could be presented to expert interventionists. They could opt for design directions which would not directly come forward from the designer point of view. Besides extended validation using experimental setups, an evaluation in a beating animal heart may be a test environment closest to the real practice.

7. Conclusion

This project was initiated to design an input control method for the *Sigma* catheter tip and shaft design to improve task performance while reducing workload of the interventionist. After evaluating the gathered theory about the instrument's work environment, the interventionist who handles the instrument and the instrumentation, a design outline was exposed. The functional design described steering of the handle, combining multiple fingers and wrist, with positive input-output coupling. Further detailing in the geometrical design showed that bending flexures in the handle together with a 180° bended shaft results in the desired input-output coupling.

To demonstrate the design, a functional prototype, the *Epsilon* catheter, was fabricated. The input control method of the *Epsilon* catheter was evaluated in an experimental setup and compared to the input control method of the *Sigma* catheter. Experimental data showed that novice participants can faster complete the targeting task with reduced workload using the *Epsilon* catheter. Although the fifth degree of freedom of the multi-steerable catheter tip is not evaluated yet. The next step towards a new development in interventional cardiac treatment is set. However, further clinical evaluation and design improvements are required to bring this technology to the clinicians.

Acknowledgements

The author would like to thank the supervisors of the project Awaz Ali, Paul Henselmans, Costanza Culmone and Paul Breedveld for their helpful feedback and guiding along the project. Additionally, the clinical experts and specialists from the cardiology department of the Erasmus Medical Centre in Rotterdam for their valuable insights and the workshop at 3ME and DEMO at

Delft University of Technology which had an important role in the manufacturing of the prototype. Especially many thanks to Remi van Starkenburg for all his dedication and effort while fabricating the prototype. Finally, many thanks to Elisabeth Strijdhorst for language feedback in the final state of the report.

References

- [1]. J. Buddeke, I. Van Dis, F. L. J. Visseren, I. Vaartjes, M. L. Bots. (2016). Hart- en vaatziekten in Nederland 2016, cijfers over prevalentie, ziekte en sterfte. [online]. Available: <https://www.hartstichting.nl/getmedia/06fb9c92-a1f7-4135-a635-ff73680bfaa6/cijferboek-hartstichting-hart-vaatziekten-nederland-2016.pdf>
- [2]. V. Feigin. (2016). Global, regional, and national life expectancy, all-cause mortality, and cause-specific mortality for 249 causes of death, 1980-2015: a systematic analysis for the Global Burden of Disease Study 2015. *The Lancet*, 388(10053), 1459-1544.
- [3]. T. Vos, C. Allen, M. Arora, R. M. Barber, Z. A. Bhutta, A. Brown, M. Coggeshall. (2016). Global, regional, and national incidence, prevalence, and years lived with disability for 310 diseases and injuries, 1990–2015: a systematic analysis for the Global Burden of Disease Study 2015. *The Lancet*, 388(10053), 1545-1602.
- [4]. N. J. Kassebaum, M. Arora, R. M. Barber, Z. A. Bhutta, J. Brown, A. Carter, L. Cornaby. (2016). Global, regional, and national disability-adjusted life-years (DALYs) for 315 diseases and injuries and healthy life expectancy (HALE), 1990–2015: a systematic analysis for the Global Burden of Disease Study 2015. *The Lancet*, 388(10053), 1603-1658.
- [5]. M. H. Forouzanfar, A. Afshin, L. T. Alexander, H. R. Anderson, Z. A. Bhutta, S. Biryukov, A.J. Cohen. (2016). Global, regional, and national comparative risk assessment of 79 behavioural, environmental and occupational, and metabolic risks or clusters of risks, 1990–2015: a systematic analysis for the Global Burden of Disease Study 2015. *The Lancet*, 388(10053), 1659-1724.
- [6]. J. H. Gibbon. (1954). Application of a mechanical heart and lung apparatus to cardiac surgery. *Minn. Med.* 37, 171–185.
- [7]. E. Crystal, S. J. Connolly, K. Sleik, T. J. Ginger, S. Yusuf (2002). Interventions on

- prevention of postoperative atrial fibrillation in patients undergoing heart surgery. *Circulation*, 106(1), 75-80.
- [8]. A. Starr. (2007). The artificial heart valve. *Nature medicine*, 13(10), 1160-1164.
- [9]. J. M. Tobis & I. Abudayyeh. (2015). New devices and technology in interventional cardiology. *Journal of cardiology*, 65(1), 5-16.
- [10]. D. Filgueiras-Rama, A. Estrada, J. Shachar, S. Castrejón, D. Doiny, M. Ortega, J. L. Merino. (2013). Remote magnetic navigation for accurate, real-time catheter positioning and ablation in cardiac electrophysiology procedures. *Journal of visualized experiments: JoVE*, (74).
- [11]. M. Padala, J. H. Jimenez, A. P. Yoganathan, A. Chin, V. H. Thourani. (2012). Transapical beating heart cardioscopy technique for off-pump visualization of heart valves. *The Journal of thoracic and cardiovascular surgery*, 144(1), 231-234.
- [12]. R. L. Mueller & T. A. Sanborn. (1995). The history of interventional cardiology: cardiac catheterization, angioplasty, and related interventions. *American heart journal*, 129(1), 146-172.
- [13]. Y. Fu, H. Liu, W. Huang, S. Wang, Z. Liang. (2009). Steerable catheters in minimally invasive vascular surgery. *The International Journal of Medical Robotics and Computer Assisted Surgery*, 5(4), 381-391.
- [14]. A. Ali, D. H. Plettenburg, P. Breedveld. (2016). Steerable Catheters in Cardiology: Classifying Steerability and Assessing Future Challenges. *IEEE Transactions on Biomedical Engineering*, 63(4), 679-693.
- [15]. S. Ernst, F. Ouyang, C. Linder, K. Hertting, F. Stahl, J. Chun, K. H. Kuck. (2004). Initial experience with remote catheter ablation using a novel magnetic navigation system. *Circulation*, 109(12), 1472-1475.
- [16]. S. C. Brown, D. E. Boshoff, B. Eyskens, L. Mertens, M. Gewillig. (2009). Use of a microcatheter in a telescopic system to reach difficult targets in complex congenital heart disease. *Catheterization and Cardiovascular Interventions*, 73(5), 676-681.
- [17]. A. Arya, G. Hindricks, P. Sommer, Y. Huo, A. Bollmann, T. Gaspar, C. Piorkowski. (2009). Long-term results and the predictors of outcome of catheter ablation of atrial fibrillation using steerable sheath catheter navigation after single procedure in 674 patients. *Europace*, 12(2), 173-180.
- [18]. R. O. Bonow, B. Carabello, A. C. de Leon, L. H. Edmunds, B. J. Fedderly, M. D. Freed, R. A. O'Rourke. (1998). Guidelines for the management of patients with valvular heart disease. *Circulation*, 98(18), 1949-1984.
- [19]. D. H. Adams, J. J. Popma, M. J. Reardon, S. J. Yakubov, J. S. Coselli, G. M. Deeb, S. Chetcuti. (2014). Transcatheter aortic-valve replacement with a self-expanding prosthesis. *New England Journal of Medicine*, 370(19), 1790-1798.
- [20]. M. R. Reynolds, E. A. Magnuson, K. Wang, Y. Lei, K. Vilain, J. Walczak, C. R. Smith. (2012). Cost-effectiveness of transcatheter aortic valve replacement compared with standard care among inoperable patients with severe aortic stenosis. *Circulation*, 125(9), 1102-1109.
- [21]. C. Tamburino, M. Barbanti, P. D'Errigo, R. Ranucci, F. Onorati, R. D. Covello, C. Grossi. (2015). 1-year outcomes after transfemoral transcatheter or surgical aortic valve replacement: results from the Italian OBSERVANT study. *Journal of the American College of Cardiology*, 66(7), 804-812.
- [22]. P. Aagaard, A. Natale, D. Briceno, H. Nakagawa, S. Mohanty, C. Gianni, L. Di Biase. (2016). Remote magnetic navigation: a focus on catheter ablation of ventricular arrhythmias. *Journal of cardiovascular electrophysiology*, 27(S1).
- [23]. S. P. Friedrich, A. D. Berman, D. S. Baim, D. J. Diver. (1994). Myocardial perforation in the cardiac catheterization laboratory: incidence, presentation, diagnosis, and management. *Catheterization and Cardiovascular Interventions*, 32(2), 99-107.
- [24]. H. Rafii-Tari, C. J. Payne, G.Z. Yang. (2014). Current and emerging robot-assisted endovascular catheterization technologies: a review. *Annals of biomedical engineering*, 42(4), 697-715.
- [25]. S. Miyazaki, A. Shah, O. Xhaët, N. Derval, S. Matsuo, M. Wright, L. Rivard. (2010). Remote magnetic navigation with irrigated tip catheter for ablation of paroxysmal atrial fibrillation. *Circulation: Arrhythmia and Electrophysiology*, CIRCEP-110.
- [26]. A. Ali, A. Sakes, E. A. Arkenbout, P. W. J. Henselmans, T. Szili-Torok, D. H. Plettenburg, P. Breedveld. (2018). Catheter Steering in Interventional Cardiology: Mechanical Analysis and Novel Solution. [unpublished].

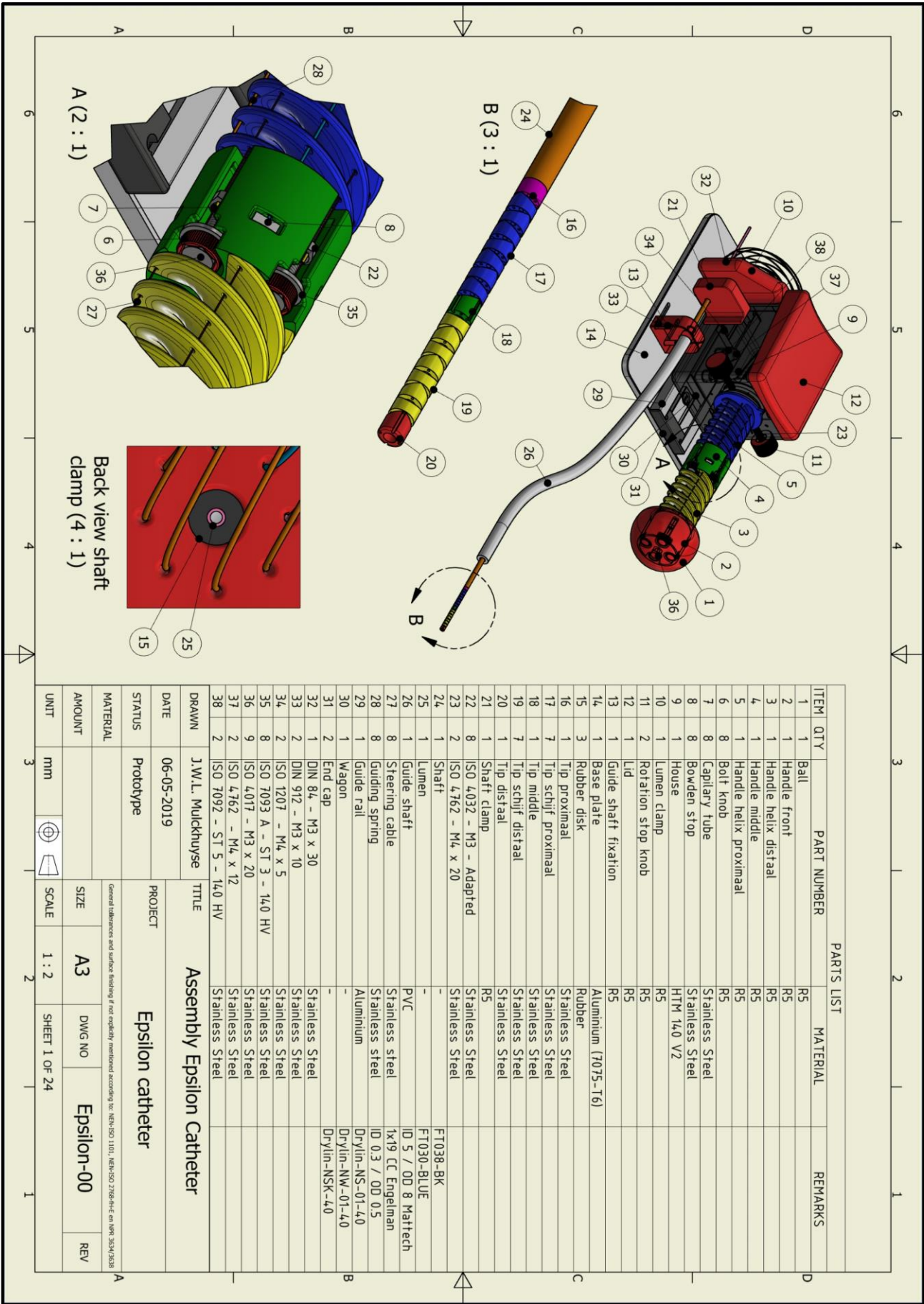
- [27]. M. K. Konings, T. G. Van Leeuwen, W. T. Mali, M. A. Viergever. (1998). Torsion measurement of catheters using polarized light in a single glass fibre. *Physics in medicine and biology*, 43(5), 1049.
- [28]. M. A. Tanner & D. Ward. (2003). Percutaneous technique for the reduction of knotted coronary catheters. *Heart*, 89(10), 1132-1133.
- [29]. I. M. Kelly & C. S. Boyd. (1999). Buckling of the tethering catheter causes migration of a temporary caval filter to the right atrium. *Clinical radiology*, 54(6), 398-401.
- [30]. P. Santangeli, & D. Lin (2015). Catheter ablation of paroxysmal atrial fibrillation: have we achieved cure with pulmonary vein isolation?. *Methodist DeBakey cardiovascular journal*, 11(2), 71.
- [31]. B. O'Brien, H. Zafar, S. De Freitas, F. Sharif. (2017). Transseptal puncture—Review of anatomy, techniques, complications and challenges. *International Journal of Cardiology*.
- [32]. J. Bismuth, E. Kashef, N. Cheshire, A. B. Lumsden. (2011). Feasibility and safety of remote endovascular catheter navigation in a porcine model. *Journal of Endovascular Therapy*, 18(2), 243-249.
- [33]. P. G  n  reux, J. G. Webb, L. G. Svensson, S. K. Kodali, L. F. Satler, W. F. Fearon, V. Babaliaros. (2012). Vascular complications after transcatheter aortic valve replacement: insights from the PARTNER (Placement of AoRTic TraNscatheterER Valve) trial. *Journal of the American College of Cardiology*, 60(12), 1043-1052.
- [34]. R. West, G. Ellis, N. Brooks. (2006). Complications of diagnostic cardiac catheterisation: results from a confidential inquiry into cardiac catheter complications. *Heart*, 92(6), 810-814.
- [35]. J. F  rster, E. T. Higgins, A. T. Bianco. (2003). Speed/accuracy decisions in task performance: Built-in trade-off or separate strategic concerns?. *Organizational Behavior and Human Decision Processes*, 90(1), 148-164
- [36]. S. Hasco  t, K. Warin-Fresse, A. E. Baruteau, K. Hadeed, C. Karsenty, J. Petit, P. Acar. (2016). Cardiac imaging of congenital heart diseases during interventional procedures continues to evolve: pros and cons of the main techniques. *Archives of cardiovascular diseases*, 109(2), 128-142.
- [37]. M. Pekař, A. F. Kolen, H. Belt, F. van Heesch, N. Mihajlovi  , I. E. Hoefer, A. F. van der Steen. (2017). Preclinical Testing of Frequency-Tunable Capacitive Micromachined Ultrasonic Transducer Probe Prototypes. *Ultrasound in medicine & biology*, 43(9), 2079-2085.
- [38]. C. Lin, S. Pehrson, P. K. Jacobsen, X. Chen. (2017). Initial experience of a novel mapping system combined with remote magnetic navigation in the catheter ablation of atrial fibrillation. *Journal of cardiovascular electrophysiology*, 28(12), 1387-1392.
- [39]. D. B. Douglas, C. A. Wilke, D. Gibson, E. F. Petricoin, L. Liotta. (2017). Virtual reality and augmented reality: Advances in surgery. *Biol*, 2(5), 1-8.
- [40]. P. Breedveld, H. G. Stassen, D. W. Meijer, L. P. S. Stassen. (1999). Theoretical background and conceptual solution for depth perception and eye-hand coordination problems in laparoscopic surgery. *Minimally invasive therapy & allied technologies*, 8(4), 227-234.
- [41]. R. H. Taylor, A. Menciassi, G. Fichtinger, P. Fiorini, P. Dario. (2016). Medical robotics and computer-integrated surgery. In *Springer handbook of robotics* (pp. 1657-1684). Springer, Cham.
- [42]. P. van Dam, J. Hauspy, L. Verkinderen, B. Trinh, L. Van Looy, L. Dirix. (2011). Do costs of robotic surgery matter?. In *Advanced Gynecologic Endoscopy*. InTech.
- [43]. S. Bagla, J. Smirniotopoulos, J. C. Orlando, R. Piechowiak. (2017). Robotic-assisted versus manual prostatic arterial embolization for benign prostatic hyperplasia: a comparative analysis. *Cardiovascular and interventional radiology*, 40(3), 360-365.
- [44]. G. Gerboni, P. W. Henselmans, E. A. Arkenbout, W. R. van Furth, P. Breedveld. (2015). HelixFlex: bioinspired maneuverable instrument for skull base surgery. *Bioinspiration & biomimetics*, 10(6), 066013.
- [45]. M. S. Hasan H. & Yu. (2017). Innovative developments in HCI and future trends. *International Journal of Automation and Computing*, 14(1), 10-20.
- [46]. R. Balasubramanian & V. J. Santos, V. J. (2014). *The human hand as an inspiration for robot hand development*(Vol. 95). Springer.
- [47]. R. M. Anderson & R. F. Romfh. (1980). Technique in the use of surgical tools. *Appleton-Century-Crofts*.

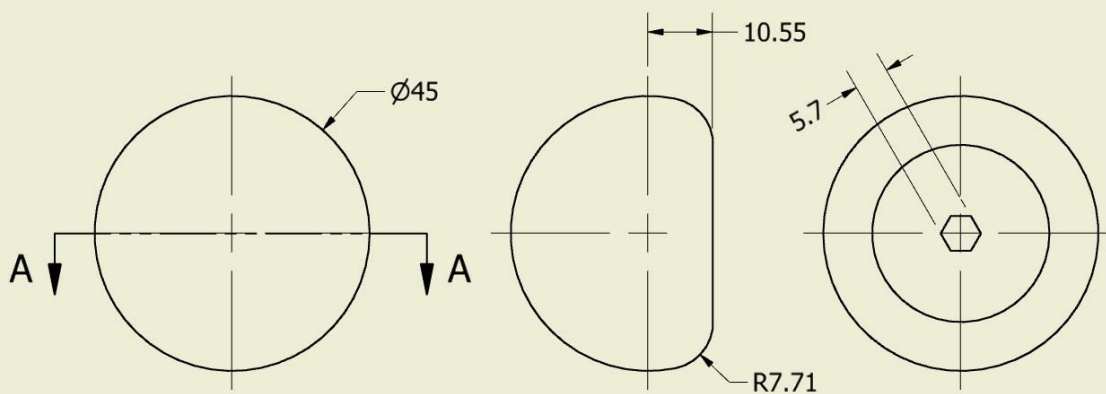
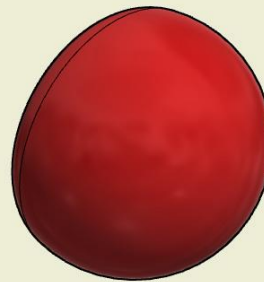
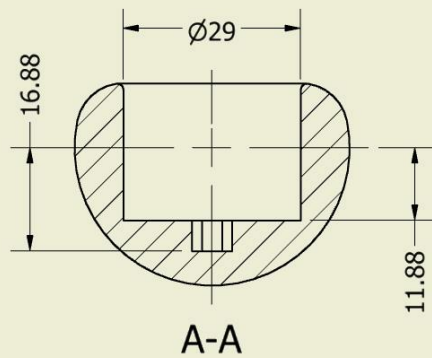
- [48]. J. P. Toombs, & K. M. Clarke. (2003). Basic operative techniques. *Textbook of small animal surgery*, 1, 199-222.
- [49]. D. A. Abbink & M. Mulder. (2010). Neuromuscular analysis as a guideline in designing shared control. In *Advances in haptics*. InTech.
- [50]. D. M. Wolpert, R. C. Miall, R. C., M. Kawato. (1998). Internal models in the cerebellum. *Trends in cognitive sciences*, 2(9), 338-347.
- [51]. C. Fan, D. Dodou, P. Breedveld. (2013). Review of manual control methods for handheld maneuverable instruments. *Minimally Invasive Therapy & Allied Technologies*, 22(3), 127-135.
- [52]. C. Fan, D. Dodou, P. Breedveld, J. Dankelman. (2015). Spatial orientation in pathway surgery. *Surgical endoscopy*, 29(9), 2705-2719.
- [53]. J. Molenbroek. (2018). *DINED anthropometric database*. [online]. Available: <https://dined.io.tudelft.nl/en>
- [54]. F. Jelinek, E. A. Arkenbout, P. W. Henselmans, R. Pessers, P. Breedveld. (2015). Classification of joints used in steerable instruments for minimally invasive surgery—A review of the state of the art. *Journal of Medical Devices*, 9(1), 010801.
- [55]. IGUS. (2018). IGUS DryLin W Linear Guide Systems. [online]. Available: https://www.igus.com/_product_files/download/pdf/drylinw.pdf
- [56]. Envisiontec. (2014). Perfactory Materials R5 and R11. [online]. Available: <https://strategic3dsolutions.com/wp-content/uploads/2014/10/MK-MTS-R5R11-V01-FN-EN.pdf>
- [57]. Engelmann. (2015). *Fine Wire Ropes*. [online]. Available: https://engelmann-online.de/wp-content/uploads/2015/09/Engelmann_Broschuere_Feinseile_EN.pdf
- [58]. Chatillon. (2018). DL Series Mechanical Forge Gauge. [online]. Available: https://www.ametektest.com/-/media/ametektest/download_links/data_mechanical_force_gauges_lg_data_sheet_english.pdf
- [59]. National Instruments. (2017). USB-6008. [online]. Available: <http://www.ni.com/pdf/manuals/375295c.pdf>
- [60]. A. R. Jensen. (2006). Clocking the mind: Mental chronometry and individual differences. *Elevier*.
- [61]. S. G. Hart & L. E. Staveland (1988) Development of NASA-TLX (Task Load Index): results of empirical and theoretical research. *Hum Ment Workload* 1:139–183
- [62]. J. C. F. de Winter. (2014) Controversy in human factors constructs and the explosive use of the NASA TLX: a measurement perspective. *Cogn Technol Work* 16:289–297
- [63]. F. Paul, E. Erdfelder, A. Lang, A. Buchner. (2007). G*Power 3: A flexible statistical power analysis program for the social, behavioral, and biomedical sciences. *Behavior Research Methods*, 39, 175-191.
- [64]. R. W. Payne & H. Gwynne Jones. (1957). Statistics for the investigation of individual cases. *Journal of Clinical Psychology*, 13(2), 115-121.
- [65]. J. Cohen. (1988). Statistical power analysis for the behavioral sciences . Hillsdale. NJ: Lawrence Earlbaum Associates, 2.
- [66]. G. J. Meyer, S. E. Finn, L. D. Eyde, G. G. Kay, K. L. Moreland, R. R. Dies, G. M. Reed. (2001). Psychological testing and psychological assessment: A review of evidence and issues. *American psychologist*, 56(2), 128.

Appendix A: List of symbols

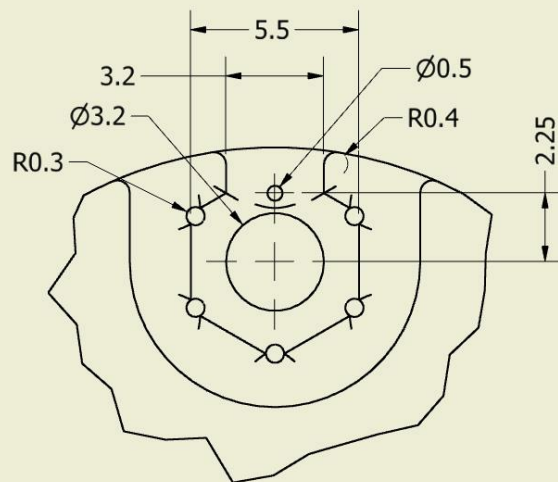
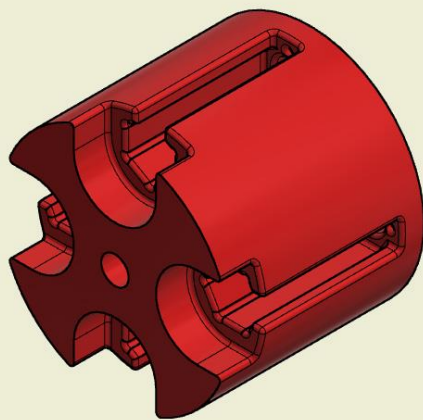
Symbol	Description
\varnothing	Diameter
μ	Mean (average)
σ	Standard deviation
α	Significance level, probability of a type I error (false positive)

Appendix B: Technical drawings Epsilon prototype

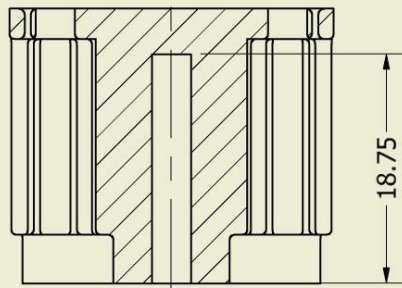




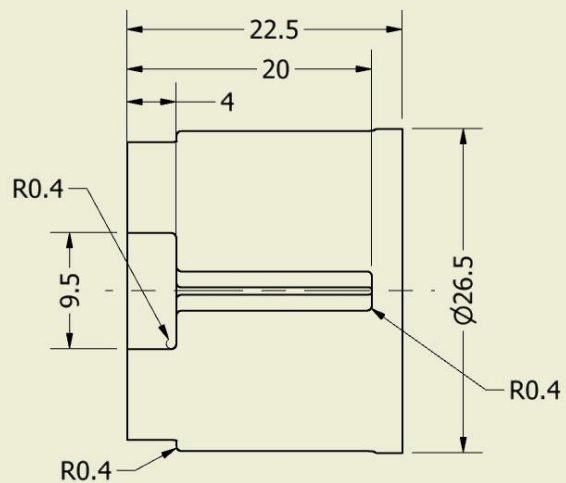
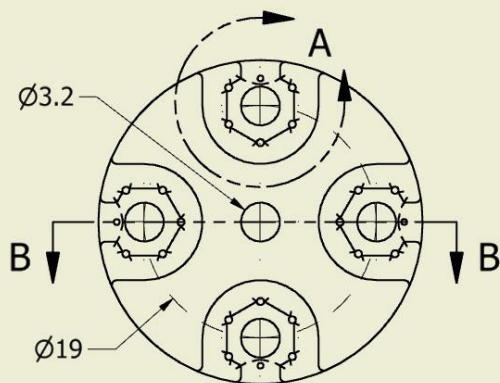
DRAWN	J.W.L. Mulckhuyse	TITLE Ball				
DATE	06-05-2019	PROJECT Epsilon catheter				
STATUS	Prototype					
MATERIAL	R5	General tolerances and surface finishing if not explicitly mentioned according to: NEN-ISO 1101, NEN-ISO 2768-FH-E en NPR 3634/3638				
AMOUNT	1	SIZE	A4	DWG NO	Epsilon-01	REV
UNIT	mm	SCALE	1 : 1	SHEET 2 OF 24		



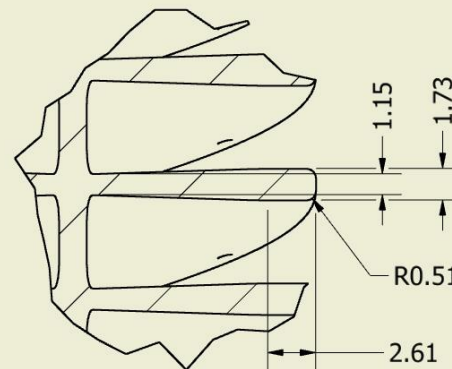
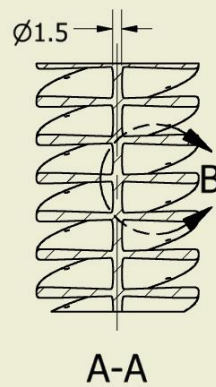
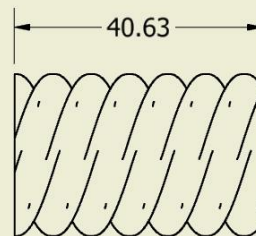
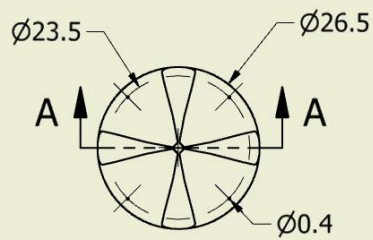
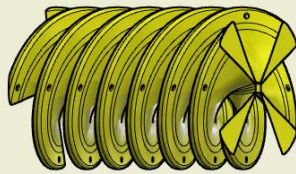
A



B-B

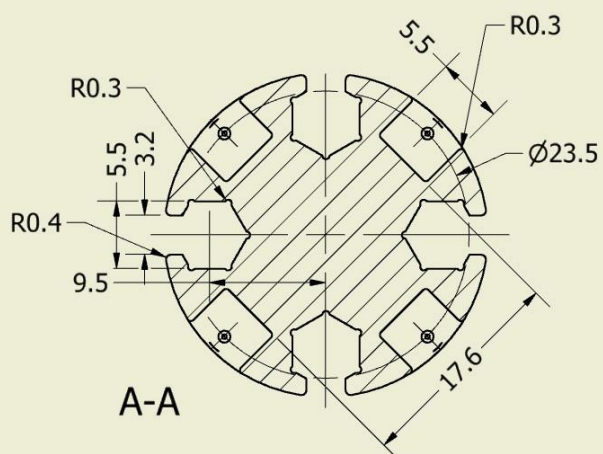
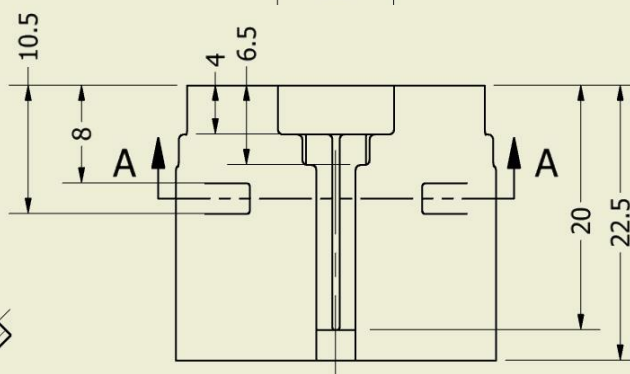
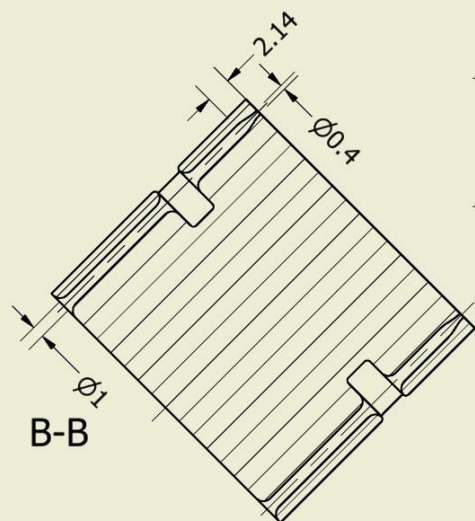
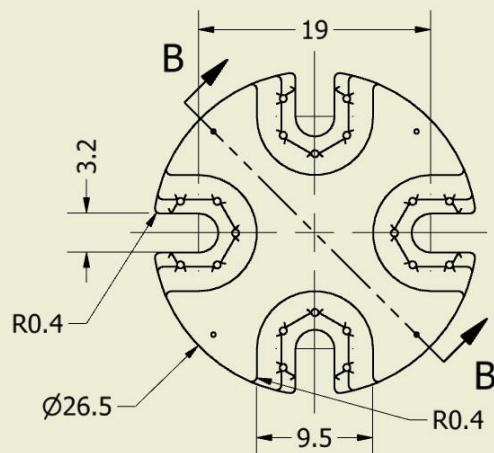
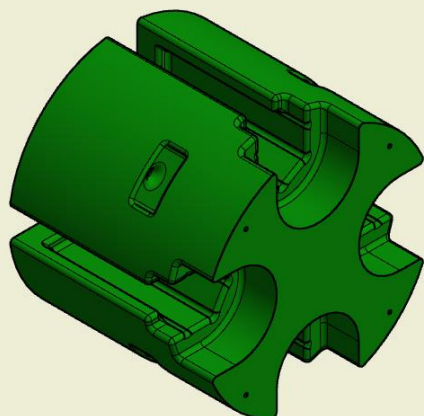


DRAWN	J.W.L. Mulckhuyse	TITLE				
DATE	06-05-2019	Handle front				
STATUS	Prototype	PROJECT				
MATERIAL	R5	Epsilon catheter				
AMOUNT	1	General tollerances and surface finishing if not explicitly mentioned according to: NEN-ISO 1101, NEN-ISO 2768-FH-E en NPR 3634/3638				
UNIT	mm	SIZE	A4	DWG NO	Epsilon-02	REV
		SCALE	2 : 1	SHEET 3 OF 24		

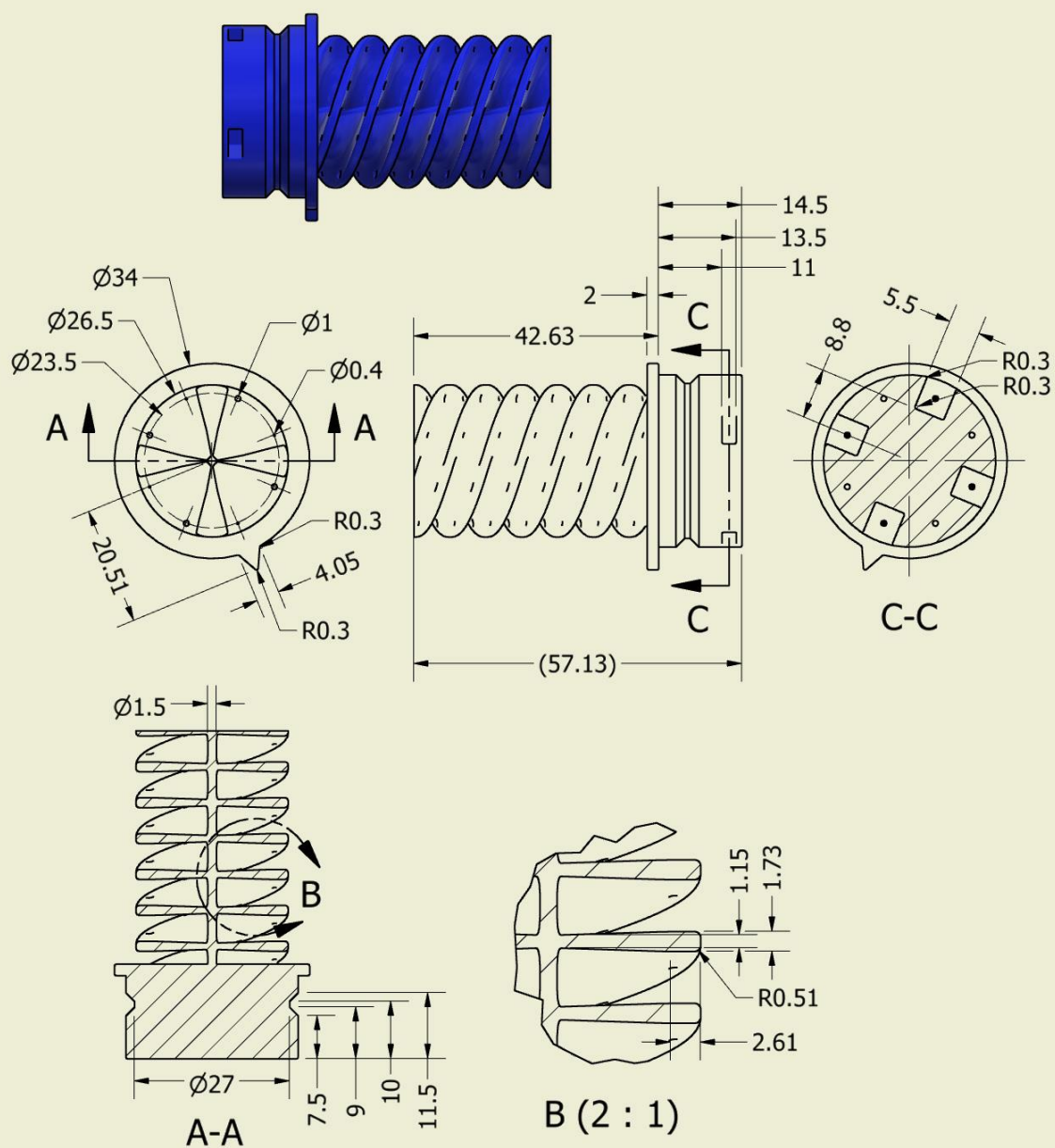


B (3 : 1)

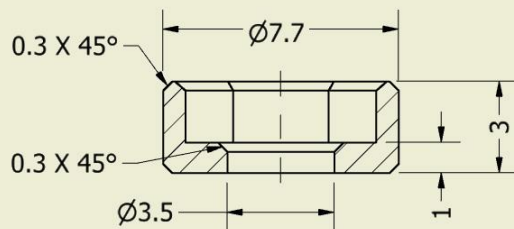
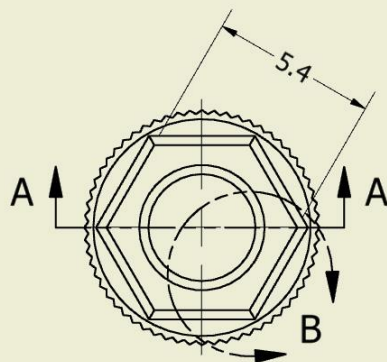
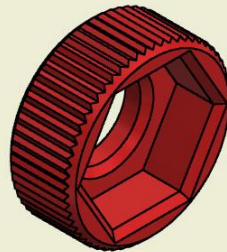
DRAWN	J.W.L. Mulckhuyse	TITLE Handle helix distaal				
DATE	06-05-2019	PROJECT Epsilon catheter				
STATUS	Prototype					
MATERIAL	R5	General tollerances and surface finishing if not explicitly mentioned according to: NEN-ISO 1101, NEN-ISO 2768-FH-E en NPR 3634/3638				
AMOUNT	1	SIZE	A4	DWG NO	Epsilon-03	REV
UNIT	mm	SCALE	1 : 1	SHEET 4 OF 24		



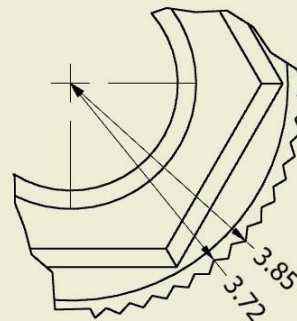
DRAWN	J.W.L. Mulckhuyse	TITLE				
DATE	06-05-2019	PROJECT				
STATUS	Prototype					
MATERIAL	R5	General tollerances and surface finishing if not explicitly mentioned according to: NEN-ISO 1101, NEN-ISO 2768-FH-E en NPR 3634/3638				
AMOUNT	1	SIZE	A4	DWG NO	Epsilon-04	REV
UNIT	mm	SCALE	2 : 1	SHEET 5 OF 24		



DRAWN	J.W.L. Mulckhuyse	TITLE Handle helix proximaal				
DATE	06-05-2019	PROJECT Epsilon catheter				
STATUS	Prototype					
MATERIAL	R5	General tollerances and surface finishing if not explicitly mentioned according to: NEN-ISO 1101, NEN-ISO 2768-FH-E en NPR 3634/3638				
AMOUNT	1	SIZE	A4	DWG NO	Epsilon-05	REV
UNIT	mm	SCALE	1 : 1	SHEET 6 OF 24		

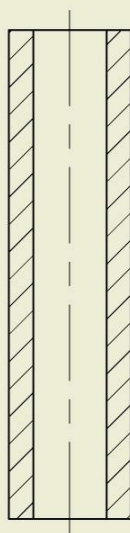
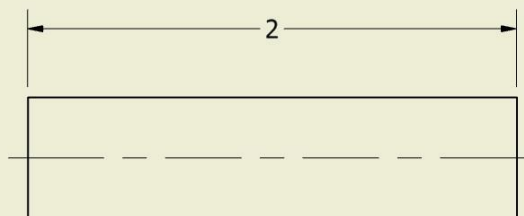
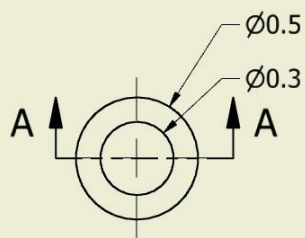


A-A

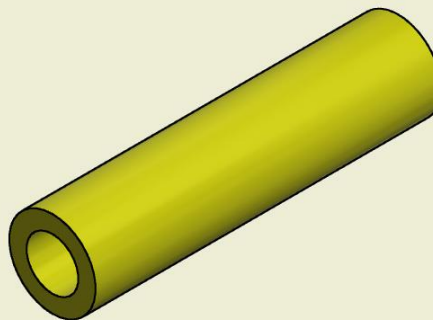


B (10 : 1)

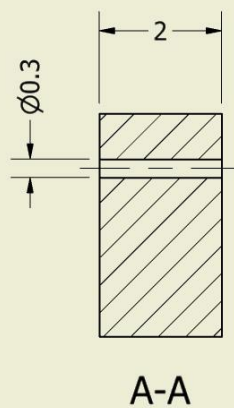
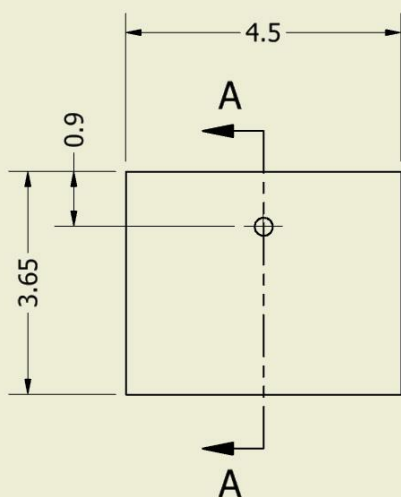
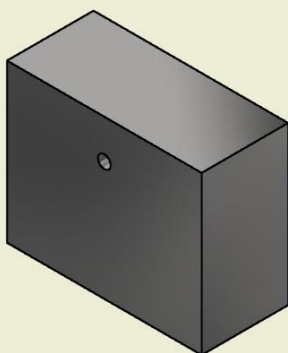
DRAWN	J.W.L. Mulckhuyse	TITLE Bolt knob				
DATE	06-05-2019	PROJECT Epsilon catheter				
STATUS	Prototype					
MATERIAL	R5	General tolerances and surface finishing if not explicitly mentioned according to: NEN-ISO 1101, NEN-ISO 2768-FH-E en NPR 3634/3638				
AMOUNT	8	SIZE	A4	DWG NO	Epsilon-06	REV
UNIT	mm	SCALE	5 : 1	SHEET 7 OF 24		



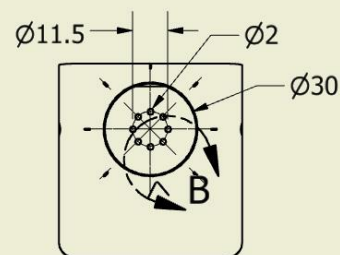
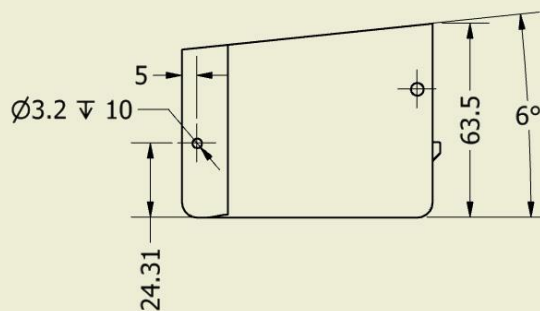
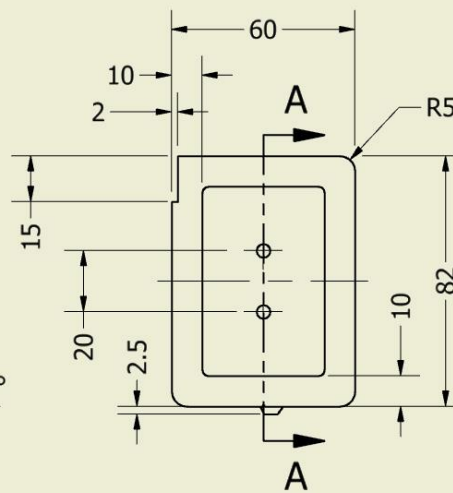
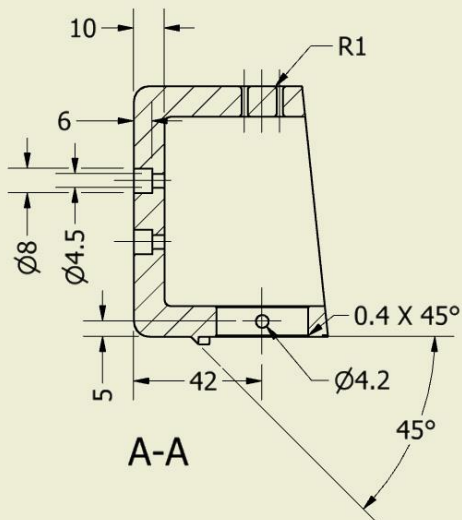
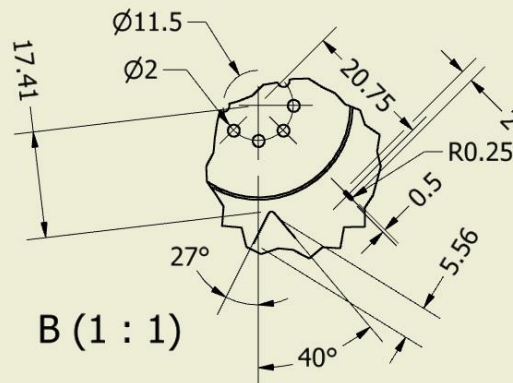
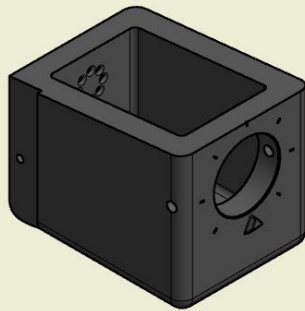
A-A



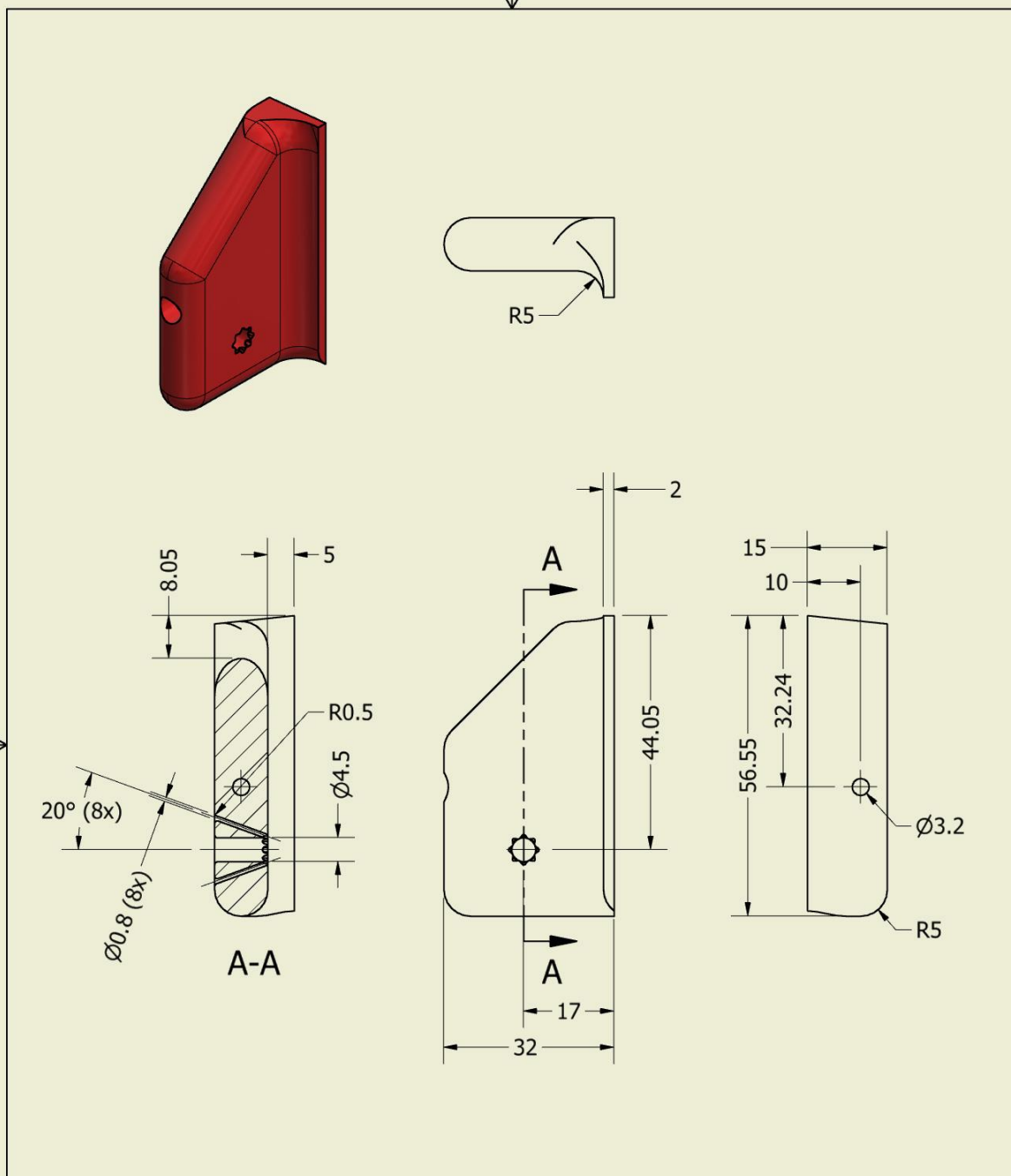
DRAWN	J.W.L. Mulckhuyse	TITLE Capillary tube				
DATE	06-05-2019	PROJECT Epsilon catheter				
STATUS	Prototype					
MATERIAL	Stainless steel	General tollerances and surface finishing if not explicitly mentioned according to: NEN-ISO 1101, NEN-ISO 2768-FH-E en NPR 3634/3638				
AMOUNT	8	SIZE	A4	DWG NO	Epsilon-07	REV
UNIT	mm	SCALE	40 : 1	SHEET 8 OF 24		



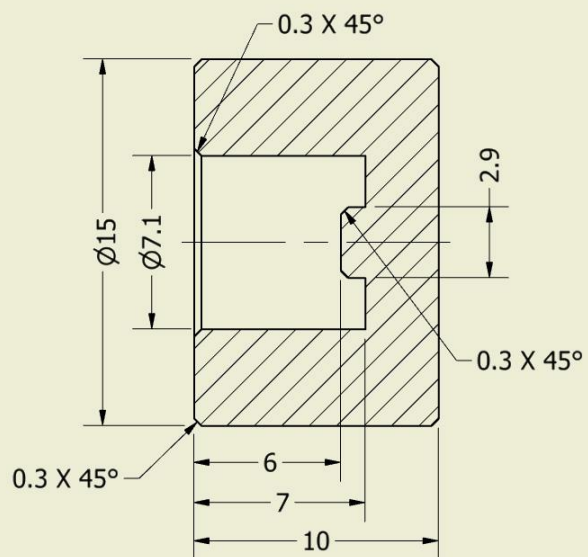
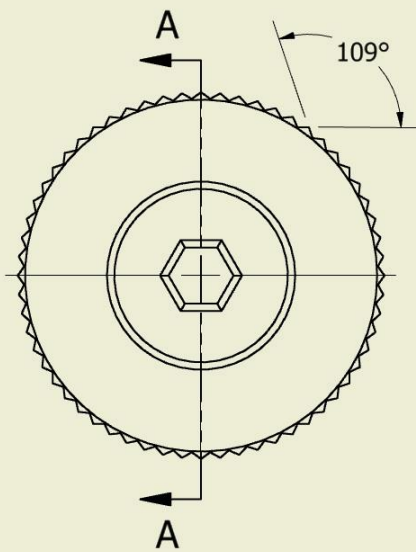
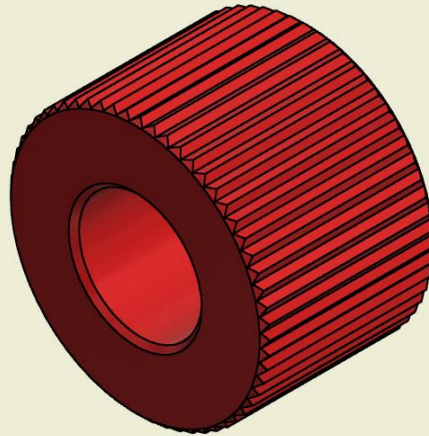
DRAWN	J.W.L. Mulckhuyse	TITLE Bowden stop				
DATE	06-05-2019	PROJECT Epsilon catheter				
STATUS	Prototype					
MATERIAL	Aluminium (7075-T6)	General tollerances and surface finishing if not explicitly mentioned according to: NEN-ISO 1101, NEN-ISO 2768-FH-E en NPR 3634/3638				
AMOUNT	8	SIZE	A4	DWG NO	Epsilon-08	REV
UNIT	mm	SCALE	10 : 1	SHEET 9 OF 24		



DRAWN	J.W.L. Mulckhuyse	TITLE House				
DATE	06-05-2019	PROJECT Epsilon catheter				
STATUS	Prototype					
MATERIAL	HTM 140 V2	General tolerances and surface finishing if not explicitly mentioned according to: NEN-ISO 1101, NEN-ISO 2768-FH-E en NPR 3634/3638				
AMOUNT	1	SIZE	A4	DWG NO	Epsilon-09	REV
UNIT	mm	SCALE	1 : 2	SHEET 10 OF 24		

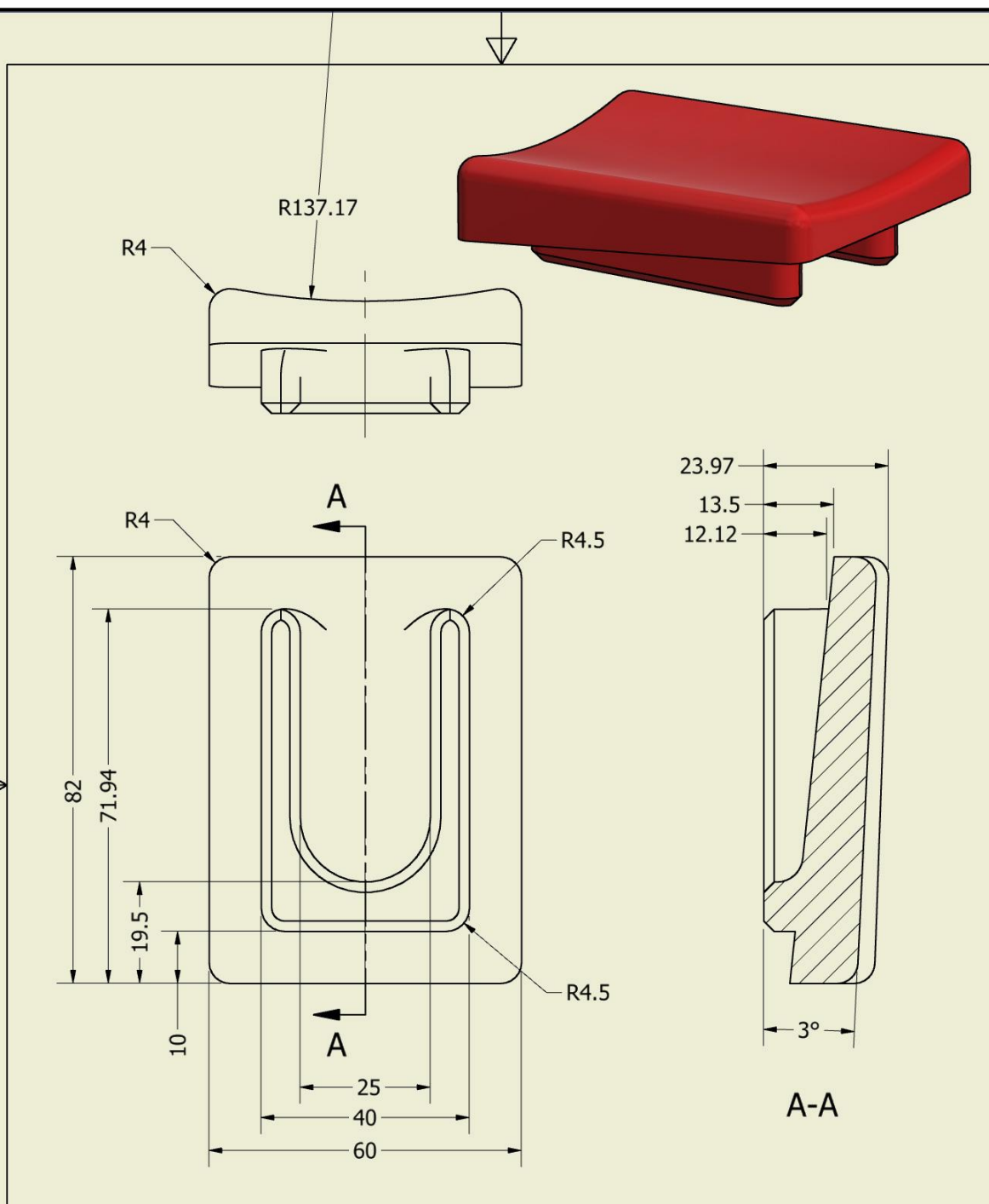


DRAWN	J.W.L. Mulckhuyse	TITLE Lumen clamp				
DATE	06-05-2019	PROJECT Epsilon catheter				
STATUS	Prototype					
MATERIAL	R5	General tolerances and surface finishing if not explicitly mentioned according to: NEN-ISO 1101, NEN-ISO 2768-FH-E en NPR 3634/3638				
AMOUNT	1	SIZE	A4	DWG NO	Epsilon-10	REV
UNIT	mm	SCALE	1 : 1	SHEET 11 OF 24		

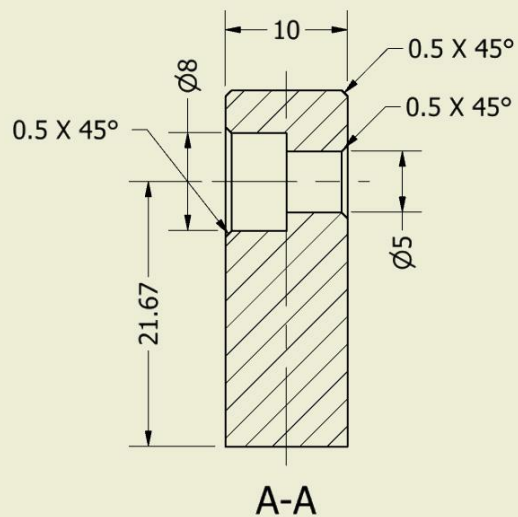
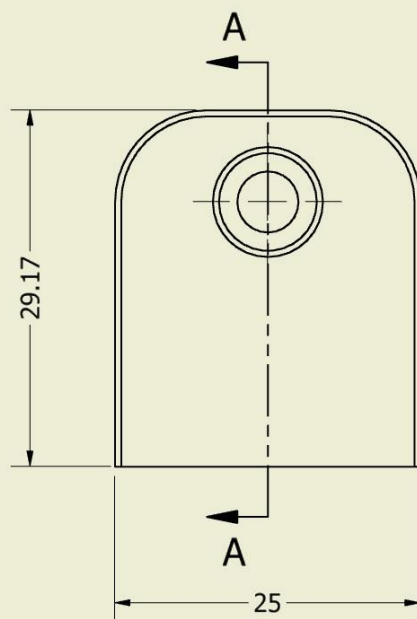
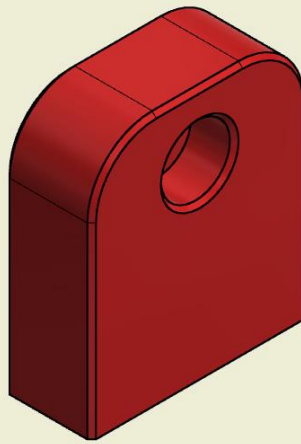


A-A

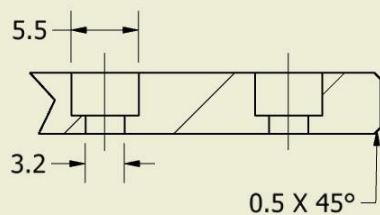
DRAWN	J.W.L. Mulckhuyse	TITLE Rotation stop knob				
DATE	06-05-2019	PROJECT Epsilon catheter				
STATUS	Prototype					
MATERIAL	R5	General tolerances and surface finishing if not explicitly mentioned according to: NEN-ISO 1101, NEN-ISO 2768-FH-E en NPR 3634/3638				
AMOUNT	2	SIZE	A4	DWG NO	Epsilon-11	REV
UNIT	mm	SCALE	4 : 1	SHEET 12 OF 24		



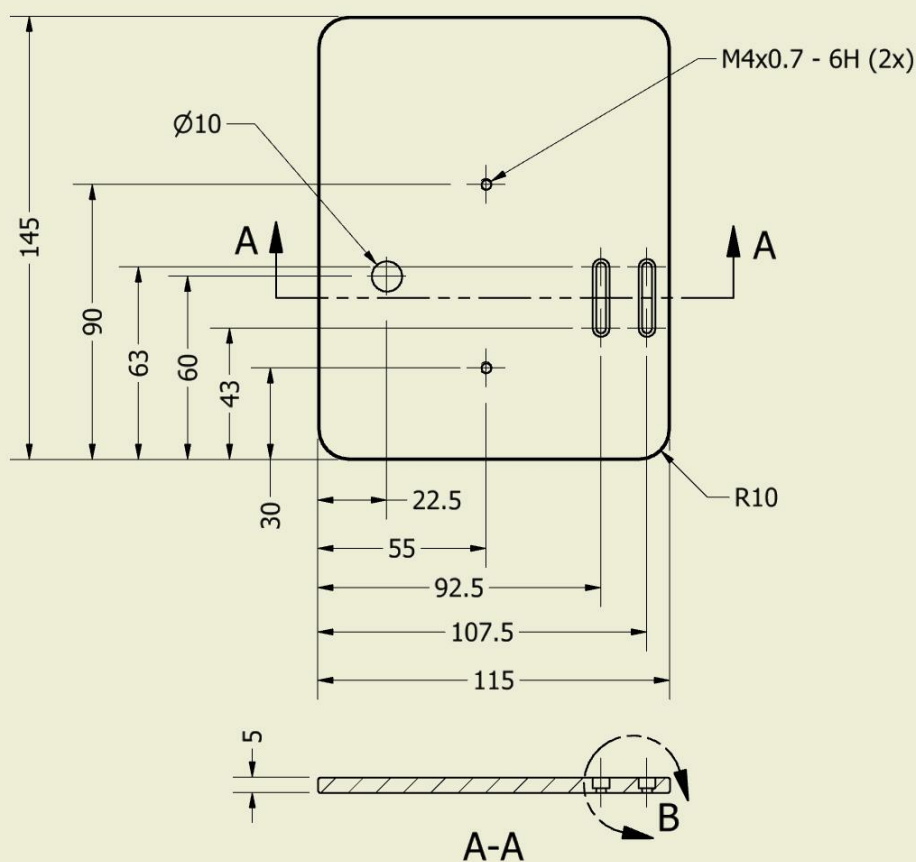
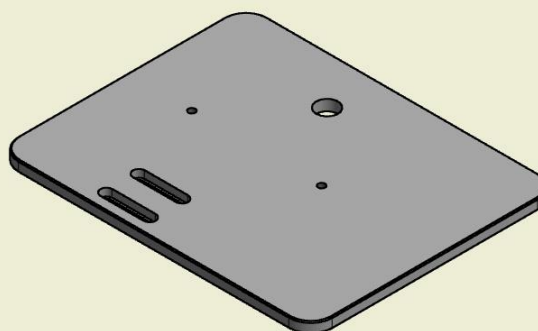
DRAWN	J.W.L. Mulckhuysen	TITLE Lid				
DATE	06-05-2019	PROJECT Epsilon catheter				
STATUS	Prototype					
MATERIAL	R5	General tolerances and surface finishing if not explicitly mentioned according to: NEN-ISO 1101, NEN-ISO 2768-FH-E en NPR 3634/3638				
AMOUNT	1	SIZE	A4	DWG NO	Epsilon-12	REV
UNIT	mm	SCALE	1 : 1	SHEET 13 OF 24		




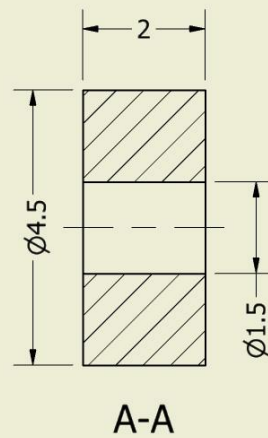
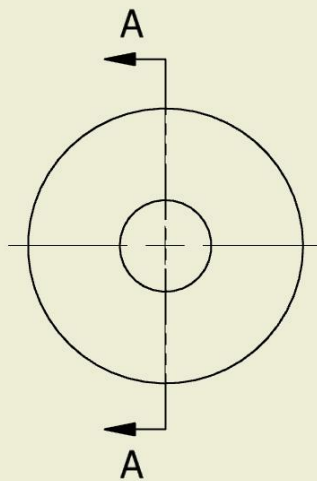
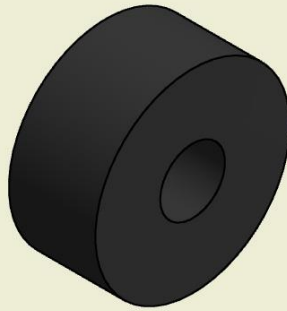
DRAWN	J.W.L. Mulckhuysen	TITLE Guide shaft fixation				
DATE	06-05-2019	PROJECT Epsilon catheter				
STATUS	Prototype					
MATERIAL	R5	General tolerances and surface finishing if not explicitly mentioned according to: NEN-ISO 1101, NEN-ISO 2768-FH-E en NPR 3634/3638				
AMOUNT	1	SIZE	A4	DWG NO	Epsilon-13	REV
UNIT	mm	SCALE	2 : 1	SHEET 14 OF 24		



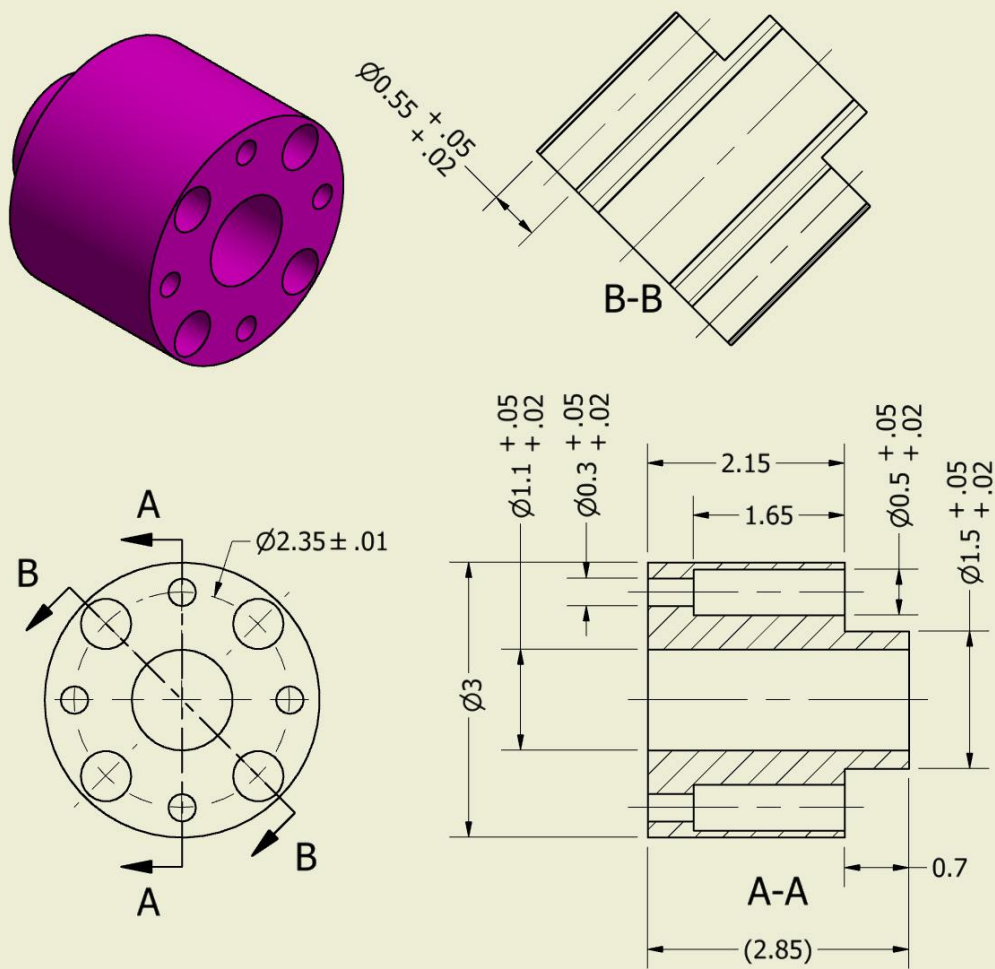
B (2 : 1)



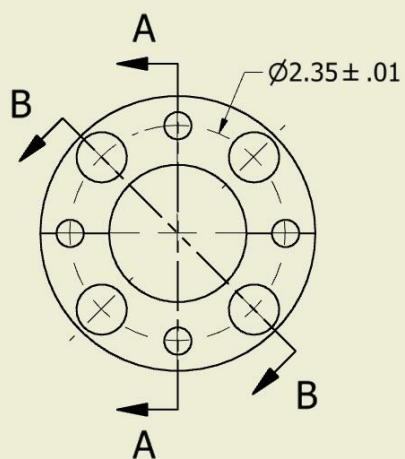
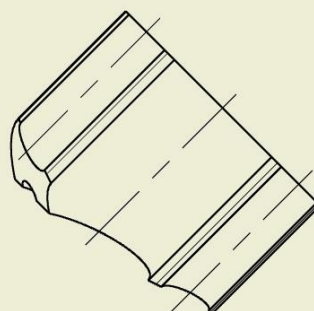
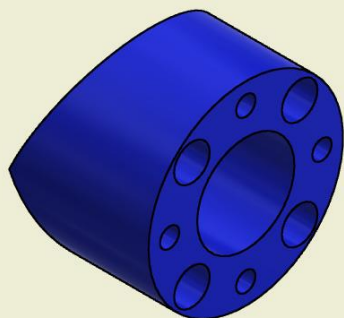
DRAWN	J.W.L. Mulckhuyse	TITLE Base plate					
DATE	06-05-2019						
STATUS	Prototype	PROJECT Epsilon catheter					
MATERIAL	Aluminium (7075-T6)						
AMOUNT	1	General tollerances and surface finishing if not explicitly mentioned according to: NEN-ISO 1101, NEN-ISO 2768-FH-E en NPR 3634/3638					
		SIZE	A4	DWG NO	Epsilon-14		REV
UNIT	mm		SCALE	1 : 2	SHEET 15 OF 24		



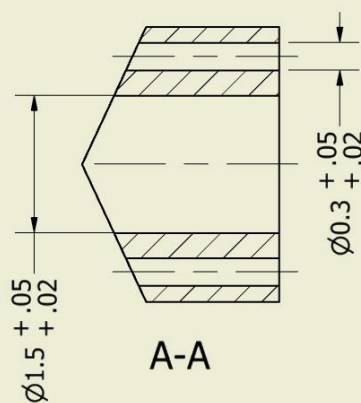
DRAWN	J.W.L. Mulckhuyse	TITLE Rubber disk				
DATE	06-05-2019	PROJECT Epsilon catheter				
STATUS	Prototype					
MATERIAL	Rubber	General tollerances and surface finishing if not explicitly mentioned according to: NEN-ISO 1101, NEN-ISO 2768-FH-E en NPR 3634/3638				
AMOUNT	3	SIZE	A4	DWG NO	Epsilon-15	REV
UNIT	mm	SCALE	10 : 1	SHEET 16 OF 24		



DRAWN	J.W.L. Mulckhuyse	TITLE				
DATE	06-05-2019	PROJECT				
STATUS	Prototype					
MATERIAL	Stainless steel	General tolerances and surface finishing if not explicitly mentioned according to: NEN-ISO 1101, NEN-ISO 2768-FH-E en NPR 3634/3638				
AMOUNT	1	SIZE	A4	DWG NO	Epsilon-16	REV
UNIT	mm	SCALE	15 : 1	SHEET 17 OF 24		

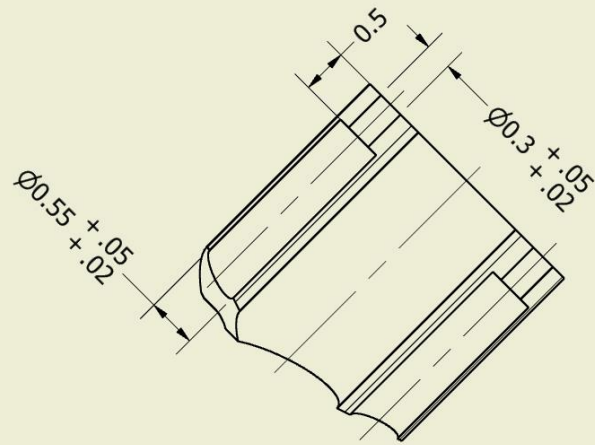
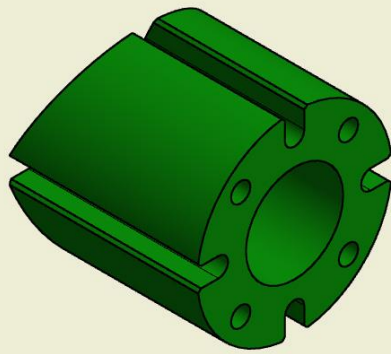


B-B

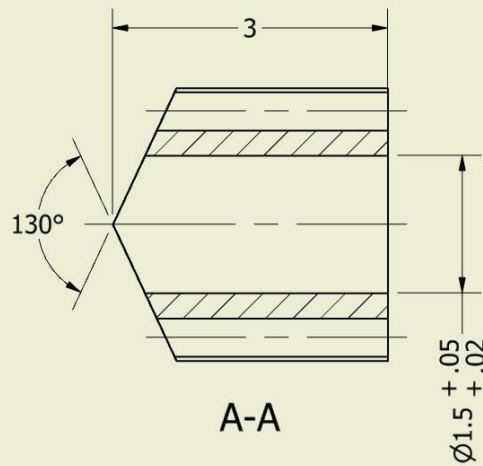
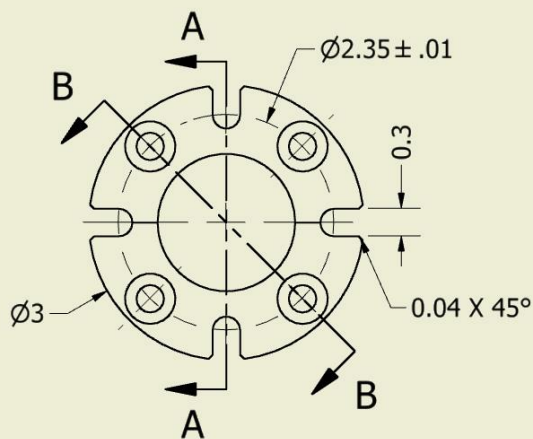


A-A

DRAWN	J.W.L. Mulckhuyse	TITLE				
DATE	06-05-2019	PROJECT				
STATUS	Prototype					
MATERIAL	Stainless steel	General tollerances and surface finishing if not explicitly mentioned according to: NEN-ISO 1101, NEN-ISO 2768-FH-E en NPR 3634/3638				
AMOUNT	7	SIZE	A4	DWG NO	Epsilon-17	REV
UNIT	mm	SCALE	15 : 1	SHEET 18 OF 24		

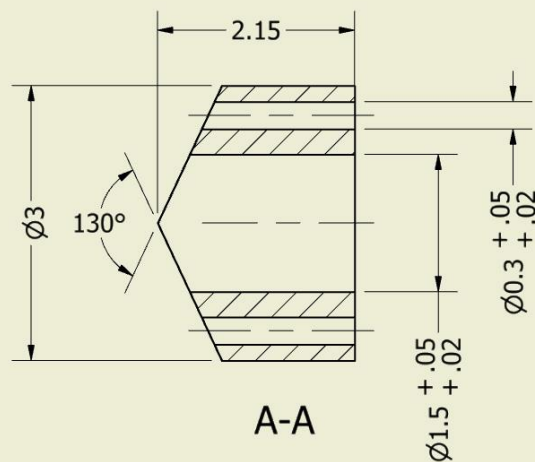
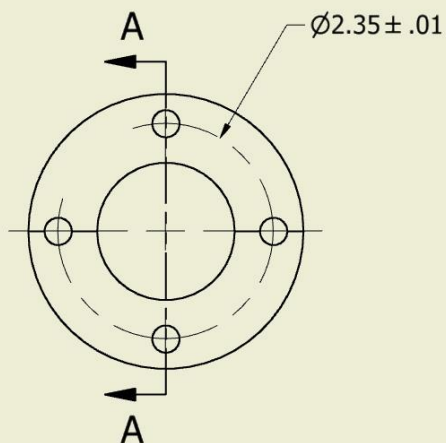
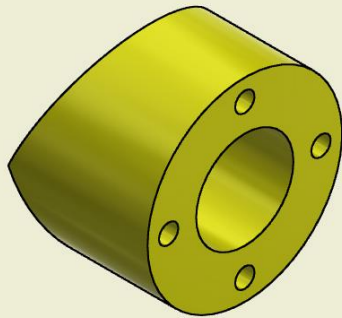


B-B

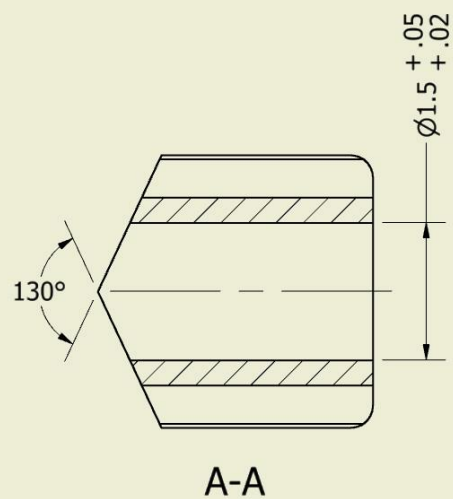
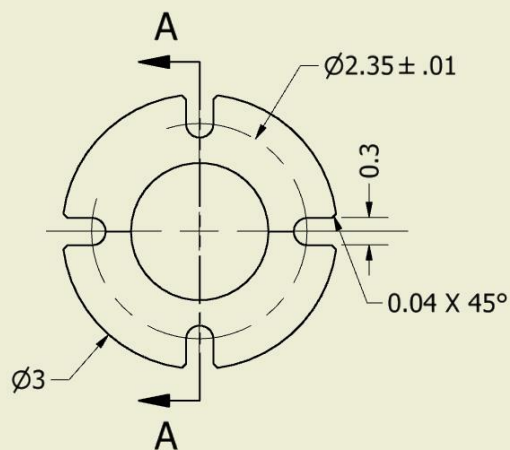
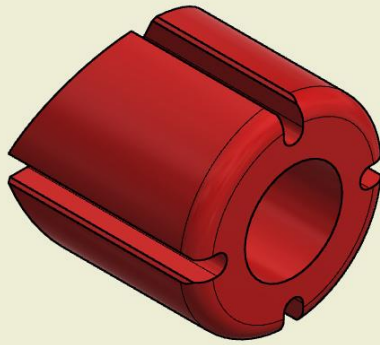


A-A

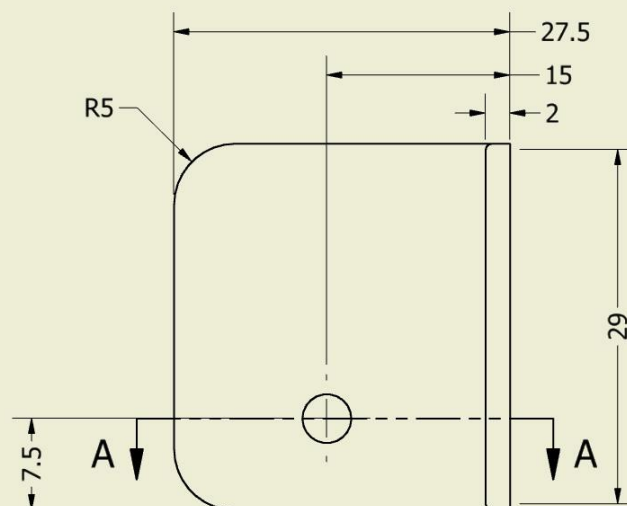
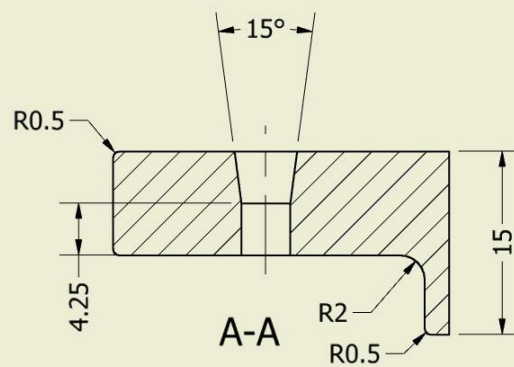
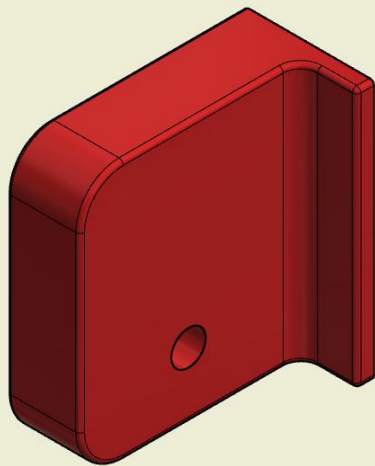
DRAWN	J.W.L. Mulckhuyse	TITLE Tip middle				
DATE	06-05-2019	PROJECT Epsilon catheter				
STATUS	Prototype					
MATERIAL	Stainless steel	General tollerances and surface finishing if not explicitly mentioned according to: NEN-ISO 1101, NEN-ISO 2768-FH-E en NPR 3634/3638				
AMOUNT	1	SIZE	A4	DWG NO	Epsilon-18	REV
UNIT	mm	SCALE	15 : 1	SHEET 19 OF 24		



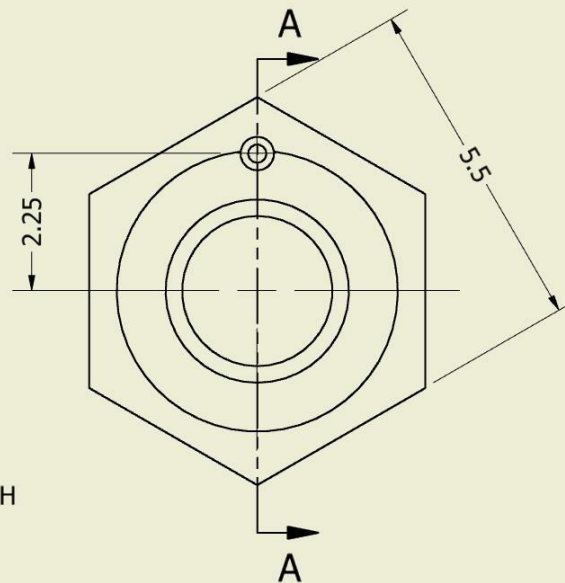
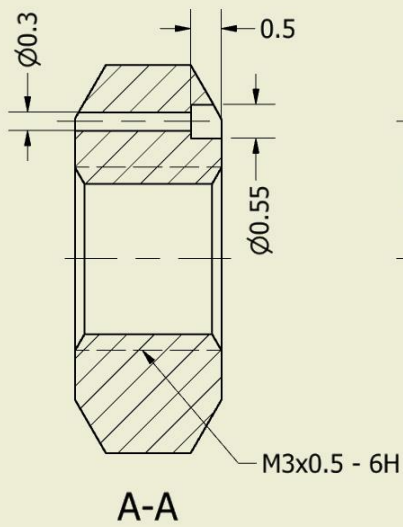
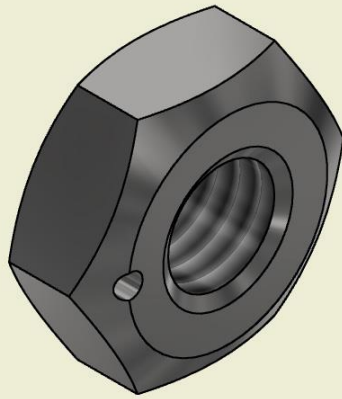
DRAWN	J.W.L. Mulckhuysen	TITLE Tip schijf distaal				
DATE	06-05-2019	PROJECT Epsilon catheter				
STATUS	Prototype					
MATERIAL	Stainless steel	General tolerances and surface finishing if not explicitly mentioned according to: NEN-ISO 1101, NEN-ISO 2768-FH-E en NPR 3634/3638				
AMOUNT	7	SIZE	A4	DWG NO	Epsilon-19	REV
UNIT	mm	SCALE	15 : 1	SHEET 20 OF 24		



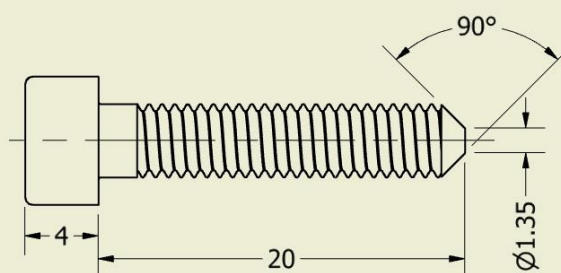
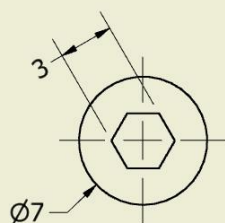
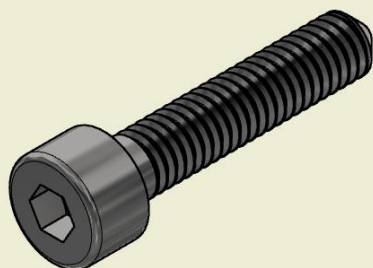
DRAWN	J.W.L. Mulckhuyse	TITLE Tip distaal				
DATE	06-05-2019	PROJECT Epsilon catheter				
STATUS	Prototype					
MATERIAL	R5	General tollerances and surface finishing if not explicitly mentioned according to: NEN-ISO 1101, NEN-ISO 2768-FH-E en NPR 3634/3638				
AMOUNT	1	SIZE	A4	DWG NO	Epsilon-20	REV
UNIT	mm	SCALE	15 : 1	SHEET 21 OF 24		



DRAWN	J.W.L. Mulckhuysen	TITLE				
DATE	06-05-2019	PROJECT				
STATUS	Prototype	Epsilon catheter				
MATERIAL	R5	General tolerances and surface finishing if not explicitly mentioned according to: NEN-ISO 1101, NEN-ISO 2768-fH-E en NPR 3634/3638				
AMOUNT	1	SIZE	A4	DWG NO	Epsilon-21	REV
UNIT	mm	SCALE	2 : 1	SHEET 22 OF 24		



DRAWN	J.W.L. Mulckhuysen	TITLE ISO 4032 - M3 - Adapted				
DATE	06-05-2019	PROJECT Epsilon catheter				
STATUS	Prototype					
MATERIAL	Stainless steel	General tolerances and surface finishing if not explicitly mentioned according to: NEN-ISO 1101, NEN-ISO 2768-FH-E en NPR 3634/3638				
AMOUNT	8	SIZE	A4	DWG NO	Epsilon-22	REV
UNIT	mm	SCALE	10 : 1	SHEET 23 OF 24		



DRAWN	J.W.L. Mulckhuysen	TITLE ISO 4762 - M4 x 20 - Adapted				
DATE	06-05-2019	PROJECT Epsilon catheter				
STATUS	Prototype					
MATERIAL	Stainless steel	General tolerances and surface finishing if not explicitly mentioned according to: NEN-ISO 1101, NEN-ISO 2768-fH-E en NPR 3634/3638				
AMOUNT	2	SIZE	A4	DWG NO	Epsilon-23	REV
UNIT	mm	SCALE	3 : 1	SHEET 24 OF 24		

Appendix C: Informed consent form

Date April 2018
Contact person Joppe Mulckhuysen
Telephone +31(0)641473718
E-mail j.w.l.mulckhuysen@student.tudelft.nl
Subject Heart Catheter Controllability experiment



Researchers:

Joppe Mulckhuysen – MSc student (e-mail: j.w.l.mulckhuysen@student.tudelft.nl)

Awaz Ali – supervisor (e-mail: a.ali@tudelft.nl)

Paul Breedveld – supervisor (e-mail: p.breedveld@tudelft.nl)

Organization: Delft University of Technology, Faculty of Mechanical, Maritime and Materials Engineering, Department of BioMechanical Engineering

Funding agent: STW

Consent Form

Dear participant,

You are invited to take part in this study to test newly developed catheter prototypes. Before you decide to participate in the experiment, it is important to know why this research is being conducted and what you will be asked to do. Please read this document carefully. If there is anything you do not understand, do not hesitate to ask.

Purpose of the research

Catheters are the most used instruments in interventional cardiology. In such procedures, a skin and vessel incision are made through which the catheter is inserted and manoeuvred towards the heart. Cardiac catheterizations are used to treat a number of heart disorders, such as an irregular heartbeat, replacing calcified valves, and retrieving biopsy samples from the heart muscle. However, because the heart has a complex shape, it can be difficult to place the catheter tip at the required location inside the heart. For this purpose, we have developed a catheter that can be steered toward the target location. The goal of this research is to determine which control method is most suitable for steering the multi-steerable catheter.

Procedures

Prior to the experiment, you will fill in a short questionnaire with demographic information and receive instructions for the experiment. Subsequently, you will test two variants of the catheter. At the end of each session, you will complete a questionnaire about your experiences during the tasks.

Duration

Your participation will last approximately 45 minutes.

Risks

The research has been reviewed and approved by the Human Research Ethics Committee of Delft University of Technology. There are no foreseen risks involved in participating in this study. If, however, you feel uncomfortable in any way during the experiment, please inform me so that you take a break or leave the experiment.

Benefits

There will be no direct benefit to you, but your participation is likely to help us find out more about instrument steerability required for cardiology procedures. With this information we can further develop our prototype.

Reimbursements

You will not be provided any reimbursement to take part in the research.

Confidentiality

The acquired data will be processed and analysed, and the results will be published in a graduation report and perhaps in scientific papers. You will not be identified by name in any reports using information obtained from this study, and your confidentiality as a participant will remain secure. Subsequent use of records and data will be subjected to standard data use policies which protect the anonymity of individuals.

Right to refuse or withdraw

This is a reconfirmation that your participation is entirely voluntary. You have the right to withdraw from the experiment at any time.

Who to contact

If you have any questions, you can ask them at any time. If you choose to ask questions after the completion of the experiment, you may contact Joppe Mulckhuysen (j.w.l.mulckhuysen@student.tudelft.nl). For research questions regarding the use of human participants, please contact Ir. J.B.J. Groot Kormelink, secretary of the Human Research Ethics Committee of the TU Delft (j.b.j.grootkormelink@tudelft.nl)

Certificate of Consent

I have read and understood all foregoing information. I have had the opportunity to ask questions about it and any questions I have asked have been answered to my satisfaction. I consent voluntarily to be a participant in this study.

Name of participant

Date

Signature of participant

Signature of investigator

Appendix D: Instructions

Date April 2018
Contact person Joppe Mulckhuysen
Telephone +31(0)64147318
E-mail j.w.l.mulckhuysen@student.tudelft.nl
Subject Heart Catheter Controllability experiment



General Instructions

Dear participant,

Thank you for participating in this experiment. Please read these instructions carefully before starting the experiment.

Intake Questionnaire

Prior to the experiment you will be asked to fill in a brief questionnaire (5 min).

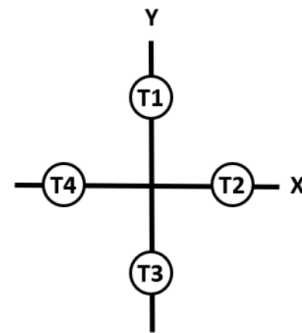
Experiment

During the experiment you will be asked to test two prototypes of a steerable catheter. There will be two sessions, one for each prototype.

Each session consists of a practice phase, a trial phase, and a questionnaire:

A. Practice Phase

- You will receive one of the prototypes:
 - 1) Sigma catheter
 - 2) Epsilon catheter
- You will find a written description of actions allowed with it on the back of this sheet.
- You will have 2 minutes to practice with the prototype.
- Make yourself familiar with manoeuvring the prototype and reaching the targets.



B. Trial Phase

- You will perform a position task with the prototype:
- You will find four targets (T1 till T4) behind holes in the black plate.
- The task time starts when you hit T1 with the tip of the catheter.
- When you hear a buzzer, you correctly contacted the target and you can continue to target T2 and accordingly T3, T4 and again T1.
- Try to reach the targets as fast as possible but be careful not break the prototype.
- Besides the task completion time, also the number of errors will be recorded.

C. Session Questionnaire

- After each session, you will be given a 5-minute break to complete a questionnaire regarding the task performance, the usability of the prototype, and your workload during the preceding session.

Final Questionnaire

After completing the third session you will be asked to fill in a brief final questionnaire regarding your experiences during the experiment (5 min).

Prototype Description

Prototype 1) Sigma catheter – double handed

- Use your primary hand to control the joystick
 - o Your thumb controls the distal (top) segment
 - o Your index finger controls the proximal (bottom) segment
- Use your secondary hand to longitudinally push/pull the shaft
 - o Keep the red line placed at the tip on top
 - o Do not torque the shaft

Prototype 2) Epsilon catheter – double handed

- Place your wrist of your primary hand on the wrist support
- Use your primary hand to control the handle using thumb, index and middle finger
- Use your secondary hand to longitudinally push/pull the shaft
 - o Keep the red line placed at the tip on top
 - o Do not torque the shaft

Appendix E: Intake questionnaire

Intake Questionnaire

Participant ID: _____

1. What is your gender?

- ☐ Male
- ☐ Female
- ☐ Other

2. What is your age?

3. In which educational phase are you currently?

- ☐ Bachelor
- ☐ Master
- ☐ PhD
- ☐ Other: _____

4. Which study direction are you following?

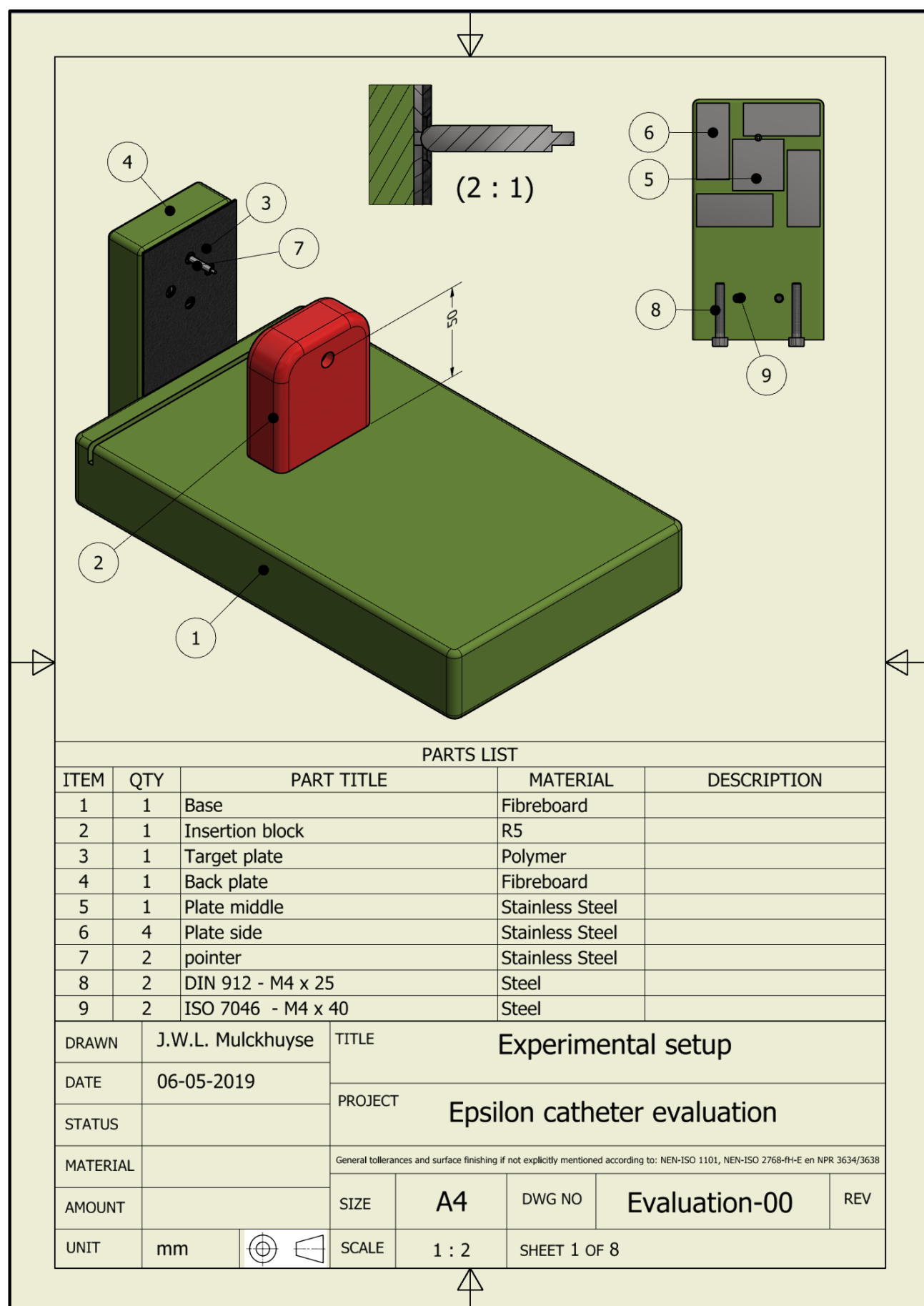
5. What is your dominant hand?

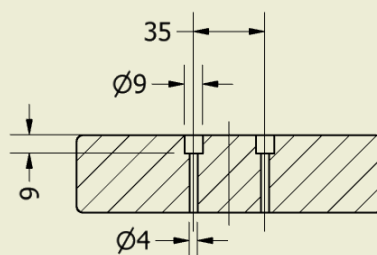
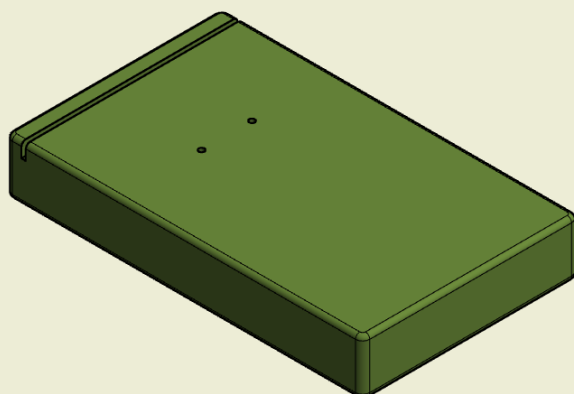
- ☐ Left hand
- ☐ Right hand
- ☐ No preference

6. How many hours did you play video games on average over the last 10 years?

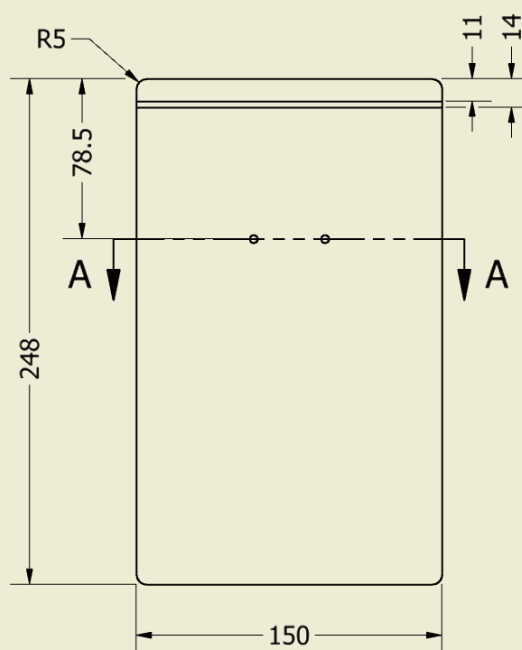
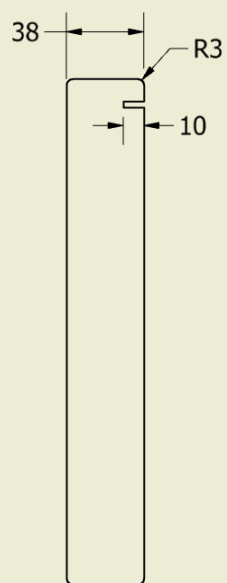
- ☐ Between 0 and 1 h/wk
- ☐ Between 1 and 3 h/wk
- ☐ Between 3 and 5 h/wk
- ☐ Between 5 and 10 h/wk
- ☐ Between 10 and 15 h/wk
- ☐ More than 15 h/wk, namely _____h/wk

Appendix F: Technical drawings experimental design

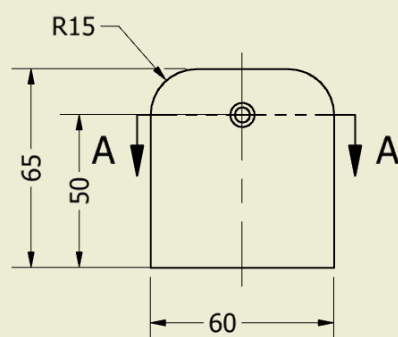
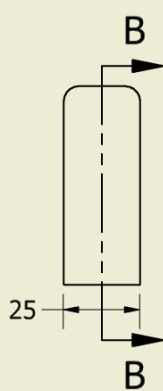
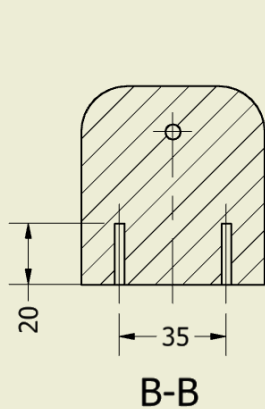
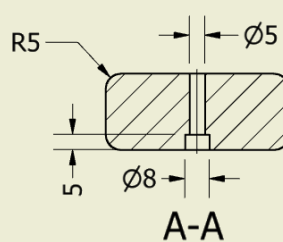
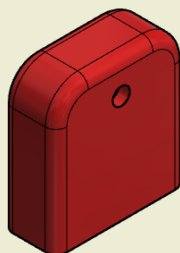





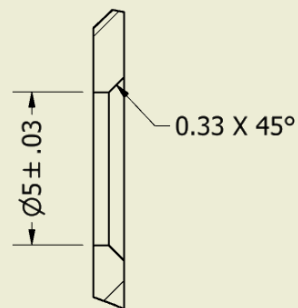
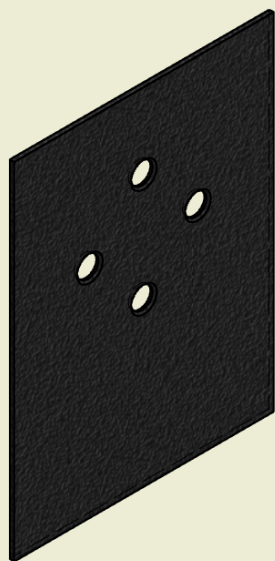
A-A



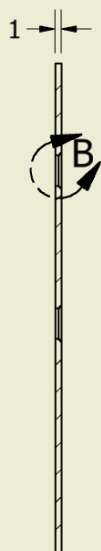
DRAWN	J.W.L. Mulckhuyse	TITLE Base				
DATE	06-05-2019	PROJECT Epsilon catheter evaluation				
STATUS						
MATERIAL	Fibreboard	General tollerances and surface finishing if not explicitly mentioned according to: NEN-ISO 1101, NEN-ISO 2768-FH-E en NPR 3634/3638				
AMOUNT	1	SIZE	A4	DWG NO	Evaluation-01	REV
UNIT	mm	SCALE	1 : 3	SHEET 2 OF 8		



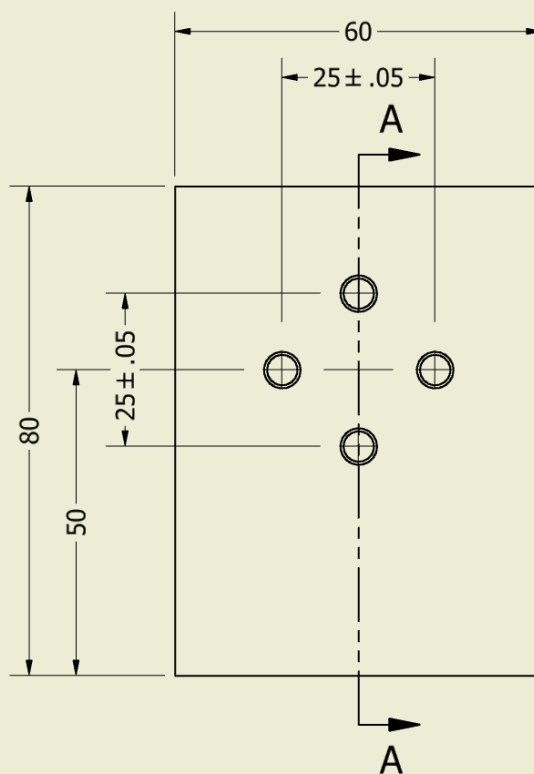
DRAWN	J.W.L. Mulckhuysen	TITLE						Insertion block	
DATE	06-05-2019	PROJECT						Epsilon catheter evaluation	
STATUS									
MATERIAL	R5	General tolerances and surface finishing if not explicitly mentioned according to: NEN-ISO 1101, NEN-ISO 2768-FH-E en NPR 3634/3638							
AMOUNT	1	SIZE	A4	DWG NO	Evaluation-02			REV	
UNIT	mm		SCALE	1 : 2	SHEET 3 OF 8				



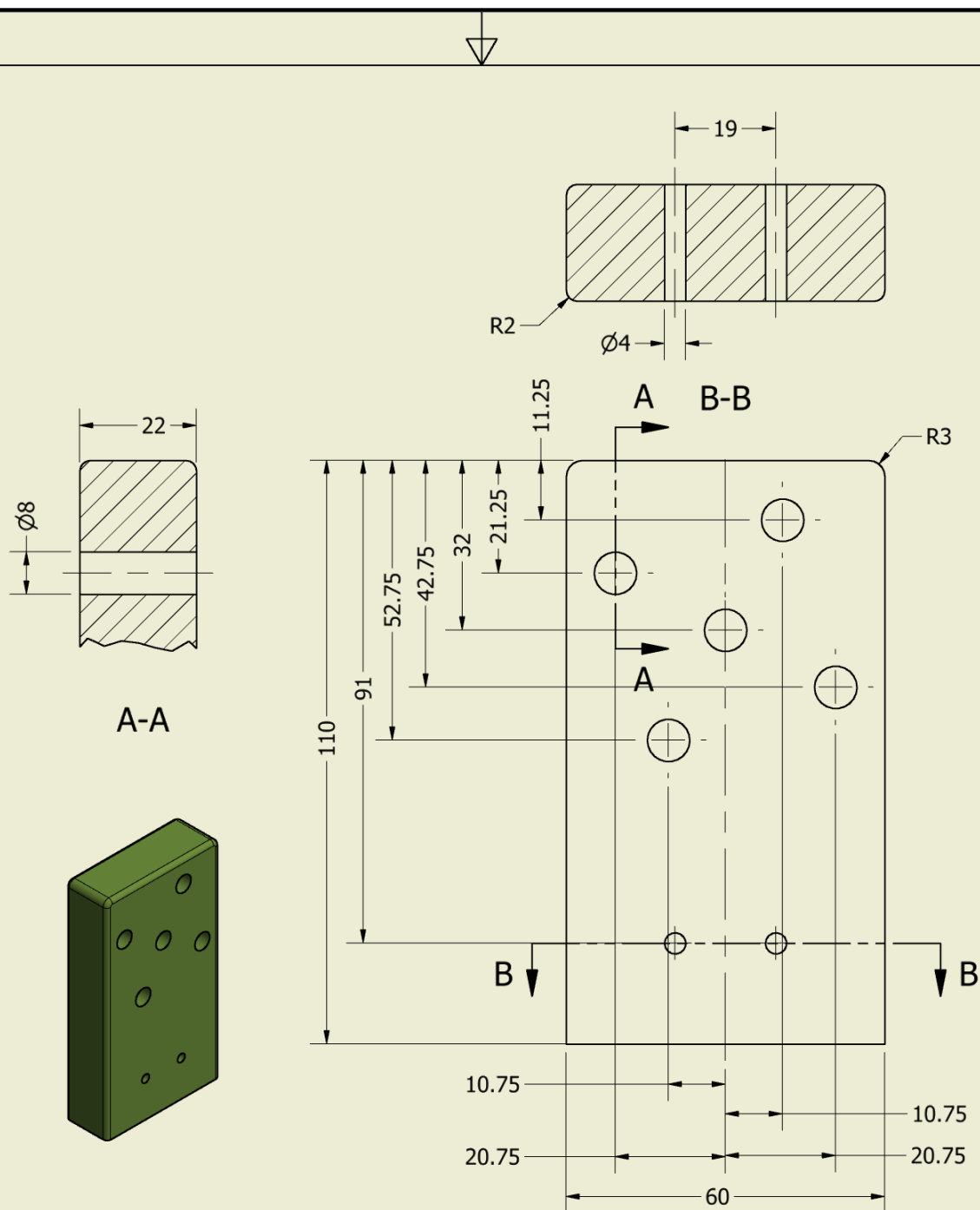
B (5 : 1)



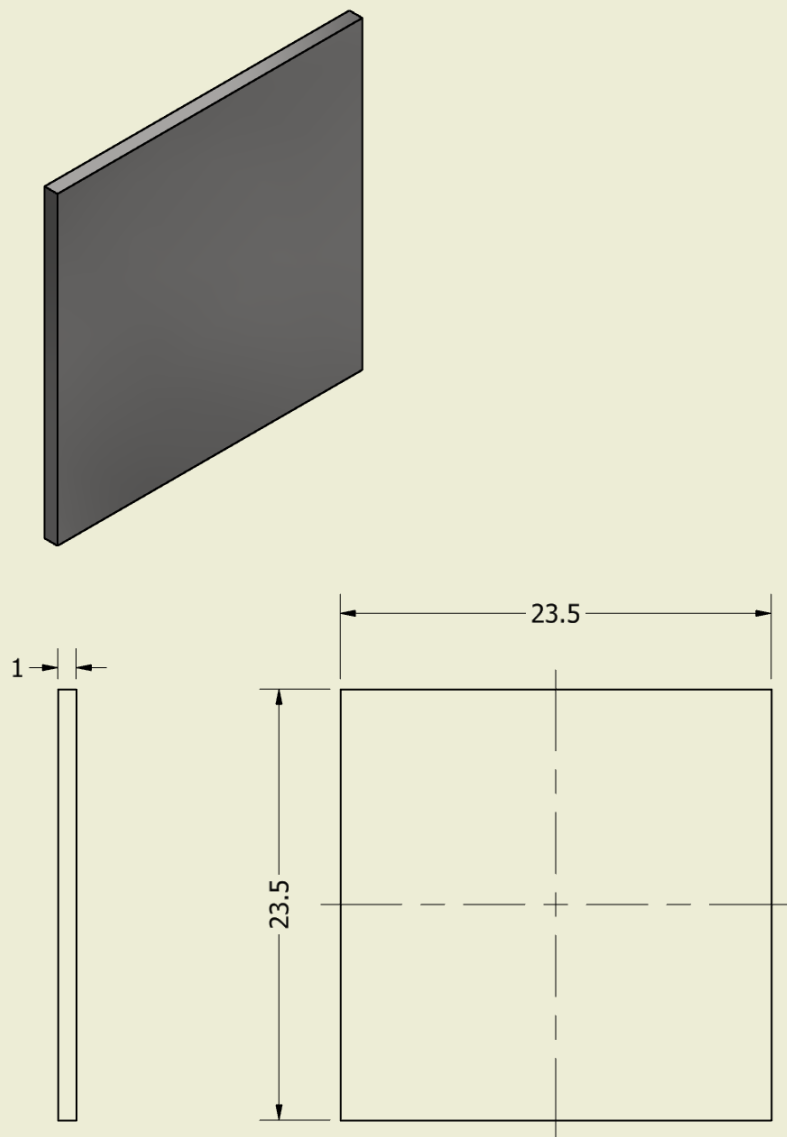
A-A



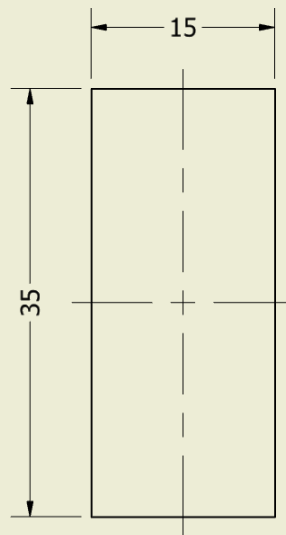
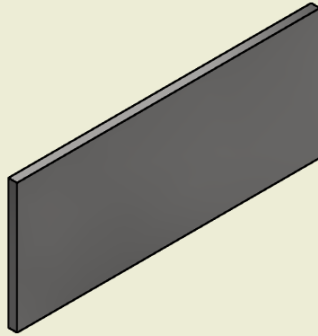
DRAWN	J.W.L. Mulckhuyse	TITLE Target plate				
DATE	06-05-2019	PROJECT Epsilon catheter evaluation				
STATUS						
MATERIAL	Polymer	General tollerances and surface finishing if not explicitly mentioned according to: NEN-ISO 1101, NEN-ISO 2768-FH-E en NPR 3634/3638				
AMOUNT	1	SIZE	A4	DWG NO	Evaluation-03	REV
UNIT	mm	SCALE	1 : 1	SHEET 4 OF 8		




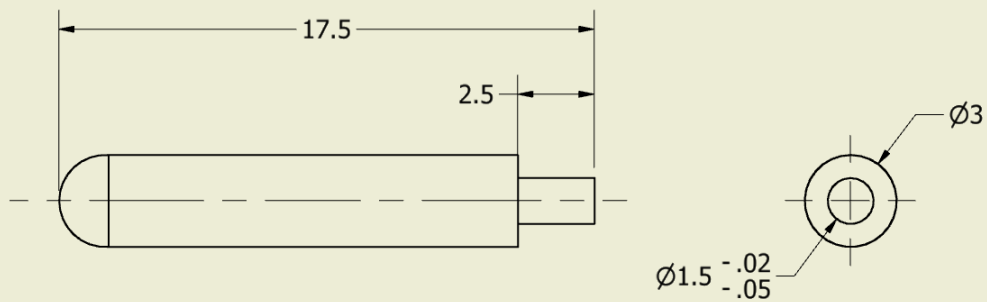
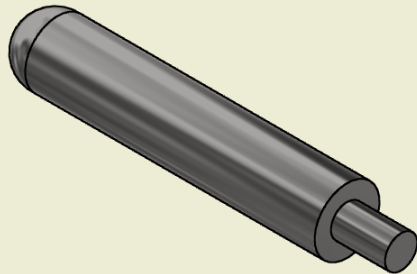
DRAWN	J.W.L. Mulckhuyse	TITLE Back plate				
DATE	06-05-2019	PROJECT Epsilon catheter evaluation				
STATUS						
MATERIAL	Fibreboard	General tollerances and surface finishing if not explicitly mentioned according to: NEN-ISO 1101, NEN-ISO 2768-FH-E en NPR 3634/3638				
AMOUNT	1	SIZE	A4	DWG NO	Evaluation-04	REV
UNIT	mm	SCALE	1 : 2	SHEET 5 OF 8		



DRAWN	J.W.L. Mulckhuyse	TITLE Plate middle				
DATE	06-05-2019	PROJECT Epsilon catheter evaluation				
STATUS						
MATERIAL	Stainless steel	General tollerances and surface finishing if not explicitly mentioned according to: NEN-ISO 1101, NEN-ISO 2768-FH-E en NPR 3634/3638				
AMOUNT	1	SIZE	A4	DWG NO	Evaluation-05	REV
UNIT	mm	SCALE	3 : 1	SHEET 6 OF 8		



DRAWN	J.W.L. Mulckhuysen		TITLE Plate side				
DATE	06-05-2019						
STATUS			PROJECT Epsilon catheter evaluation				
MATERIAL	Stainless steel						
AMOUNT	4		General tolerances and surface finishing if not explicitly mentioned according to: NEN-ISO 1101, NEN-ISO 2768-FH-E en NPR 3634/3638				
UNIT	mm		SIZE	A4	DWG NO	Evaluation-06	REV
			SCALE	2 : 1	SHEET 7 OF 8		



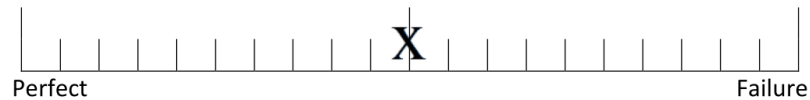
DRAWN	J.W.L. Mulckhuyse	TITLE Pointer				
DATE	06-05-2019	PROJECT Epsilon catheter evaluation				
STATUS						
MATERIAL	Stainless steel	General tolerances and surface finishing if not explicitly mentioned according to: NEN-ISO 1101, NEN-ISO 2768-FH-E en NPR 3634/3638				
AMOUNT	2	SIZE	A4	DWG NO	Evaluation-07	REV
UNIT	mm	SCALE	5 : 1	SHEET 8 OF 8		

Appendix G: TLX questionnaire

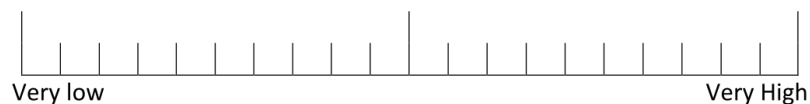
TLX Questionnaire Condition: _____

Participant ID: _____

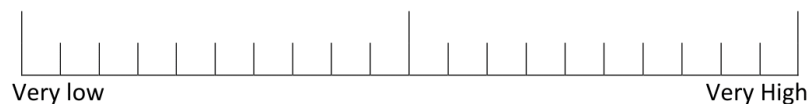
Instruction: The following questions have to be answered like this: put the cross on the line



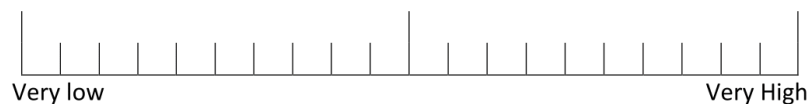
1. How mentally demanding was the task?



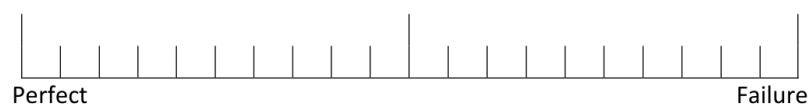
2. How physically demanding was the task?



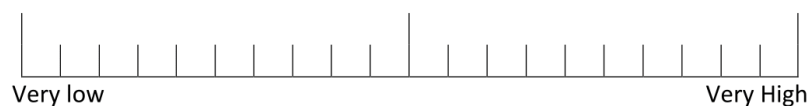
3. How hurried or rushed was the pace of the task?



4. How successful were you in accomplishing what you were asked to do?



5. How hard did you have to work to accomplish your level of performance?



6. How insecure, discouraged, irritated, stressed, and annoyed were you?



Appendix H: Final questionnaire

Final Questionnaire

Participant ID: _____

1. Which prototype has your personal preference?

- ☐ Sigma catheter
- ☐ Epsilon catheter

2. Which prototype is the easiest to steer?

- ☐ Sigma catheter
- ☐ Epsilon catheter

3. Which prototype is the fastest to steer?

- ☐ Sigma catheter
- ☐ Epsilon catheter

4. Which prototype is the most precisely to steer?

- ☐ Sigma catheter
- ☐ Epsilon catheter

5. Do you have any comments regarding the prototypes or experiment?

Appendix I: Raw data of experiment

Table 6: Raw intake questionnaire data

<i>ID</i> Topic	1	2	3	4	5	6	μ	σ
Gender	Female	Male	Male	Female	Male	Male	67% Male	
Age [years]	25	25	25	26	25	23	25	0.98
Educational Phase	Master	Master	Master	Master	Master	Master	-	-
Study Direction	Architecture	Mechanical Engineering	Civil Engineering	Mechanical Engineering	Mechanical Engineering	Mechanical Engineering	-	-
Dominant hand	Right hand	Right hand	Right hand	Right hand	Left hand	Right hand	83% Right handed	
Video games [hours/per week]	0.5	0.5	0.5	0.5	2	7.5	1.92	2.80

The responses of the Raw TLX questionnaire questions vary from -10 to 10.

Table 7: Raw TLX data of Sigma catheter.

<i>ID</i> Topic	1	2	3	4	5	6	μ	σ
Mental Demand	4	4	3	10	4	4	4.8	2.6
Physical Demand	-4	2	-4	8	4	4	1.7	4.8
Temporal Demand	-2	1	5	0	2	-5	0.2	3.4
Performance	0	4	6	7	3	0	3.3	2.9
Effort	4	5	5	10	0	0	4.0	3.7
Frustration	-5	3	5	7	5	0	2.5	4.4
Total							2.8	3.8

Table 8: Raw TLX data of Epsilon catheter.

<i>ID</i> Topic	1	2	3	4	5	6	μ	σ
Mental Demand	-3	-6	-6	5	-5	0	-3	4.3
Physical Demand	-5	-7	-6	-2	-6	-2	-5	2.2
Temporal Demand	-6	-2	2	3	-2	-5	-2	3.6
Performance	-4	-4	-9	-6	-5	-5	-6	1.9
Effort	2	3	-6	8	-5	-7	-1	6.0
Frustration	-7	-4	-8	-5	-8	-5	-6	1.7
Total							-3.6	3.9

Table 9: Target-to-target times of experiment [ms]

ID	Sigma catheter											
	Trial 1				Trial 2				Trial 3			
	T1-T2	T2-T3	T3-T4	T4-T1	T1-T2	T2-T3	T3-T4	T4-T1	T1-T2	T2-T3	T3-T4	T4-T1
1	14119	27631	21017	30125	17074	20659	28083	13814	19428	24456	5856	63009
2	10520	3756	36184	16772	15570	11417	12200	21680	9857	10914	3436	17862
3	34899	14206	33827	97757	56060	21280	6379	30298	8203	11366	19530	12612
4	15446	58287	72558	22122	15411	20322	19783	22900	15255	18368	52615	28027
5	14852	3154	7597	2910	10490	18621	25373	54916	4102	17623	14493	16672
6	5238	3954	10108	5807	16037	13263	9167	13962	2901	10212	7890	4054
	Epsilon catheter											
1	8213	14670	8617	21629	9119	15464	6558	14512	9665	20180	8135	8265
2	4210	3802	3556	6254	4504	6860	7510	5360	2054	7160	2608	3653
3	2035	8658	7655	7605	2155	3705	5959	3106	1983	5409	2351	2300
4	16993	18469	10967	13119	10062	7958	10615	4756	8462	6408	5453	3550
5	2987	11814	1826	2554	1753	5709	2001	1502	1553	1856	1953	2202
6	6008	6762	5512	6668	8467	2751	3005	2501	6008	6762	5512	6668

Appendix J: MATLAB code for data processing of the experiment

```
%% Joppe Mulckhuyse 17-05-2018
% Data Processing for Heart Catheter Controllability experiment 18 mei 2018
clear all
close all
clc

%% Variables
% Conditions 1: Sigma | condition 2: Epsilon
N = 6; % # participants

%% Initialize
TLX1 = xlsread('Results.xlsx','TLX','B3:G8'); % Get scores from TLX questionnaires
TLX2 = xlsread('Results.xlsx','TLX','B12:G17');

data_timestamp = zeros(N,30); % time when target is hit since researcher started the
measurement [ms]
data = data_timestamp; % actual time between two targets [ms]
for n = 1:N
    a = 0;
    for c = 1:6
        raw = xlsread(strjoin({'Raw Data\Time measurement\'
sprintf('%d_%d.xlsx',n,c)}, ''));
        j = 2;
        for k = 1:size(raw,1)
            if j <= 5 && raw(k,j) <= 1
                if c == 2
                    a = 5;
                elseif c == 3
                    a = 10;
                elseif c == 4
                    a = 15;
                elseif c == 5
                    a = 20;
                elseif c == 6
                    a = 25;
                end
                data_timestamp(n,j-1+a) = raw(k,1);
                j = j+1;
            end
            if j >= 4
                data(n,a+j-3)=data_timestamp(n,1+a+j-3)-data_timestamp(n,a+j-3);
            end
            if j == 6 && raw(k,2) <= 1
                data_timestamp(n,j-1+a) = raw(k,1);
                data(n,a+j-3)=data_timestamp(n,1+a+j-3)-data_timestamp(n,a+j-3);
                j = j+1;
            end
        end
    end
end
end

data( :, ~any(data,1) ) = []; % remove empty columns
```

```

data_c1 = zeros(N,12); % time between targets for condition 1 [ms]
data_c2 = data_c1; % time between targets for condition 2 [ms]
% Since odd participants started with condition 1 and
% even participants with condition 2 the data should be sorted out
for n = 1:N
    if mod(n,2) == 1
        data_c1(n,:) = data(n,1:12);
        data_c2(n,:) = data(n,13:24);
    elseif mod(n,2) == 0
        data_c1(n,:) = data(n,13:24);
        data_c2(n,:) = data(n,1:12);
    end
end

%% Visualise results
% Scatter plot of individual measurements
figure(1)
clf(1)
hold on
for n=1:N
    range = 1:12;
    range = range+n/6;
    scatter(range,data_c1(n,:)./10^3,'o')
    scatter(range,data_c2(n,:)./10^3,'+')
end
legend('Sigma','Epsilon')
xlabel('Trails')
ylabel('Time between targets [s]')
title({'Time measurement of Heart Catheter Controllability experiment',
       'Scatter plot of individuel measurements of all participants'})

%% Box plot representation of all time measurements
figure(2)
clf(2)
boxplot([reshape(data_c1,1,[],[]); reshape(data_c2,1,[],[])]'/10^3,...
        'Labels',{'Sigma','Epsilon'})
ylabel('Time between targets [s]')
title({'Time measurement of Heart Catheter Controllability experiment',...
       'Box plot representation for all time measurements combined'})

%% Box plot representation of time measurements for each participant
figure(3)
clf(3)
boxplot([reshape(data_c1(1,:),1,[]); reshape(data_c2(1,:),1,[]);
        reshape(data_c1(2,:),1,[]); reshape(data_c2(2,:),1,[]);
        reshape(data_c1(3,:),1,[]); reshape(data_c2(3,:),1,[]);
        reshape(data_c1(4,:),1,[]); reshape(data_c2(4,:),1,[]);
        reshape(data_c1(5,:),1,[]); reshape(data_c2(5,:),1,[]);
        reshape(data_c1(6,:),1,[]); reshape(data_c2(6,:),1,[])]'/10^3,...
        'Labels',{'1_S','1_E','2_S','2_E','3_S','3_E',...
                  '4_S','4_E','5_S','5_E','6_S','6_E'})
xlabel({'Participant ID _ Catheter','S = Sigma | E = Epsilon'}, 'Interpreter',
'none')
ylabel('Target-to-target time [s]')
% title({'Time measurement of Heart Catheter Controllability experiment',...
%       'Box plot representation of time measurements for each participant'})

```



```

%% Results from NASA-TLX Questionnaires
figure(4);
boxplot([TLX1(1,:); TLX2(1,:);
        TLX1(2,:); TLX2(2,:);
        TLX1(3,:); TLX2(3,:);
        TLX1(4,:); TLX2(4,:);
        TLX1(5,:); TLX2(5,:);
        TLX1(6,:); TLX2(6,:); ], 'Labels', {'MD1', 'MD2', 'PD1', 'PD2'...
        , 'TD1', 'TD2', 'P1', 'P2', 'E1', 'E2', 'F1', 'F2' })
ylim([-10 10])
title({'Results from NASA-TLX Questionnaires of', 'Heart Catheter Controllability
experiment'})
xlabel({'Condition 1: Sigma | Condition 2: Epsilon',
        'MD = Mental Demand | PD = Physical Demand | TD = Temporal Demand',
        'P = Performance | E = Effort | F = Frustration'})
ylabel('Scores (lower is desired)')

%% Statistical Test
TLX1_avg = mean(TLX1(:));
TLX2_avg = mean(TLX2(:));
TLX1_std = std(TLX1(:));
TLX2_std = std(TLX2(:));

TLX_cor = corrcoef(TLX1, TLX2);

data_c1_avg = mean(data_c1(:))/10^3; % Average time TA to TB [s]
data_c2_avg = mean(data_c2(:))/10^3;

data_c1_std = std(data_c1(:))/10^3; % Standard deviation time TA to TB [s]
data_c2_std = std(data_c2(:))/10^3;

data_cor = corrcoef(data_c1, data_c2);

% within subject design --> paired-samples t test
[Ht, Pt, CIt, STATSt] = ttest(data_c1, data_c2, 'Tail', 'Both', 'Alpha', 0.05); %Time
[H, P, CI, STATS] = ttest(TLX1, TLX2, 'Tail', 'Both', 'Alpha', 0.05); %TLX

%% effect size (cohen's d)
d_time = ones(N,1);
for n=1:N
    x1 = data_c1(n,:)/10^3;
    x2 = data_c2(n,:)/10^3;
    n1=length(x1);
    n2=length(x2);
    d_time(n) = (mean(x1)-mean(x2))/(sqrt(((n1-1)*std(x1)^2+(n2-1)*std(x2)^2)/(n1+n2-
2))));
end

d_tlx = ones(N,1);
for n=1:N
    x1 = TLX1(n,:);
    x2 = TLX2(n,:);
    n1=length(x1);
    n2=length(x2);
    d_tlx(n) = (mean(x1)-mean(x2))/(sqrt(((n1-1)*std(x1)^2+(n2-1)*std(x2)^2)/(n1+n2-
2))));
end

```

```

% all target-to-target data points
x1 = reshape(data_c1,1,[]);
x2 = reshape(data_c2,1,[]);
n1=length(x1);
n2=length(x2);
d_all_time = (mean(x1)-mean(x2))/(sqrt(((n1-1)*std(x1)^2+(n2-1)*std(x2)^2)/(n1+n2-2)));
[ht,pt,~,statst] = ttest(x1,x2,'Tail','Both','Alpha',0.05);

% all TLX data points
x1 = reshape(TLX1',1,[]);
x2 = reshape(TLX2',1,[]);
n1=length(x1);
n2=length(x2);
d_all_TLX = (mean(x1)-mean(x2))/(sqrt(((n1-1)*std(x1)^2+(n2-1)*std(x2)^2)/(n1+n2-2)));
[h,p,~,stats] = ttest(x1,x2,'Tail','Both','Alpha',0.05);

% difference between targets
x1 = [data_c1(:,1:4);data_c1(:,5:8);data_c1(:,9:12)];
x2 = [data_c2(:,1:4);data_c2(:,5:8);data_c2(:,9:12)];
[hT,pT,~,statsT] = ttest(x1(:,1),x1(:,2),'Tail','Both','Alpha',0.05);

```